IMMOBILIZATION OF ENZYMES ON POROUS MATERIALS AND THEIR CATALYTIC APPLICATIONS

A THESIS

Submitted to the

BHAVNAGAR UNIVERSITY, Bhavnagar

for the Degree of

DOCTOR OF PHILOSOPHY

in

CHEMISTRY

by

KANNAN. K

Under the guidance of

DR. RAKSH VIR JASRA

Discipline of Inorganic Materials and Catalysis
Central Salt and Marine Chemicals Research Institute (CSMCRI)
Council of Scientific and Industrial Research (CSIR)
Bhavnagar - 364 021, India

September 2010


Dedicated to my Beloved
Family & Teachers

27 September 2010

Candidate's Statement

I hereby declare that the work incorporated in the thesis entitled **"Immobilization of Enzymes on Porous Materials and their Catalytic Applications"** is original and has not been submitted to any university / institution for the award of any diploma / degree.

I further declare that the results presented in the thesis and the considerations made therein, contribute in general to the advancement of knowledge in chemistry and biochemistry in particular to enzyme immobilization, porous silica synthesis, silica surface functionalization, immobilization method, stability, reusability, protein engineering, reversible denaturisation, novel enzyme design, activity with substrate.

(KANNAN. K)

Reg. No. 1164

27 September 2010

Certificate by the Ph.D. Supervisor

This is to certify that the contents of this thesis entitled **"Immobilization of Enzymes on Porous Materials and their Catalytic Applications"** are the original research work of **Mr. Kannan. K (**Reg. No. 1164) carried out under my supervision at Discipline of Inorganic Materials and Catalysis, Central Salt and Marine Chemicals Research Institute, Bhavnagar.

I further certify that the work has not been submitted either partly or fully to any university / institution for the award of any diploma / degree.

Dr. Raksh Vir Jasra
Ph. D Supervisor

ACKNOWLEDGEMENTS

First, I would like to express my prodigious grateful to my research supervisor **Dr. Raksh Vir Jasra,** who allowed me think independently and crystallized out with a right shape and properties through his inspiring guidance and constant motivation. He has taught me scientific and non-scientific lessons better and to remain optimistic. I preserve an everlasting gratitude for him.

I am indebted to **Dr. Pushpito K. Ghosh**, Director, CSMCRI, for providing me his kind permission to carry out this research work at CSMCRI, Bhavnagar

I would like to place honest gratitude to Dr. H.C. Bajaj, Discipline coordinator, Discipline of Inorganic Materials and Catalysis, CSMCRI, Bhavnagar.

I express my sincere gratitude to Dr. R.J. Tayade, Dr. M. Chidambaram and Dr. Amith Dubey for paving the path to carry out this research work.

I would like to place my respect and deep sense of gratitude to Dr. S. Kannan, Dr. R.S. Somani, Dr. R.S. Shukla, Dr. S.H.R. Abdi, Dr. S.D. Bhatt, Dr. R.I. Kureshy, Dr. N.H. Khan, Dr. H.M. Mody, Dr. Beena Tyagi and Dr. A.B. Boricha at CSMCRI Bhavnagar and Dr. Sharad Lande, Dr. A. Sakthivel, Dr. S.M. Pillai, Dr. Jince Sepastine, Dr. Nagesh Sharma, Dr. S. Unnikrishnan, Dr. K.V. Murthy, Dr. Vivek Srivastava, Mr. Pankaj Chavda, Mr. Vipul Chahwala, Mr. K.N. Pathak and Mr. Krishna at RTG, VMD for their encourage and support.

I render my thankfulness to Dr. P. Paul, DC, Analytical Science Discipline, for providing various instrumental facilities. I am thankful to Mr. P.G. Mohanan Pillai, Mr. K. Rajagopalan, Mr. P. Balakrishnan, Mr. V.C. Zala, and Mr. V.M. Rajan for the support and I also acknowledge Mr. Bharat B. Parmar, Mr. Jayanthi M. Parmar, and Mr. Ali H. Lakhani for their prompt help rendered during this period.

I always had a learning inspiration from my colleague and seniors: Mr. Sunil A.P, Dr. Renjith S. Pillai, Mr. Prasanth. K.P, Dr. Praveen K. Surolia, Mr. Jinka Krishnamohan, Mr. M.V. Patil, Mr. Manoj A. Lazar, Mr. Phani, Mr. G.P. Dangi, Mr. Munusamy. K, Mrs. Nirali, Mr. Manoj J.C. Raj, Mr. Thillai Sivakumar and Mr. Dinesh Patil.

I am also thankful to Mr. Mosae selvakumar, Mr. Suresh. M, Mr. Churchil A. Angel, Mr. Subratha padra, Mr. Manu. V, Mr. Jinesh, C.M, Mr. Amal Cherian. K, Sudheesh. N, Mr. Gnana Sekar, Mr. Vijay Anand, Mr. Rathish and Mr. Selva kumar for their charming company, help and everlasting prayer.

I am very much gratified to the staff from canteen, library, I. T. cell, BDIM, electrical, mechanical, carpentry, refrigeration, store & purchase, administration, finance & accounts and watch & ward sections for their co-operation during this period. I would also like to express my sincere thanks to all the staff members of CSMCRI for their cooperation and assistance throughout my tenure directly or indirectly.

I would also like to acknowledge the support of my friends and colleagues Dr. Srinivasan, Dr. Lakshmi Narayanan, Dr. Amilan Jose, Dr. Krishna Kumar, Dr. Gnanaprakasam, Dr. Manish Mishra, Mr. Ravikumar, Dr. Hasmukh Patel, Dr. Sumeet Sharma, Mr. Arunachalam, Dr. Presanjith Kar, Dr. Amritha, Dr. Santosh Agarwal Dr. Vishal J. Mayani, Dr. Munir D. Khokhar, Mr. Nisar, Mr. Murugan, Mr. Asif, Mr. Koil Raj, Mr. Siva Shanmugam, Mr. Jeyaprathap, Mr. Sumit Jadav, Mr. Radheshym Pawar, Mr. Pravin Ingole, Mr. Sandesh, Mr. Abhinav, Mr. Kunal, Mr.Yogesh, Mr. Bhavesh, Mr. Gopala Krishnan and Dr. Smithra for providing a good friendly working atmosphere.

My special heartfelt thanks to my graduation teachers Dr. A. Thamarai selvan, Dr. A. Veluchamy and Dr. A. Elangovan, who have founded to become skilled at the scientific taste and they are absolutely inspired me to remain in science. I cannot fail to acknowledge my classmates, Mr. Kalidasan, Mr. Ramkumar, Mr. Kandhasamy, Mr. Bala Subramanian, Mr. Thamarai Selvan, Mr. Suresh Kumar, Mrs. Nithya, Mrs. Deepa, Mrs. Kavitha and Mrs. Banu. I would also thank friends at Palayanoor and all my FOPE friends in Vadodara, those were spared with me in memorable days.

I am grateful to my schooling teachers Mr. Ravanan, Mr. Kesavan and Mr. Babu lal for their parental care and constant encouragement throughout my studies.

This thesis would have been impossible without the moral support from my father **Shri. Kayambu**, mother **Smt. Ponnuthai**, brother Mr. Manivannan, sister Mrs. Anantha Jothi, brother-in-law Mr. Mahesh, sister-in-law Mrs. Muthumeena and niece Udaya Krishma. So I believe it becomes success only because of the constant support, encouragement, genuine care and their deep faith in god.

I place my regards to all those who helped me consciously or unsuspectingly. Above all, I am grateful for the providential blessing showered on me in abundance, which enabled me to successfully complete my thesis work.

Finally, my acknowledges are due to the financial assistance from the Council of Scientific and Industrial Research (CSIR), New Delhi, India for granting Senior Research Fellowship and the CSIR network project on catalysis.

(KANNAN. K)

TABLE OF CONTENT

LIST OF FIGURES

LIST OF TABLES

Chapter 1

Introduction to Enzymes, immobilization and protein engineering

1.1. Introduction

Enzymes are mainly catalytic proteins, that increase the rates of chemical reactions.[1] In enzymatic reactions, the molecules at the beginning of the process are called substrates, and the enzyme converts them into different molecules, called the products. Almost all processes in a biological cell need enzymes to occur at significant rates. Since enzymes are selective for their substrates and speed up only a few reactions from among many possibilities, the set of enzymes made in a cell determines which metabolic pathways occur in that cell. Acting in organized sequences, they catalyze the hundreds of stepwise reactions that degrade nutrient molecules, conserve and transform chemical energy, and make biological macromolecules from simple precursors. Through the action of regulatory enzymes, metabolic pathways are highly coordinated to yield a harmonious interplay among the many activities necessary to sustain life.

Like all catalysts, enzymes work by lowering the activation energy ($E_a^{\ddagger}$) for a reaction, thus dramatically increasing the rate of the reaction. Most enzyme reaction rates are millions of times faster than those of comparable un-catalyzed reactions. As with all catalysts, enzymes are not consumed by the reactions they catalyze, nor do they alter the equilibrium of these reactions. However, enzymes do differ from most other catalysts by being much more specific. Enzymes are known to catalyze about 4,000 biochemical reactions.[2] A few RNA molecules called ribozymes also catalyze reactions.[3-4] Synthetic molecules called artificial enzymes also display enzyme-like catalysis.[5]

1.2 A short history of enzymes

Enzymes had been used for thousands of years without a clear understanding of their nature and mechanism. As early 1800s, the digestion of meat by stomach secretions and the conversion of starch to sugars by plant extracts and saliva were known.[1]

In 19th century, when studying the fermentation of sugar to alcohol by yeast, Louis Pasteur introduced “ferments” and concluded that "alcoholic fermentation is an act correlated with the life and organization of the yeast cells, not with the death or putrefaction of the cells".[6]

In 1878, German physiologist Wilhelm Kühne (1837–1900) first used the term *enzyme*, which comes from Greek *ενζυμον*, "in leaven" to describe this process. In 1897, Eduard Buchner began to study the ability of yeast extracts to ferment sugar, noticed that there were no living yeast cells in the mixture and named the enzyme to cause fermentation “zymase”. In 1907, he received the nobel Prize in Chemistry” for his discovery of cell-free fermentation.[7]

In 1926, James B. Sumner crystallized the enzyme catalase which helped to determine biochemical nature of enzyme. In 1965, first lysozyme could be crystallized its structure was solved by X-ray crystallography.[8] This high-resolution structure of lysozyme marked the beginning of the field of structural biology and the effort to understand how enzymes work at an atomic level.

1.3 Enzymes structures and specificity

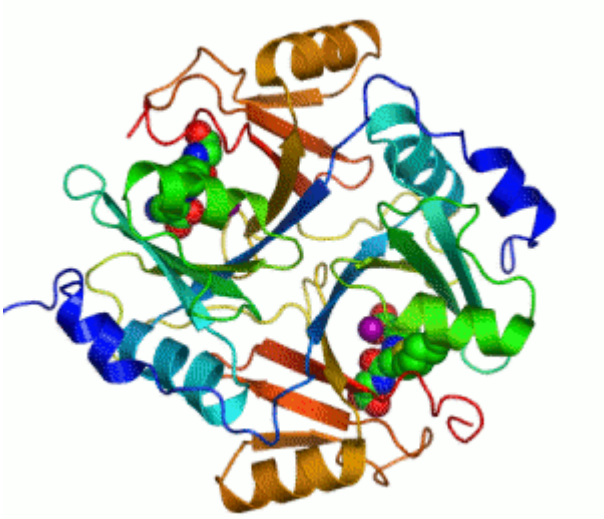

Fig. 1.1 Human glyoxalase I. Two zinc ions that are needed for the enzyme to catalyze its reaction are shown as purple spheres, and an enzyme inhibitor called S-hexylglutathione is shown as a space-filling model, filling the two active sites

Enzymes are generally globular proteins, range from just 62 amino acid residues in size and small number of RNA-based biological catalysts exist, with the most common being the ribosome; these are referred to as either RNA-enzymes or ribozymes. The activities of enzymes are determined by their three-dimensional structure.[9] However, although structure does determine function, predicting a novel enzyme's activity just from its structure is a very difficult problem that has not yet been solved.[10]

Most enzymes are much larger than the substrates they act on, and only a small portion of the enzyme (around 3–4 amino acids) is directly involved in catalysis. The region that contains these catalytic residues, binds the substrate, and then carries out the reaction is known as the active site. Complementary shape, charge and hydrophilic/hydrophobic characteristics of enzymes and substrates are responsible

for this specificity. Enzymes can also show impressive levels of stereospecificity, regioselectivity and chemoselectivity.[11]

Enzymes can also contain sites that bind cofactors, which are needed for catalysis. Enzymes that require a cofactor but do not have one bound are called apoenzymes or apoproteins. An apoenzyme together with its cofactor(s) is called a holoenzyme (this is the active form). Cofactors can be either inorganic (*e.g.*, metal ions and iron-sulfur clusters) or organic compounds (e.g., flavin and heme). Organic cofactors can be either prosthetic groups, which are tightly bound to an enzyme, or coenzymes, which are released from the enzyme's active site during the reaction. Coenzymes include reduced nicotinamide adenine dinucleotide (NADH), reduced nicotinamide adenine dinucleotide phosphate (NADPH) and adenosine triphosphate (ATP). These molecules transfer chemical groups between enzymes.[1]

Inhibitors are molecules that decrease enzyme activity; activators are molecules that increase activity. Activity is also affected by temperature, chemical environment (*e.g.*, pH), and the concentration of substrate.

1.4 Nomenclature for enzymes

An enzyme's name is often derived from its substrate or the chemical reaction it catalyzes, with the word ending in ***-ase***. The International Union of Biochemistry and Molecular Biology have developed a nomenclature for an enzyme as described in Table 1.1.

Table 1.1 Nomenclature for enzymes

No	Class	Type of reaction catalyzed
1	Oxidoreductases	Transfer of electrons (hydride ions or H atoms)
2	Transferases	Group transfer reactions
3	Hydrolases	Hydrolysis reactions (transfer of functional groups to water)
4	Lyases	Addition of groups to double bonds, or formation of double bonds by removal of groups
5	Isomerases	Transfer of groups within molecules to yield isomeric forms
6	Ligases	Formation of C–C, C–S, C–O, and C–N bonds by condensation reactions coupled to ATP cleavage

1.5 Thermodynamics and Mechanisms

As all catalysts, enzymes do not alter the position of the chemical equilibrium of the reaction. Usually, in the presence of an enzyme, the reaction runs in the same direction as it would without the enzyme, just more quickly. However, in the absence of the enzyme, other possible uncatalyzed, "spontaneous" reactions might lead to different products, because in those conditions this different product is formed faster.

Enzymes can act in several ways, all of which lower $\Delta G^{\ddagger}$ shown in Fig. 2.

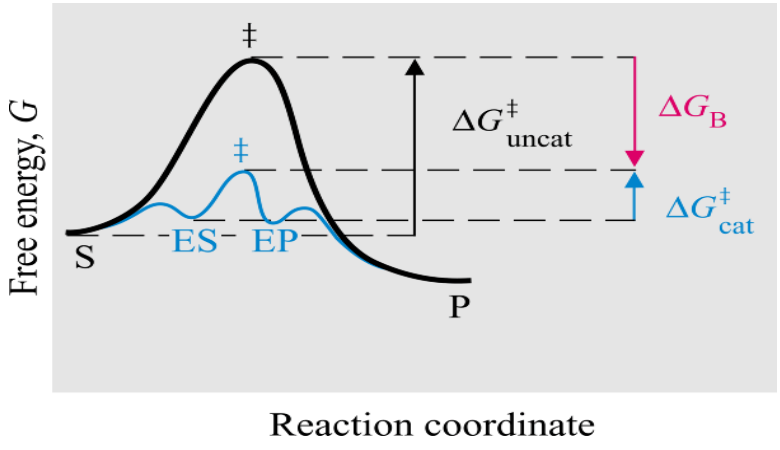

Fig. 2.2. The effect of substrate concentration on reaction velocity

The catalysed reaction pathway goes through the three transition states, with standard free energy of activation $\Delta G_{cat}^{\ddagger}$, whereas the uncatalysed reaction goes through one transition state with standard free energy of activation $\Delta G_{uncat}^{\ddagger}$. In this example the rate limiting step would be the conversion of ES into EP. Reactions involving several substrates and products, or more intermediates, are even more complicated.

The Michaelis-Menten reaction would give a similar profile but without the EP-complex free energy trough. The schematic profile for the uncatalysed reaction is shown as the black line. It should be noted that the catalytic effect only concerns the lowering of the standard free energy of activation from $\Delta G_{uncat}^{\ddagger}$ to $\Delta G_{cat}^{\ddagger}$ and has no effect on the overall free energy change (i.e. the difference between the initial and final states) or the related equilibrium constant.

1.5.1. Transition State Stabilization and dynamics

The most effective way for reaching large stabilization is the use of electrostatic effects, in particular, by having a relatively fixed polar environment that is oriented toward the charge distribution of the transition state.[12]

The internal dynamics of enzymes is connected to their mechanism of catalysis.[13-14] Internal dynamics are the movement of parts of the enzyme's structure, such as individual amino acid residues, a group of amino acids, or even an entire protein domain. These movements occur at various time-scales ranging from femto seconds to seconds. Networks of protein residues throughout an enzyme's structure can contribute to catalysis through dynamic motions.[15-17]

1.5.2. Lock and key model

Enzymes are very specific, and it was suggested by Emil Fischer in 1894 that this was because both the enzyme and the substrate possess specific complementary geometric shapes that fit exactly into one another.[18] This is often referred to as "the lock and key" model. However, while this model explains enzyme specificity, it fails to explain the stabilization of the transition state that enzymes achieve. The "lock and key" model has proven inaccurate, and the induced fit model is the most currently accepted enzyme-substrate-coenzyme.

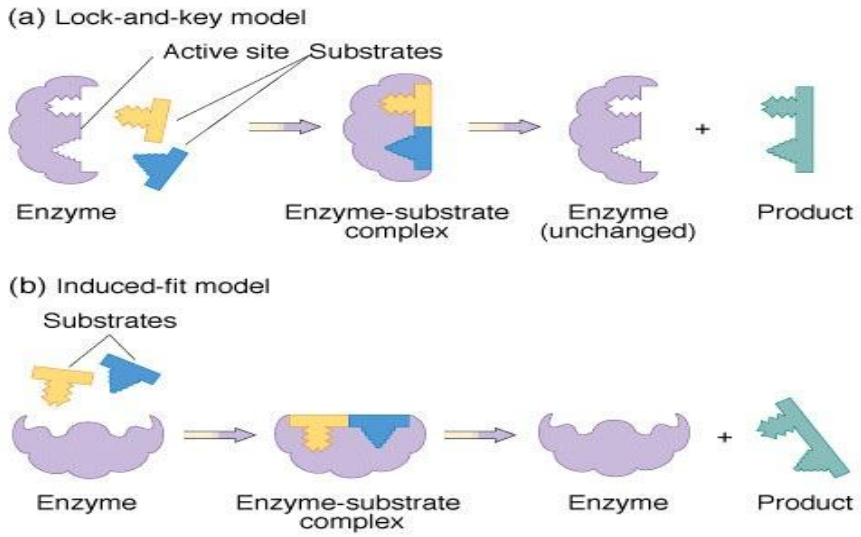

Fig. 1.3 Lock-and-key and induced fit hypothesis of enzyme action

1.5.3. Induced fit model

In 1958, Daniel Koshland suggested a modification to the lock and key model: since enzymes are rather flexible structures, the active site is continually reshaped by interactions with the substrate as the substrate interacts with the enzyme.[19] As a result, the substrate does not simply bind to a rigid active site; the amino acid side

chains which make up the active site are molded into the precise positions that enable the enzyme to perform its catalytic function. The active site continues to change until the substrate is completely bound, at which point the final shape and charge is determined.[20]

1.6. Enzyme Kinetics

The rate of reaction will increase as substrate concentration increases, eventually becoming saturated at very high concentrations of substrate (Fig.1.4). The effect of substrate concentration on reaction velocity is showed in Fig. 1.5. With the substrate concentration increase, the reaction rate increases a lot and shows as a first-ordered reaction at the very beginning. When every enzyme molecule is occupied by substrate, that is, enzyme molecules are saturated; the reaction rate gets close to a constant, that is, the maximum reaction rate. At this point, it goes to zero-ordered reaction.

Fig.1.4 The concentration of substrate and enzyme molecules

Enzyme kinetics is the investigation of how enzymes bind substrates and turn them into products. The rate data used in kinetic analyses are obtained from enzyme assays.

In 1902 Victor Henri[21] proposed a quantitative theory of enzyme kinetics, but his experimental data were not useful because the significance of the hydrogen ion concentration was not yet appreciated. After Peter Lauritz Sørensen had defined the logarithmic pH-scale and introduced the concept of buffering in 1909[22] the German chemist Leonor Michaelis and his Canadian postdoc Maud Leonora Menten repeated Henri's experiments and confirmed his equation which is referred to as Henri-Michaelis-Menten kinetics (sometimes also Michaelis-Menten kinetics).[23] Their work was further developed by G. E. Briggs and J. B. S. Haldane, who derived kinetic equations that are still widely used today.[24]

1.6.1 Michaelis–Menten kinetics

As enzyme-catalysed reactions are saturable, their rate of catalysis does not show a linear response to increasing substrate. If the initial rate of the reaction is measured over a range of substrate concentrations (denoted as [S]), the reaction rate (v) increases as [S] increases, as shown on the left. However, as [S] gets higher, the enzyme becomes saturated with substrate and the rate reaches V_{max}, the enzyme's maximum rate.

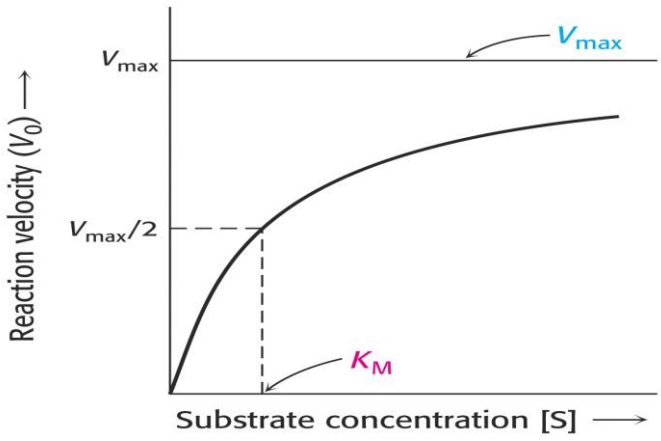

Fig. 1.5. Relation between the concentration of substrate and rate of reaction

The Michaelis-Menten kinetic model of a single-substrate reaction is shown on the right. There is an initial bimolecular reaction between the enzyme E and substrate S to form the enzyme–substrate complex ES.

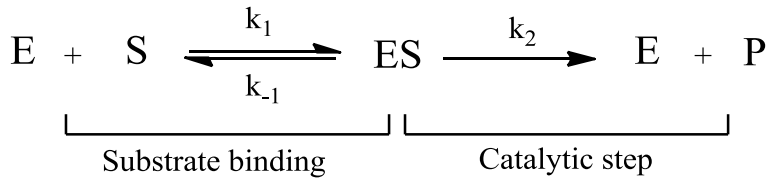

k_1, k_{-1} and k_2 are the rate constants for the individual steps. Although the enzymatic mechanism for the unimolecular reaction reaction can be quite complex, there is typically one rate-determining enzymatic step that allows the mechanism to be modeled as a single kinetic step of rate constant k_2.

$$\upsilon = k_2 [ES] \text{-------(1).}$$

k_2 is also called k_{cat} or the *turnover number*, the maximum number of enzymatic reactions catalyzed per second.

At low concentrations of substrate [S], the enzyme exists in an equilibrium between both the free form E and the enzyme–substrate complex ES; increasing [S] like wises increases [ES] at the expense of [E], shifting the binding equilibrium to the right. Since the rate of the reaction depends on the concentration [ES], the rate is sensitive to small changes in [S]. However, at very high [S], the enzyme is entirely saturated with substrate, and exists only in the ES form. Under these conditions, the rate ($v \approx k_2[E]_{tot} = V_{max}$) is insensitive to small changes in [S]; here, $[E]_{tot}$ is the total enzyme concentration

$$[E]_{tot} = [E] + [ES] \text{.....(2)}$$

which is approximately equal to the concentration [ES] under saturating conditions.

The Michaelis–Menten equation[23] describes how the reaction rate *v* depends on the position of the substrate-binding equilibrium and the rate constant k_2. Michaelis and Menten showed when k_2 is much less than k_{-1} (the equilibrium approximation) they could derive the following equation:

The Michaelis–Menten equation still holds under these more general conditions, as may be derived from the steady-state approximation. During the initial-rate period, the reaction rate *v* is roughly constant, indicating that [ES] is similarly constant.

$$\frac{d}{dt}[ES] = k_1[E][S] - k_2[ES] - k_{-1}[ES] \approx 0$$

Therefore, the concentration [ES] is given by the formula

$$[ES] \approx \frac{[E]_{tot}[S]}{[S] + K_m} \quad \text{.....(3)}$$

where the Michaelis constant K_m is defined

$$K_m \stackrel{\text{def}}{=} \frac{k_2 + k_{-1}}{k_1} \approx \frac{[E][S]}{[ES]} \quad \text{.....(4)}$$

([E] is the concentration of free enzyme). Taken together, the general formula for the reaction rate *v* is again the Michaelis-Menten equation:

$$v = k_2[ES] = \frac{k_2[E]_{tot}[S]}{[S] + K_m} = \frac{V_{max}[S]}{[S] + K_m} \qquad \boxed{v = \frac{V_{max}[S]}{K_m + [S]}}$$

This is the Michaelis- Menten equation. υ is the reaction rate. Commonly, researchers use initial velocity to express reaction rate here. As the definition of K_m (so-called Michaelis-Menten constant) showed, we can easily figure out that K_m shows the

affinity of enzyme to the substrate. The larger K_m is, the lower affinity to substrate the enzyme has V_{max} is the maximum velocity enzyme can achieve.

1.6.2. Linear plots of the Michaelis-Menten equation

Using an interactive Michaelis–Menten kinetics tutorial at the University of Virginia, USA (www.virginia.edu) the effects on the behaviour of an enzyme of varying kinetic constants can be explored.

The plot of *v* versus [S] above is not linear; although initially linear at low [S], it bends over to saturate at high [S]. Before the modern era of nonlinear curve-fitting on computers, this nonlinearity could make it difficult to estimate K_m and V_{max} accurately. Therefore, several researchers developed linearizations of the Michaelis-Menten equation, such as the Lineweaver-Burk plot and the Eadie-Hofstee diagram.

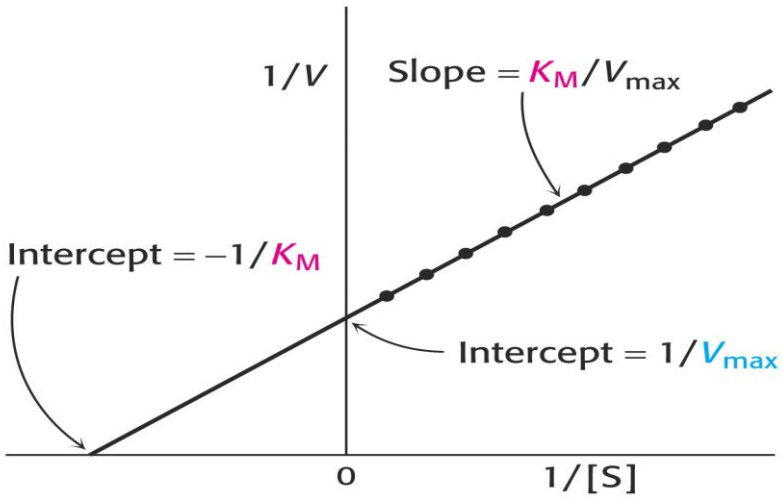

Fig. 1.6 Lineweaver–Burk plot of kinetic data

The Lineweaver-Burk plot or double reciprocal plot is common way of illustrating kinetic data. This is produced by taking the reciprocal of both sides of the Michaelis–Menten equation. As shown on the right, this is a linear form of the

Michaelis–Menten equation and produces a straight line with the equation $y = mx + c$ with a *y*-intercept equivalent to $1/V_{max}$ and an *x*-intercept of the graph representing $-1/K_m$.

$$\frac{1}{v} = \frac{K_m}{V_{max}[\mathrm{S}]} + \frac{1}{V_{max}}$$

Naturally, no experimental values can be taken at negative 1/[S]; the lower limiting value 1/[S] = 0 (the *y*-intercept) corresponds to an infinite substrate concentration, where $1/v=1/V_{max}$ as shown at the right; thus, the *x*-intercept is an extrapolation of the experimental data taken at positive concentrations. More generally, the Lineweaver-Burk plot skews the importance of measurements taken at low substrate concentrations and, thus, can yield inaccurate estimates of V_{max} and K_m.[23] A more accurate linear plotting method is the Eadie-Hofstee plot although, in modern research, all such linearizations have been superseded by more reliable nonlinear regression methods.

1.7 Enzymes applications and needs

During the last three decades, enzymology and enzyme technology have progressed considerably and, as a result, there are many examples of industrial applications where enzymes, in the native or immobilized form, are being used. These include food industry, materials processing, textiles, detergents, biochemical and chemical industries, biotechnology, and pharmaceutical uses.[93]

Table 1.2. Biochemical function of enzymes in living systems

Enzyme	Tissue	Application	Related Disease
Alcohol dehydrogenase	Liver	Facilitate the inter conversion between alcohol and aldehyde or ketones with the reduction of NAD^+ to NADH.[25]	Hepatitis B[26]
L-lactate dehydrogenase	Blood serum, heart	Inter conversion of pyruvate and lactate with inter conversion of NADH and NAD^+.[27]	Cardiovascu-lar Diseases [28]
Malate dehydrogenase	Liver	Conversion of malate into oxaloacetate (using NAD^+) and vice versa.[29]	Kidney Failure[30]
Inosine monophosphate dehydrogenase	Lymphocyte, Lymphoblast	Inosine monophosphate dehydrogenate to xanthosine monophosphate in presence of NAD^+ and H_2O.[31]	
D-proline reductase (dithiol)	Fibroblast	D-proline synthesis from 5-aminopentanoate and lipoate.[32]	Hepatitis B [33]
Cytochrome-b5 reductase	Liver	Converts methemoglobin to haemoglobin in presence of NADH.[34]	
11beta-hydroxysteroid dehydrogenase	Brain, Liver, Neocortex	Reduces cortisone to the active hormone cortisol that activates glucocorticoid receptors.[35]	Late pregnancy [36]
Luciferase		Light is produced by oxidation of a luciferin in presence of O_2.[37]	
Dihydrofolate reductase	WIL-2 cell	Reduces dihydrofolic acid to tetrahydrofolic acid using NADPH as electron donor.[38]	Chagas Disease [39]
3-oxoacyl-[acyl-carrier-protein] reductase	Flower, seed	Converts (3R)-3-hydroxyacyl-[acyl-carrier-protein] into 3-oxoacyl-[acyl-carrier-protein] in presence of $NADP^+$.[40]	Tuberculosis [41]
Cholesterol oxidase	Liver	Converts cholesterol into cholest-4-en-3-one in presence of O_2.[42]	
Aldehyde reductase	Kidney, Liver	Converts glucose into sorbitol in presence of NADPH.[43]	Kidney Failure [44]
Hydroxymethyl glutaryl-CoA reductase (NADPH	Keratinocyte	Converts (R)-mevalonate, CoA into (S)-3-hydroxy-3-methylglutaryl-CoA in presence of $NADP^+$. [45]	Hypercholest erolemia [46]

Enzyme	Tissue	Application	Related Disease
Catalase	Blood	Catalyse the decomposition of H_2O_2 into H_2O and O_2.[47-48]	
Pyrroline-5-carboxylate reductase	SW-620 cell, RKO cell	Converts L-Proline into L-pyrroline-5-carboxylate in presence of NAD^+ and $NADP^+$.[49]	Meningitis [50]
Succinate dehydrogenase (ubiquinone)	Kidney, Liver	Catalyses the oxidation of succinate to fumarate with the reduction of ubiquinone to ubiquinol.[51]	Hyper-glycemia [52]
Butyryl-CoA dehydrogenase	Amygdale, Brain, Cerebral cortex	Converts butanoyl-CoA into 2-butenoyl-CoA in presence of $NADP^+$.[53]	Axonal neuropathy [54]
3-oxo-5alpha-steroid 4-dehydrogenase	Semen	Converts testosterone, the male sex hormone into the more potent dihydro testosterone.[55]	Testicular dysfunction [56]
Glutaryl-CoA dehydrogenase	Colorectal cancer cell, Intestinal epithelium	Alters the expression level of glutaryl in colorectal cancer cell.[57]	Neurodegene-rative Diseases [58]
Glucose oxidase	Blood	Catalyses the oxidation of glucose to H_2O_2 and D-glucono-δ-lactone.[59-60]	
D-amino-acid oxidase	Kidney, liver	Oxidize D-amino acids to the corresponding imino acids, producing NH_3 and H_2O_2.[61]	Glycosuria [62]
Protopor-phyrinogen oxidase	Liver	Removes hydrogen atoms from protoporphyrinogen IX.	Porphyria [63]
Amine oxidase (copper-containing)	Plasma	Primary amines converted into aldehyde in presence of H_2O and O_2.[64]	Asthma [65]
Protein-lysine 6-oxidase	Skin	Catalyses formation of aldehydes from lysine residues in collagen and elastin.[66]	Alzheimer's Disease [67]
Thiopurine S-methyl transferase	Erythrocyte	Converts S-adenosyl-L-methionine into S-adenosyl-L-homocysteine. [68]	Hepatitis [69]
L-Serine ammonia lyase		Catalyse the production of pyruvate from L-serine with liberation of NH_3.[70-71]	

Enzyme	Tissue	Application	Related Disease
Protein-L-isoaspartate(D-aspartate) O-methyl-transferase	Erythrocyte, Blood, Brain	Catalyses the transfer of a methyl group from S-adenosyl-L-methionine to the free carboxyl groups of D-aspartyl and L-isoaspartyl residues.[72]	Spinal Dysraphism [73]
D-glutamyl transferase	Blood serum	Produces 5-glutamyl-D-glutamyl-peptide from D-glutamine and D-glutamyl-peptide with elimination of NH_3.[74]	Heart Failure [75]
Alanine-glyoxylate transaminase	Kidney	Produces pyruvate and glycine from L-alanine.[76]	Kidney Failure [77]
Ethanolamine kinase	Lens	Converts ethanolamine into phosphoethanolamine in presence of ATP by transferring phosphorus containing group.[78]	Fetal Death [79]
DNA-directed DNA polymerase	Placenta	Polymerization of new DNA or RNA against an existing DNA or RNA template in the processes of replication and transcription.	DNA damage [80]
Acylglycerol lipase	Brain	Catalyses to break the glycerol monoesters into long chain fatty acids using water.[81]	Head ache [82]
Aminoacyl-tRNA hydrolase	Erythroblast	Converts N-substituted aminoacyl-tRNA into N-substituted amino acid and tRNA using H_2O.[83]	Tuberculosis [84]
Fructose-bisphosphatase	Kidney, Liver	Converts frunctose-1,6-bisphosphate to fructose 6-phsphate in gluconeogenesis.[85]	Diabetes Mellitus [86]
Sphingomyelin phosphodi-esterase	Brain, Blood	Breaks sphingomyelin (SM) into phosphocholine and ceramide.[87]	Alzheimer Disease [88]
Calf thymus ribonuclease H	T24 cell, Placenta	Cleaves the 3'-O-P bond of RNA in a DNA/RNA duplex to produce 3'-hydroxyl and 5'-phosphate terminated products.[89]	Chromosome Breakage [90]
Ribonuclease P	Embryo, Liver	Cleave off an extra, or precursor, sequence of RNA on tRNA molecules.[91]	Autoimmune Diseases [92]

The use of enzymes in medical applications has been less extensive as those for other types of industrial applications. For example, pancreatic enzymes have been in use since the nineteenth century for the treatment of digestive disorders. At present, the most successful applications of enzymes in medicine are extracellular, such as topical uses, removal of toxic substances, and the treatment of life-threatening disorders within the blood circulation.[101] The some of the biochemical function of enzymes in living system are given Table 1.2, thus the proteins are responsible for most of the functions in the living cell.

The production of therapeutic enzymes has progressed, but the costs of enzyme production, isolation, and purification are still too high to make them available for clinical applications. Furthermore, the ability to store unstable enzymes for long periods of time is also a limitation for their more widespread use. Most applications in the biomedical field are still in the state of basic studies rather than definite applications, owing to the absence of the necessary information on toxicology, hemolysis, allergenicity, immunological reactions, and chemical stability of the system in vivo.[101-102]

Immobilized enzymes are already being used in medical applications for clinical diagnosis and also for intra- and extracorporeal enzyme therapy. Applications in clinical analysis are mainly related to biosensors, which have been used to detect the presence of various organic compounds for many years. For example, glucose oxidase and catalase have been used to measure blood glucose concentration, and cholesterol oxidase and cholesterol esterase to determine cholesterol levels. In addition, enzymes can be immobilized on different prosthetic devices or used

extracorporeally (e.g., artificial heart, artificial lung, artificial kidney, equipment for hemodialysis and specific blood purification) as surface modifiers in order to increase the biocompatibility of these devices and to prevent blood clotting.[101]

The overall impact of enzymes on industrial and medical applications is, still quite limited due to their relative instability under operational conditions, which may involve high temperatures, organic solvents, and exposure to other denaturants. Various approaches, including, among others, addition of additives,[94-95] chemical modification, [96-97] protein engineering, [98] and enzyme immobilization, [93,99] have been assessed for their ability to increase the stability of enzymes toward pH, heat, denaturants and repetitive use of single batch. [99-100]

1.8 Immobilization of enzymes

By definition, enzyme immobilization is the technique for restriction of an enzyme artificially with retention of catalytic function. Immobilization often stabilizes structure of the enzymes, thereby allowing their applications even under harsh environmental conditions. The use of a relatively expensive catalyst as an enzyme requires, in many instances, its recovery and reuse to make an economically feasible process. Moreover, the use of an immobilized enzyme permits to greatly simplify the design of the reactor and the control of the reaction.[103-104] The simple filtering of the enzyme stops the reaction; it is possible to use any kind of reactor, etc. Thus, immobilization is usually a requirement to the use of an enzyme as an industrial biocatalyst, and is the simplest solution to the solubility problem of these interesting biocatalysts.

However, the idea of enzyme reuse implicitly means that the stability of the final enzyme preparation should be high enough to permit this reuse. Therefore, the enzyme needs to be very stable or to become highly stabilized during the immobilization process to be a suitable process. Thus, although there are hundreds of immobilization protocols,[105-106] the design of new protocols that may permit to improve the enzyme properties during immobilization is still a exciting goal.

Moreover, bearing in mind that the final use will be as industrial catalyst, the ideal immobilization processes should limit the use of toxic or highly unstable reagents, be very simple, robust, etc.

1.9 Selection of suitable immobilization conditions

Although some of the immobilization methods may be expected using a correct support activated with a proper group, the selection of suitable immobilization conditions is critical to maximize the multipoint attachment of enzyme with support. Immobilization conditions should favour the enzyme–support reaction.[107-108]

Some of these critical variables are:

• *Reaction time*. Although immobilization may be very rapid, multipoint interaction between the non-complementary enzyme and support surfaces is a slow and time-dependent process: it requires the correct alignment of groups located in the already immobilized, and partially rigidified enzyme, and the rigid surface of the support.

• *pH value*. Although immobilization may be performed at neutral pH value in many cases, incubation at alkaline pH values, where the reactivity of the nucleophiles of the protein (usually Lys) may be improved, is convenient to reach a high enzyme–support reaction. It should be kept in mind that while terminal amino groups may have a p*K* between 7 and 8, exposed Lys groups will present a p*K* over 10.5.

• *Temperature*. Moderately high temperature may favour the vibration of enzyme and support, increasing the possibilities of getting more enzyme–support linkages.

• *Buffers*. It should be chosen buffers that do not interfere in the reaction. For example borate may interfere in the aldehyde–amine reaction; amino compounds (Tris, ethanol amine) may modify epoxy supports or compete with the Lys by aldehyde groups.[107]

• *Inhibitors or other protein protectors*. Multipoint immobilization, or the immobilization conditions, may reduce the enzyme activity. The presence of inhibitors and other compounds may reduce this lost in activity.[107]

1.10. Selection of proper immobilization supports

Immobilization of enzymes involves certain costs associated with the cost of materials (e.g. polymer matrix, cross-linkers) and processing time. The two major driving concerns in an industrial scale process are to lower the unit cost and to increase the unit production per fixed time. Immobilization becomes economically feasible only if it allows the repetitive use of enzyme in multiple batches to reduce the unit production cost. Further, immobilized-enzyme beads can be packed into a bed or a column for continuous flow-through reactions, if applicable, to reduce costs

associated with otherwise labour intensive processes. Such a reactor also simplifies the separation of enzyme from product: alleviating some down-stream processing costs.

The appropriate immobilization matrix is chosen based on several different properties which affect the production process (Tischer and Wedekind 1999):

- **Surface area and porosity**: It is desirable to have materials with high surface areas (> 100 m^2/g), for high enzyme loadings, and high porosity to provide enzyme access for the substrate. Pore sizes >30 nm are ideal for the diffusion of enzymes during the immobilization process.
- **Surface functional groups**: The degree of enzyme loading onto a carrier matrix also depends on the loading density of functional groups on the surface and its distribution. Choice of functional groups also affects the activity yield and material stability.
- **Mechanical and chemical stability**: Many immobilized enzyme operations are conducted as a stirred-tank or packed-bed reactor. To prevent enzyme loss, the matrix integrity must be maintained under the shear-stresses or back-pressures present in these reactors. In addition the matrix must be resistant to chemical degradations which will also result in the loss of enzyme.
- **Size and shape**: To simplify handling of the immobilized enzyme (i.e. stirring, filtration) it is ideal to have particles of uniform shape and size. For this reason, the use of a uniform spherical matrix is preferred and also results in the reduction of back-pressures in column reactors. In addition, spherical particles are also more easily characterized for modeling purposes.

- **Microbial resistance**: A major concern of any immobilized enzyme process is the presence of microbes. The durability of the carrier is often determined by its resistance to microbial degradation.
- **Hydrophobic/hydrophilic nature**: The compatibility of the support with the liquid phase is important to insure the free exchange of substrate and product between the matrix and bulk phase. It can also determine the life-time of the matrix due to the surface adsorption of materials through non-specific interactions.

Immobilization allows the enzyme to be used in a continuous-flow mode which provides several benefits: 1) continuous removal of products from the reactor, which can be beneficial for systems that suffer from product inhibition; 2) product separation through column retention, reducing the burdens for downstream purification by affinity columns; and 3) increased enzyme stability will allow the enzyme to maintain activity for longer periods of use and in more extreme conditions.

Among the immobilization protocols described in literature, there are some that may fulfil most of these requirements. Supports like agarose beads, zeolites, porous glass, epoxy resins like Sepabeads, offer large areas for enzyme–support interactions.

Among the reactive groups, epoxy or glyoxyl groups may be considered very adequate.[107,109] Glyoxyl agarose has the additional advantage that directs the immobilization via the richest area(s) in reactive residues of the protein, enabling intense multipoint enzyme–support reaction.[110-111]

Glutaraldehyde chemistry is other popular technique to immobilize enzymes. It has given some good stabilization factors in many instances.[112-114] The glutaraldehyde technique is very versatile and may be used in very different fashions.[115-117]

However, in terms of stabilization, the treatment with glutaraldehyde of proteins previously adsorbed in supports bearing primary amino groups offers in many cases very good results, because permit the crosslink between glutaraldehyde molecules bound to the enzyme and glutaraldehyde molecules bound to the support. However, it implies the chemical modification of the whole enzyme surface.[118]

1.11. Operational stabilization of enzymes by immobilization on porous supports

Immobilization of enzymes in porous support will permit majority of the enzymes inside the pores. Very few molecules are located on the external surface of the support. Thus, the enzyme molecules fully dispersed and restrict the possibility of interacting with any external surface molecule interaction. Moreover, the immobilized enzyme molecules will not be in contact with any external hydrophobic interface, such as air bubbles (Fig. 1.7) originated by supplying some required gases or promoted by strong stirring, necessary to control pH. These gas bubbles may produce enzyme inactivation of soluble proteins,[119-122] but cannot inactivate the enzymes immobilized on a porous solid [123-124]

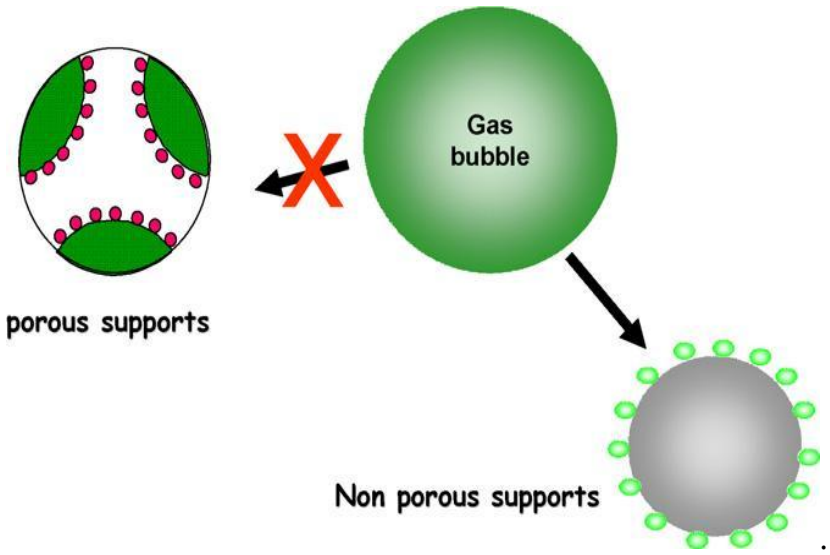

Fig. 1.7 Effect of the type of support on the immobilized enzyme stability against inactivation by gas bubbles

In the presence of an organic solvent phase, the enzymes may be in contact with the solvent molecules. In general enzymes are soluble in the aqueous phase, but not with the organic phase interface, which could inactivate the enzyme. Thus, any immobilization protocol of an enzyme which yields the enzyme immobilized inside a porous solid as the final product may permit an "operational stabilization" of the enzyme, even without really affecting the structural stability of the enzyme, simply by the mechanisms described above.

However, this stabilization is not only associated to the porous support, the increasingly popular use of non-porous nano-particles (mainly magnetic nano-particles) to immobilize enzymes.[125-127] These supports needs to consider that all the mechanisms of enzyme stabilization described above (section 1.10) are lost in this case. Enzymes immobilized on nano-particles are now able to interact with external interfaces, or even with enzyme molecules immobilized on other particles.[128]

1.12 The features of ordered mesoporous silica (MPS)

One unique advantage of ordered mesoporous solids over disordered, high surface area silicas, such as those prepared by sol–gel or aerosol methods, is that as well as having a narrow pore size distribution, the geometry and connectivity of their pores is very well defined. Transmission electron micrographs of the structures (Fig. 1.8 a–d) not only reveal these features with great clarity, they can also inspire and help the chemists design the optimum mesoporous molecular sieve for a given application. In that sense, the ordered mesoporous silicas act as ideal 'model systems'.

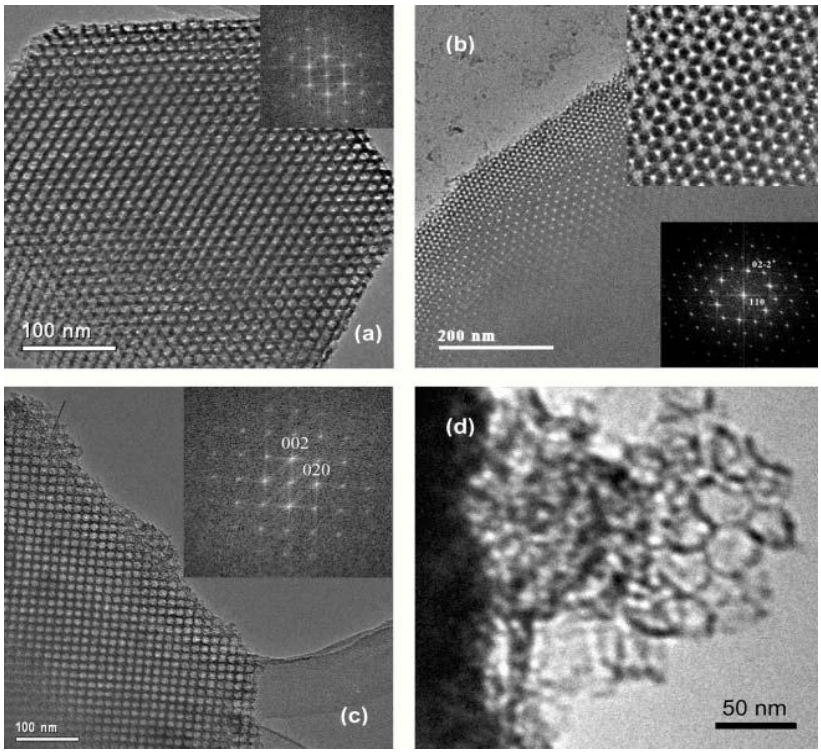

Fig.1.8 TEM micrograms of (a) SBA-15, (b) FDU-5, (c) FDU-12 and (d) MCF

Among the ordered mesoporous silicas of interest for the adsorption and immobilization of enzymes, only those wider than several nanometres at their narrowest point are of interest for all but the smallest enzymes. This narrows the

candidates down to those in Table 1.3, which are of two types, those with pores of uniform diameter and those with cage-like structure, in which large cages are connected via restrictions. The former include silicas with the two dimensional hexagonal p6mm structure (MCM-41, SBA-15)[129] and the bicontinuous cubic Ia3d structure (FDU-5).[130] The second type include the three dimensional Fm3m, face centred cubic structure (FDU-12)[131] and the body centred Im3m structure (SBA-16).[132-133] Careful manipulation of the synthetic conditions for the cage-like structures is required to ensure the restrictions can allow biomolecules larger than 5 nm full access to their internal volumes. The size of these restrictions can be estimated from the desorption branches of the N_2 adsorption isotherms, which show marked hysteresis.[134]

Table 1.3 Structural characteristics of mesoporous materials employed for enzyme immobilization

Porous material	Derivation	Typical template used	Pore Size/nm	BET surface (m^2g^{-1})
MCM-41	Mobile composite material No.41	CTAB; C_nTMA^+ (n = 14–18); $C_{16\text{-}n\text{-}16}$ (n = 4,6,7,8,10)	2.5–12	300–1200
FSM-16	Folded sheet Material No.16	CTAB; C_nTMA^+ (n = 14–18); $C_{16\text{-}n\text{-}16}$ (n = 4,6,7,8,10)	3–9	500–900
SBA-15	Santa Barbara Amorphous Material No.15	P123 ($EO_{20}PO_{70}EO_{20}$)	5–20	500–1400
BA-16	Santa Barbara Amorphous Material No.16	F127 ($EO_{106}PO_{70}EO_{106}$)	3–15	600–1200
FDU-12	Fluorodeoxyuridine	F127 ($EO_{106}PO_{70}EO_{106}$) + TMB and KCl	10–15	200–700
MCF	Meso Cellular Foam	P123 ($EO_{20}PO_{70}EO_{20}$) + mesitylene	25–40	500–1000

Careful electron microscopic studies of precious metal casts of these mesoporous silicas indicate that the mesopores are connected via microporous channels.[135] While not assisting in the transport of the biomolecules themselves, these will facilitate diffusion of substrate and product molecules from the active sites of immobilized enzymes. Whether high internal loading of biomolecules can be achieved will depend on the nature of the adsorption. If the adsorption is reversible, then the pore size needs only to be greater than the molecular size. The same criterion applies if rapid, reversible adsorption is followed by slower, irreversible immobilization.

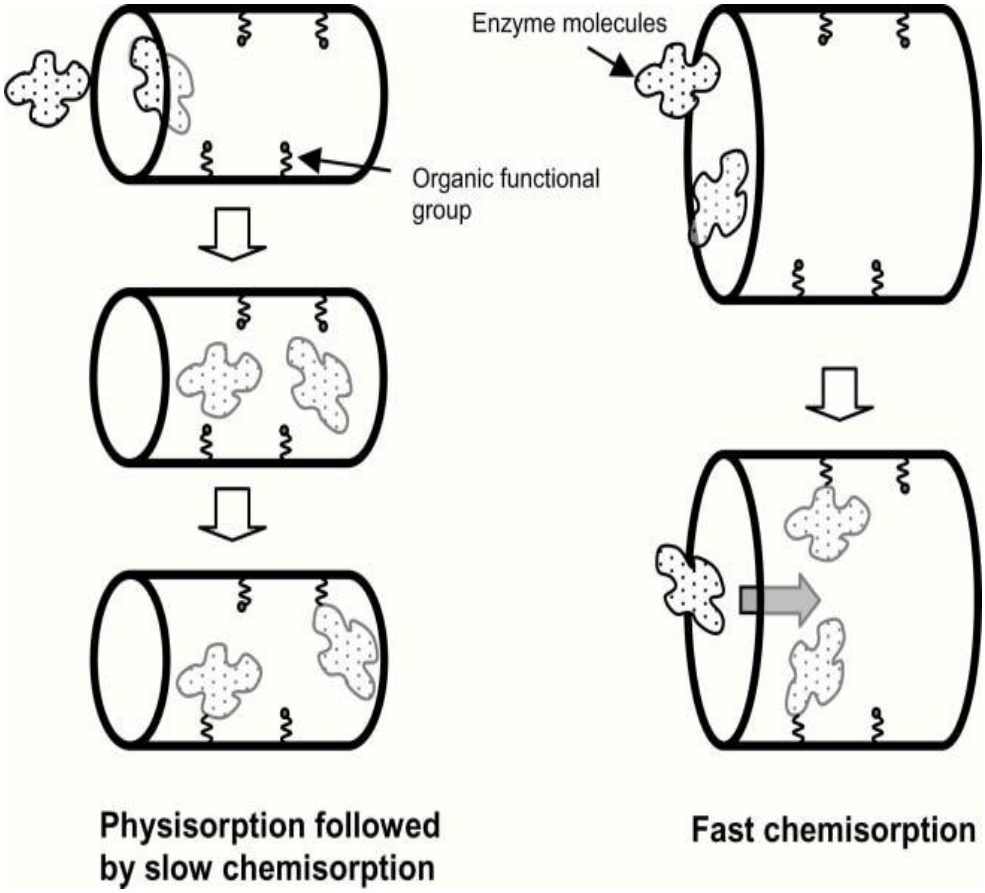

Fig. 1.9 Illustration showing two possible mechanism of protein binding onto the functionalized surface of mesoporous silica

However, if the irreversible immobilization is fast, the pore diameter must be at least three times the molecular diameter to enable full access to the internal pores (see Fig. 1.9). It is also possible to imagine an intermediate situation, in which the biomolecules are covalently bonded by tethers present at low concentration within the pores. It would be unlikely for two such tethering points to be present at any one position in the channels, so that a pore diameter of more than twice the biomolecular radius would be required in this case. In any cases where blocking could occur, the cubic structures with three-dimensional connectivity would possess an inherent advantage over one dimensional channel structures.

The pore size of the mesoporous silicas can be increased by a nanometre or so by the addition of swelling agents, such as 1,3,5-trimethylbenzene, that segregate to the hydrophobic pore of the templating micelles to enlarge them. Addition of higher concentrations of these molecules results in loss of long range order and the formation of mesocellular foams (Fig. 1.8d). While these can possess still larger pores, their irregularity renders characterization of their pore structure ambiguous, particularly in terms of the geometry of the inter pore restrictions.

The size selectivity of ordered mesoporous solids has been demonstrated clearly in several studies.[136] Also, the measured uptakes are clearly shown to be on the internal surfaces when the adsorption of the same species by porous solids in the as-prepared state, i.e. that still contain the template, are many times lower. Uptakes of 5–20 wt% of the biomolecules are commonly observed.[137-138]

1.13 Surface functionalization of MPS's

Silica-based materials are well suited to act as hosts for immobilization. They can be made in a wide variety of high surface area forms, some very well ordered, and they may be functionalized by a range of available organic linkers, that are suitable for immobilizing biomolecules. Reviews on methods for the functionalization of mesoporous silica materials with organic groups are widely available. Generally, organic–inorganic hybrid mesoporous molecular sieves can be prepared by two routes: (1) in situ functionalization during synthesis or (2) post-synthesis functionalization (see Fig. 1.10).

The former route involves the cocondensation of a functionalized and an unfunctionalized alkoxysilane (e.g. 3-aminopropyltriethoxysilane with tetraethoxysilane (tetraethylorthosilicate, TEOS)). The alkoxysilanes must hydrolyze at a similar rate to the tetraethoxysilane or a heterogeneous gel will form and the functional groups will not be evenly distributed. Once formed, the surfactant template of these materials has to be removed by solvent extraction and extraction is typically only ca. 80% successful, probably because residual block copolymer remains trapped in micropores within the silica walls. For in situ functionalized mesoporous molecular sieves, the percentage of functional groups is limited to ca. 20% and a loss of structural order usually occurs with high functional group contents as the number of Si–O– bonds available for linkage is reduced. In some cases, the addition of a functionalized alkoxysilane alters the structure type of the silica that forms.

The post-synthetic route involves a reaction of the functionalized siloxane with a calcined mesoporous molecular sieve, suitably rehydrated to generate surface hydroxyl groups. Since all the template molecules have been removed during calcination before functionalization, there is no residual template in the hybrid mesoporous molecular sieve. However, it is more difficult to achieve uniform coverage by this route and the siloxane is likely to be attached to the surface by less than three Si–O–Si linkages. Fig. 1.10 shows preparation routes for post-synthesis functionalization of a mesoporous molecular sieve. The conditions for these reactions are widely available in the literature.[139-142]

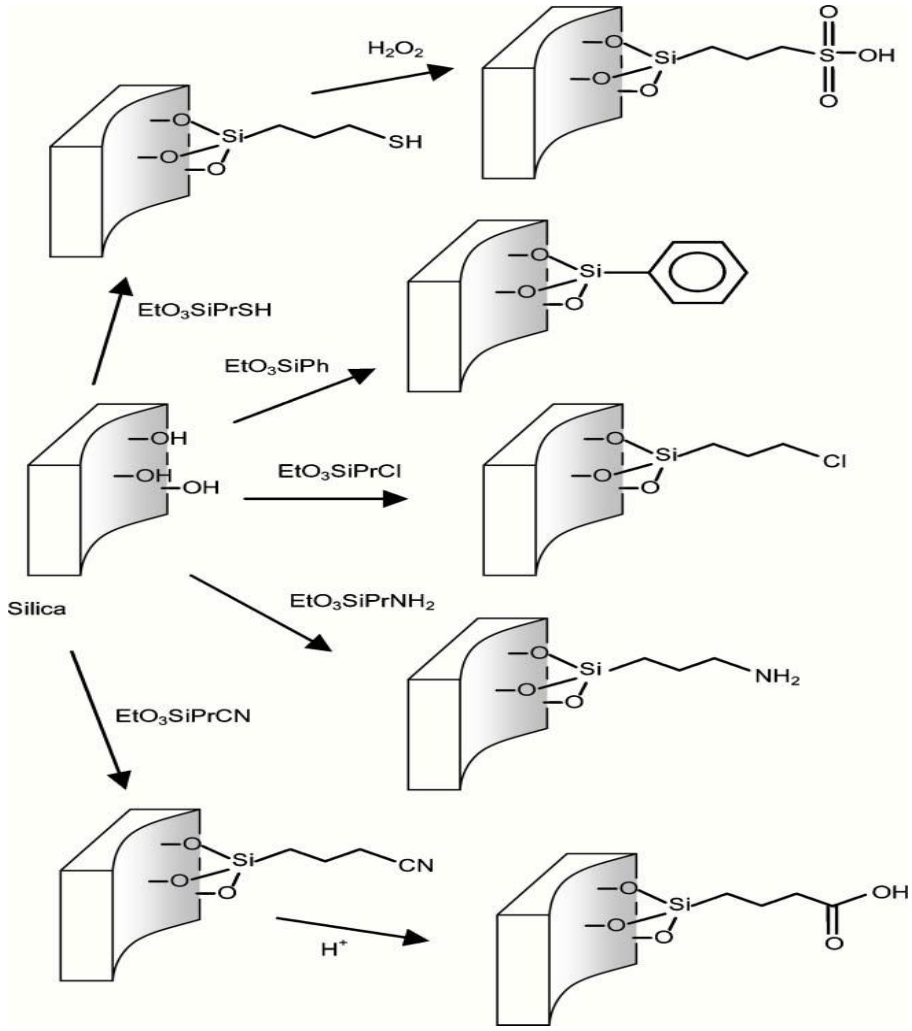

Fig. 1.10 Post-synthesis functionalization of silica's using organotriethoxysilanes

The inclusion of functional groups on silicas is, therefore, a well established procedure. Amine, thiol, carboxylate, chloride, alkyl, vinyl and phenyl are among the most commonly included groups, but the method is very generally applicable. As a result, the ability of a surface to interact by hydrogen bonds or van der Waals force, electrostatic or covalent bonds can be manipulated. For example, to enhance electrostatic interactions with negatively charged adsorbents, amine functionalization will introduce positive charge to the silica surface which would otherwise be positive. Han et al.[143] showed that the post-synthetic modification of SBA-15 using 3-aminopropyltriethoxysilane could be used to adsorb anionic proteins at pH 7 whereas a carboxy-functionalized surface, which would give a negative surface charge, readily adsorbed proteins that were cationic at the same pH. Subsequent modification of the electrostatic interaction, either by changing pH or strongly increasing the ionic strength, can result in release of the protein back into solution.

The inclusion of functional groups also opens up the possibility to tether molecules covalently. For proteins this can take the form of reactions with amine, carboxylic acid or disulfide bridges. Such immobilization procedures have been developed for protein immobilization[144] and examples of their use on high surface area silicas are described below.

In summary, in order to incorporate biomolecules into ordered mesoporous silica materials, a suitable channel size is required for internal adsorption. Moreover, the surface chemistry of the mesoporous solid also plays an important role in binding proteins as this will influence the strength of the interaction between the biomolecules and the internal surface of the ordered mesoporous silica. A charged surface can bind

proteins with opposite charge and release the adsorbants by changing the pH. For permanent binding, the formation of covalent bonds is the obvious choice.

1.14. Enzyme–mesoporous silica hybrid materials

The first report of mesoporous molecular sieves as carriers in enzyme immobilization was published in 1996 by Diaz and Balkus.[145] Since 1996, research in this area has developed rapidly. Within these studies, three main methods (physical adsorption, encapsulation and chemical binding) have been used to immobilize enzyme molecules inside the mesopores of the carriers as illustrated in Fig. 1.11 and Table 1.4. A number of studies have also appeared where the enzymes would seem to be far too large to be taken up within the mesopores, and must exist on the internal surface.[146] There have also been reports of the immobilization of whole cells on mesoporous particles, for which the same applies.[147] These are not discussed here.

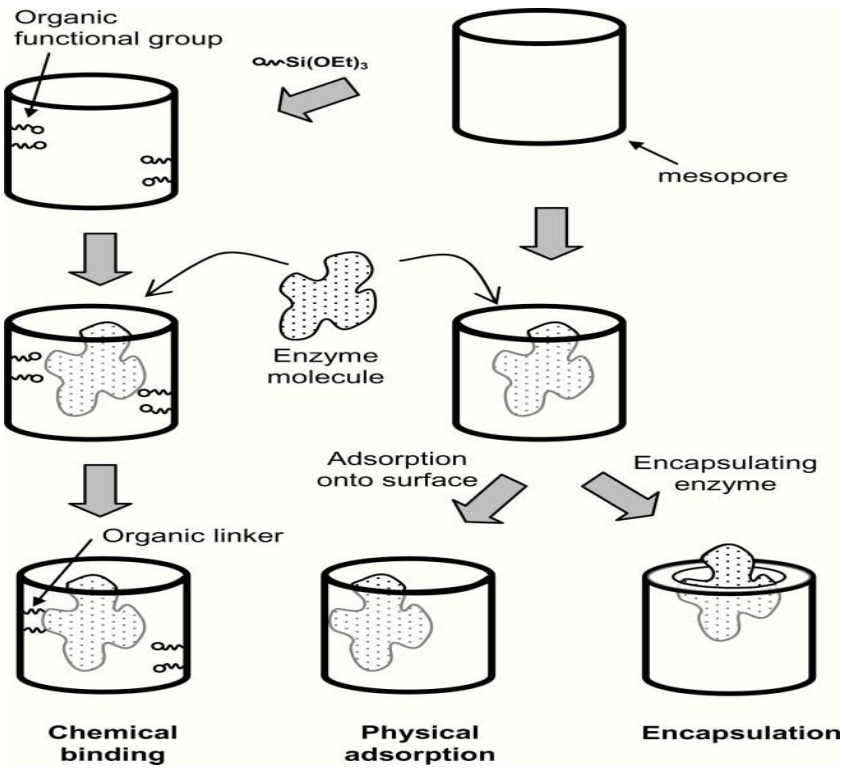

Fig.1.11 Strategies of three commonly used methods for enzyme immobilization

Table 1.4 Advantages and disadvantages of three immobilization methods: encapsulation, physical and chemical binding

Immobilization method	Advantage	Disadvantage
Encapsulation	Enzyme molecules retained Enzyme molecules free to move inside channels	Complicated experimental procedure Reactive species and toxic solvents may denature enzymes Reduced pore opening may decrease diffusion rate of reactants and products
Physical adsorption	Simple experimental procedure No toxic solvents	Leaching of enzymes during reaction
Chemical binding	No leaching of enzyme molecules Wide choice of organic linkers available	More complicated procedure No leaching of enzymes during reaction

1.15 Physisorption of enzyme onto pure silicas

Physical adsorption is the simplest method of immobilizing enzyme onto ordered mesoporous silicas. Since there is no further treatment, denaturation of the enzymes is avoided. In this method, the mesoporous silica is simply suspended in a buffered enzyme solution for about 24 h, and the composite is recovered by centrifugation.

Trypsin has been immobilized onto pure siliceous MCM-41, MCM-48 and SBA-15 and the effect of pore size on the activity studied.[148] The hydrolysis of N-α-benzoyl-DL-arginine-4-nitroanilide (BAPNA) was used as a model reaction, by monitoring the formation of p-nitroaniline spectrophotometrically. The activity of the immobilized enzyme was found to increase as the pore size increased probably due to the enhanced diffusion of the reactants and the products. However, leaching of enzymes is a major problem as the enzyme molecules are only loosely adsorbed onto the internal surface of the mesoporous silica carriers.

Most of these immobilized enzymes have been examined in aqueous medium. However, for applications in chemical industries, establishing their activity in non-aqueous media would be an important step forward for enzyme immobilization.[149] Additionally, once supported, the solubility of an enzyme in an organic solvent may be very low, and leaching is avoided in this way. An example of this is the immobilization of horseradish peroxidase (HRP). HRP has been used extensively in industry as an environmentally friendly catalyst for oxidation reactions with hydrogen peroxide as the most common oxidant.[150] The enzyme is of an appropriate size to adsorb within the pores of large pore mesoporous solids.

Takahashi et al. immobilized HRP onto FSM-16, MCM-41 and SBA-15 with different pore sizes and their activity was tested in an organic medium, using toluene as a solvent.[151-152] The HRP molecule has an oval shape with dimensions 3.7 nm x 4.3 nm x 6.4 nm which are commensurate with the mesopores of these carriers. FSM-16 and MCM-41 showed the highest maximum loadings (89 to 183 mg g^{-1}).[161] The activity of the immobilized HRP was monitored by the catalytic oxidation of 1,2-diaminobenzene in toluene at 37 °C with tert-butylhydroperoxide as the oxidant. HRP immobilized onto FSM-16 (pore size 5 nm) exhibited the highest activity, some ten times the activity of free HRP. The increase in activity was possibly due to the size of the mesopores which matches the dimensions of the HRP molecules. This was thought to prevent the HRP being exposed to environmental changes that arise when fully immersed in the organic medium. A simple test for the thermal stability of the immobilized HRP demonstrated that the thermal stability of the HRP was improved upon immobilization: the most active sample, HRP immobilized on FSM-16, showed a 20% loss in activity upon exposure to a buffer solution at 70 °C for 120 min while the free HRP showed a 60% loss in activity after 30 min.

Chen et al. reported the use of SBA-15 as a carrier for a crude lipase, Newlase F, which contains lipase and acid protease from Rhizopus niveus.[153] A simple adsorption method was employed in this research and the lipase activity was found to be up to four times that of the free enzyme with more than 90% of the lipase adsorbed onto the SBA-15. An increase in lipase activity upon immobilization is not uncommon, possibly because the hydrophilic surface of the carrier aids the adsorption of reactants.[154] Interestingly, in the same experiment, the protease activity of the supernatant was 80% of that of the free enzyme, and much more than that of the enzyme–SBA-15 composite. This indicates that the SBA-15 carrier selectively adsorbed lipase (4.9 nm x 4.9 nm x 4.6 nm) rather than acid protease (6.5 nm x 5.3 nm x 4.0 nm). Therefore, in this work, SBA-15 acted not only as a carrier for enzyme immobilization but also as the stationary phase for enzyme separation. There have also been several reports of the adsorption of electroactive enzymes within mesoporous solids, with the aim of preparing biosensors.

Dai et al. conducted electrochemical studies on hemoglobin[155] and myoglobin[156] immobilized onto HMS-silica. The enzyme–HMS composite materials were supported onto glassy carbon electrodes. The immobilized enzymes showed significant responses to the reduction of hydrogen peroxide and nitrite. There have also been efforts to prepare composites of redox enzymes with mesoporous metal oxides that could themselves show conductivity, such as titanium or niobium oxides, in order to improve the response. Initial results suggest that these also give reusable biosensors for H_2O_2.[157] The forces binding proteins to hydrated silica surfaces include electrostatic, hydrogen bonding and weak van der Waals interactions. Electrostatic protein–surface interactions are likely to be the strongest, particularly

when the adsorption is performed at a pH where the enzyme possesses a positive charge, because silica carries negative charges at pH values above 3.

Table 1.5 pI values of some proteins

Protein	pI value
Pepsin	1.0
Serum albumin (human)	4.0
Tropomyosin	5.1
Insulin (bovine)	5.4
Fibrinogen (human)	5.8
c-Globuline (human)	6.6
Collagen	6.6
Myoglobin (horse)	7.0
Hemoglobin (human)	7.1
Ribonuclease A (bovine)	7.8
Cytochrome c (horse)	10.6
Histone (bovine)	10.8
Lysozyme (hen)	11.0
Salmine (salmon)	12.1

The sign of the overall charge on a surface can readily be predicted on the basis of the isoelectric point (the pH at which the overall charge is zero). This pI value of an protein molecule depends on the balance of surface functional groups (e.g. $–NH_2$, –COOH) which may have opposite charges: pI values are given for selected proteins in Table 1.5.

When the adsorption is performed at a pH lower than the pI of the enzyme (but higher than pI of the silica) the protein will be positively charged. The greater the positive charge, the stronger the attraction between protein and surface, but the stronger the repulsion between adsorbed molecules. According to Su et al., surface

adsorption capacities of proteins are found to vary with the pH of adsorption according to a bell-curve, the maximum of which occurs at the isoelectric point of the protein.[158-159] It therefore follows that by judicious variation of the pH, proteins could be adsorbed selectively and desorbed by changing the pH. Measurements of physical adsorption on SBA-15 of proteins small enough to enter the channels, performed at pH 8.4, was found to obey a simple the Langmuir model, as expected where adsorption terminates at a monolayer and the adsorption sites are very similar.[160] Monolayer coverages of around 120 mg g^{-1}[161] were measured for myoglobin and β-lactoglobulin.

Vinu et al. carried out detailed adsorption experiments of the protein lysozyme on MCM-41 and SBA-15.[162] Lysozyme is a relatively small protein (molecular weight = 14.4 kDa, 3 nm x 3 nm x 4.5 nm) and can adsorb in both materials, but SBA-15 was found to have a higher capacity, indicating that the pores were large enough to allow two molecules to pack across a pore diameter. Detailed studies of the pH dependence of adsorption indicated that adsorption isotherms at pH 6.5 to 10.5 obey Langmuir dependence. As the pH is raised and the lysozyme becomes less positively charged (the isoelectric point is at pH 11) the monolayer coverage on both solids is observed to increase. This is attributed to reduced enzyme–enzyme repulsion and closer packing or even aggregation. Notably, at a higher pH (pH=12) the adsorption is no longer Langmuirian, and indicates that the enzyme–support interaction is no longer much stronger than the enzyme–enzyme interaction, due to the enzyme picking up negative charge. In related studies, the kinetics of the adsorption mechanism of peroxidase onto MCM-41 was modelled by rapid the Langmuir type physisorption followed by slow chemisorption.[163-164]

1.16 Encapsulation of enzyme molecules in MPS's

One way to prevent enzyme leaching from within mesoporous silicas is to physically encapsulate them inside the pore spaces. Several routes have been tried, including silanation or coating with microporous silicas produced via sol–gel routes. In the first publication of mesoporous molecular sieves in enzyme immobilization, the encapsulation method was applied to immobilize enzyme molecules such as trypsin inside the mesopores of pure siliceous MCM-41.[145] Fig. 1.11 shows a simplified scheme of this mechanism. In this method, the enzyme molecules were first dissolved in a buffer solution and MCM-41 was then suspended in the solution to permit uptake of the enzyme.

Finally the opening of the mesopores was reduced in size through silanation with the use of 3-aminopropyltriethoxysilane in order to prevent subsequent leaching out of the enzymes during reaction. After silanation, the diameter of the mesopore openings was reduced by about 1 nm. Although this process stopped the leaching, it also strongly reduced the activity of the immobilized enzyme, probably due to denaturing of trypsin during silanation and reduction in the accessibility of the substrate to the active site of the trypsin molecules inside the mesopores. Immobilization and encapsulation of porcine pancreatic lipase (PPL, 4.6 nm x 2.6 nm x 1.1 nm) onto MCM-41 has been performed in a similar way, with the pore opening being reduced by silylation.[165] The activity of the immobilized lipase was examined using the hydrolysis of acetin as a test reaction. Upon immobilization, just over 50% of the activity was retained. The immobilized lipase was also recycled, resulting in a decrease of 45% in activity after 4 cycles.

Once enzymes have been adsorbed within the mesopores of such solids, the encapsulation approach can be adopted, in a similar way to that adopted for the well ordered mesoporous solids. Wang and Caruso showed that the enzyme catalase C-100 (MW = 250 kDa) could be encapsulated in bimodal mesoporous silica (BMS) spheres, 2–4 mm in diameter, containing interconnected cages ca. 300 nm in diameter, by subsequent coating with alternate layers of polyelectrolytes such as poly(diallyldimethylammonium chloride) and silica nanoparticles.[166] This coating sharply reduced loss of the enzyme and the enzyme retained its activity for the appropriate assay (the decomposition of hydrogen peroxide to water and dioxygen) after many cycles.

The immobilized enzyme was active over a wider pH range than the free enzyme and could be recycled with a more gradual loss of activity. In a related approach, the enzyme butyrylcholinesterase was encapsulated among silica nanospheres formed by adding polypeptides (similar to those found in diatoms) to catalyze the silica condensation under mild conditions (pH 7, room temperature and pressure). Silaffin polypeptides catalyze the formation of the delicate silicate skeletons of diatoms, but in this case give robust silica nanospheres suitable for use in a continuous flow reactor. The activity of the enzyme, as measured by the assay of indophenyl acetate hydrolysis, was retained in this process.[167]

1.17. Adsorption and covalent binding onto functionalized silica

In efforts to overcome the problems of leaching without the subsequent deactivation by addition of reactive siloxanes, it has been found that organic modification of the silica surface can strengthen the binding strength of the enzyme on the surface via either electrostatic or covalent mechanisms (see Fig. 1.11). For

enzyme or protein immobilization, the most potentially useful surface functional groups are thiols, carboxylic acids, alkyl chlorides and amines. Other functional groups such as alkyl, phenyl and vinyl can be added to modify the enzyme's environment by increasing the hydrophobicity of the surface.

In 2001, Yiu et al. used functionalized SBA-15 in enzyme immobilization.[168] Trypsin was immobilized onto SBA-15 materials with different surface functional groups (–SH, –Ph, –Cl, $–NH_2$, and –COOH) prepared via in situ and post synthesis routes. Leaching of the enzyme was largely solved by using SBA-15 functionalized with groups such as –SH, –Cl and –COOH. Trypsin immobilized on iPrSH-SBA-15 (prepared via in situ functionalization) showed the highest catalytic activity. Remarkably, immobilized enzyme retained 96% activity of the free trypsin with negligible leaching. After recovery, the immobilized enzyme was reused, and gave 66% of the original activity. The cause of the increase in the strength of trypsin immobilization upon inclusion of functional groups was not identified unambiguously. Various covalent linkages between functionalized support and enzymes are given in Table 1.6.

Trypsin immobilized on isPrSH-SBA-15 in the hydrolysis of a series of proteins (cytochrome c, lysozyme, myoglobin, lactoglobolin, ovalbumin, bovine serum albumin, and conalbumin) with use of MALDI-TOF mass spectrometry for monitoring the protein fragments. Among these proteins, only smaller proteins were fragmented while ovalbumin, bovine serum album and conalbumin were not hydrolyzed, indicating that enzyme–mesoporous silica hybrid materials can introduce extra size selectivity to catalytic reactions.

Table 1.6 Various covalent linkages between functionalized support and enzyme

Support functional group	Enzyme functional group	Covalent binding	Name of binding
Support-NH_2	H_2N-Enzyme	Support–N=N–Enzyme	Diazotization
Support-COOH	H_2N-Enzyme	Support–CO–NH–Enzyme	Amide bond formation
Support-CH_2-X X = F, Cl, Br or I	H_2N-Enzyme HS-Enzyme	Support–CH_2–NH–Enzyme Support–CH_2–S–Enzyme	Alkylation and Arylation
Support-CHO	H_2N-Enzyme	Support–CH=N–Enzyme	Schiff's base formation
Support-$NH(CH_3)$	HOOC-Enzyme	Support–(CH_3) NH–O=C–Enzyme	Amidation reaction
Support-SH	HS-Enzyme	Support–S–S–Enzyme	Thiol-Disulfide Linkage
Support-NH_2	H_2N-Enzyme	Support-N=$CH(CH_2)_3$ CH=N–Enzyme	Carrier bind with bifunctional reagents

In other studies, SBA-15 solids functionalized with $–NH_2$ and –COOH groups were used as carriers for the immobilization of organophosphorus hydrolase (OPH), an enzyme that has been widely investigated for biosensing and the decontamination of poisonous agents.[169] The mesoporous carrier with 2% –COOH exhibited the highest protein loadings (4.7% w/w) and the highest activity (4182 units mg support).[161] By contrast, the carrier with 20% $–NH_2$ was found to have a very low loading. The results with OPH can be rationalized by the effect of surface charge. The immobilization and the activity measurements were performed at pH 7.5. At this pH the OPH (isoelectric point, pI = 8.3) will possess an overall positive charge, whereas carboxylic acid groups on the solid will be negatively charged and amine groups on the surface will be positively charged, giving rise to net attraction and repulsion of the enzyme, respectively. Furthermore, OPH immobilized on carboxy-functionalized SBA-15 was found to possess significantly enhanced longevity.

Table 1.7 A summary of reported research in enzyme immobilization using mesoporous molecular sieves as supports

Enzyme	**Support**	**Loading/mgg^{-1}**	**Ref.**
Encapsulation			
Cytochrome c, Trypsin, papain, horseradish peroxidase	MCM-41	0.4–5.8	77
Cytochrome c	MCM-48, SBA-15, Nb-TMS-4	6.2–11.8	108
Lipase	MCM-41	380	97
Physical adsorption			
Trypsin	SBA-15, MCM-41, MCM-48	24	80
Penicillin acylase	MCM-41	230	96
Horseradish peroxidase	FSM-16, MCM-41, SBA-15	10–183	83
Lipase	MCM-41, Al-MCM-41	2.1–4.6	109
Crude lipase	SBA-15	40	85
Trypsin	MCM-41	100	110
α-Chymotrypsin	MCM-41	170	111
Cytochrome P450	MCM-41, Al-MCM-41	0.02–0.06	112
Myoglobin	HMS	11.3	88
Lysozyme	SBA-15	174–482	93
Cytochrome c, protease, catalase	Bimodal mesoporous silica	53–250	113
Chemical Binding			
Trypsin	SBA-15 (–SH, –Cl, –COOH, etc.)	24	98
α-Chymotrypsin	SBA-15 (–CHO)	5.4	100
Organophosphorus hydrolase	SBA-15 (–COOH)	31	101
Penicillin acylase	SBA-15 (–NH2, –SH, –Ph, –COOH)	2.24	114
Chloroperoxidase	MCF, SBA-15, SBA-16, MCM-48 (–NH2)	122	103
α-Amylase	MCF, SBA-15 (–CHO)	0.5–1.75	104
Glucose oxidase	MCF (–CHO)	210	105

Formation of covalent bonds with functionalized surfaces ensures strong binding and negligible leaching. In such an approach, an aldehyde-functionalized SBA-15 material has been used as a carrier for immobilizing the enzyme α-chymotrypsin.[170] Aldehyde-functionalized supports are a popular choice for protein immobilization[171] because an imine binding can form easily between the surface aldehyde groups and the amine groups on the protein molecules. Unfortunately, aldehyde-functionalized alkoxysilane is not commercially available and was synthesized using a rhodium phosphine catalyst.[172]

A summary of reported research in enzyme immobilization using mesoporous molecular sieves as supports is given in Table 1.7. The aldehyde-functionalized SBA-15 was prepared via a post-synthesis route with the trimethoxysilylpropanal. The activity of immobilized enzyme in the hydrolysis of N-succinyl-Ala-Ala-Pro-Phe p-nitroanilide (SAAPPN) was found to decrease to only 5% of that of the free enzyme but the activity in transesterification of N-acetyl-L-phenylalanine ethylester (APEE) in organic media increased by more than 200% when compared with the free enzyme. It seems that the SBA-15 carrier protects the enzyme molecules from denaturation in organic media. To prove this assumption, the α-chymotrysin-SBA-15 composite was suspended in pure methanol at room conditions and the half-life of the immobilized enzyme was found to increase over 100-fold.The thermal stability of this immobilized enzyme was also improved.

In the work of Han et al., pure silica MCF with a pore size of 15 nm was used to immobilize CPO (SBA-15, SBA-16 and MCM-48 were also studied for comparison). The activity of the immobilized CPO was monitored using the monochlorodimedone (MCD) assay.[173] CPO remained active in MCF and SBA-15

(pore size 7 nm) but low activities were recorded from the immobilized CPO on MCM-48 (3.2 nm) and SBA-16 (8.2 nm). The pore size of MCM-48 was too small for CPO (7.7 nm 6 6.5 nm 6 4.6 nm) immobilization while SBA-16 was also unsuitable. Although SBA-16 has a pore size of 8.2 nm, the size of the openings between cages is only 4.7 nm which inhibits immobilization. This highlights an important consideration in the use of some of the new mesoporous structures, where the window size may be much smaller than the pore size.

Besides the pore structure of the carrier, the loading of CPO was also affected by the pH of the solution during the immobilization process with a maximum loading at pH = 3.5. At this pH, which is slightly below the isoelectric point of CPO (pI = 4), the enzyme has a net positive charge and the silica (isoelectric point pI = 2) a net negative charge, accounting for the high loading of CPO on MCF. CPO remains active at these pH values and the specific activity of CPO supported on MCF was around one half of that of the free enzyme. The decrease in activity was attributed to steric constraints preventing free access to the active site of the enzyme molecule.

Pandya et al. showed that the large enzyme α-amylase, active for the hydrolysis of starch, could be more successfully immobilized within MCF materials of pore diameter 33.5 nm than in SBA-15 of pore size 5–6 nm, as a result of molecular sieving.[174] Notably, the enzyme molecules had been immobilized on solids that had been functionalized post-synthesis by using alkylamines and glutaraldehyde to produce aldehyde groups that were subsequently reacted with amine groups of the enzyme. The activity of the immobilized α-amylase was measured for the chemical reaction of interest, the hydrolysis of starch to dextrin, and was found to show high specific activity, and improved thermal stability and longevity.

A similar approach was adopted to immobilize glucose oxidase (GOx, 33 kD) in MCF, which was much more successful than parallel attempts with SBA-15.[175a] The properties of siliceous mesostructured cellular foams (MCF) with the surface functionalised using different organosilanes to immobilize covalently trypsin have been studied.

Four organosilanes were applied: 3-aminopropyltriethoxysilane, 2-aminoethyl-3-aminopropylmethyldimethoxysilane, 2-aminoethyl-3-aminopropyl trimethoxy silane and 3-glicydoxypropyl-triethoxysilane. The samples modified using alkylamines were further activated with glutaraldehyde (GLA), a cross-linker. Commercially available silica gels and Eupergit C were used for comparison. Activity of MCF-based biocatalysts expressed in BAPNA and casein conversion, was significantly higher than of the silica gel- and Eupergit C-based counterparts. In the best systems the determined activity of trypsin was higher than of a free enzyme. The GLA-amino linkages appeared the most effective systems for the covalent immobilization of trypsin.[175b]

1.18. Protein Engineering

Improvement in the activity and usefulness of an existing enzyme or creation of a new enzyme activity by making suitable changes in its structure or amino acid sequence is called enzyme engineering. When this approach is used to modify the properties of any protein, whether enzyme or nonenzyme, it is termed as protein engineering.[183]

Since enzymes are proteins, enzyme engineering is a part of the larger activity of protein engineering. Enzyme engineering utilizes recombinant DNA technology to introduce the desired changes in the amino acid sequences of enzymes.

Recombinant DNA technology is also used to transfer genes encoding useful enzymes from dangerous, unapproved, slow growing or low producing microorganisms into safe, fast growing and high producing microorganisms.[184]

In addition, the level of production of an enzyme may be increased by introducing more copies of the gene into the concerned organism. Such applications of recombinant DNA technology are enzyme or protein engineering, which must rest on modification of the amino acid sequence of the concerned enzyme or protein.

The major goal of protein engineering is the generation of novel molecules, intended as both proteins endowed with new functions by mutagenesis and completely novel molecules. This definition, which may sound broad and perhaps ambitious, in fact pinpoints one of the most promising developments in our ability to understand and control a protein's function. After the revolution introduced in proteins science by the advent of genetic engineering, protein engineering can be considered as a second wave of innovation which is providing important breakthroughs in basic research and application, useful for studies on structure function relations and for exploitation in industry.

Genetic engineering makes available unlimited amounts of purified proteins, whereas protein engineering produces tailor-made proteins redesigned such as to make them more suited to industrial requirements. On this basis it becomes evident that industrial biotechnology will enormously benefit of this possibility.[185]

1.18.1. Objectives of Enzyme Engineering

The chief objective of enzyme engineering is to produce an enzyme that is more useful for industrial, medical and other applications.[186-187] The various properties of an enzyme that may be modified to achieve this objective are as follows:

- Improved kinetic properties,
- Novel enzyme activity,
- Elimination of allosteric regulation,
- Enhanced substrate and reaction specificity,
- Increased thermostability,
- Alteration in optimal pH,
- Suitability for use inorganic solvents,
- Increased/decreased optimal temperature, etc.

1.19. Design and Engineering Novel Metalloproteins Based on Native Protein scaffolds

Protein folding is primarily dictated by noncovalent, relatively weak intramolecular forces. Considerable evidence has now been accumulated to indicate that folding of a protein into native conformation proceeds through various intermediate species.[188] In the *in vitro* system many unfolded polypeptides can refold to regain native-like activity in a spontaneous process dictated solely by their primary structure. But the recovery is not always total and certainly depends on the state of unfolding of the polypeptide in a given denaturant. The refolding of the population which has lost the signal posts for correct interactions can sometimes be guided to the productive pathway with the aid of effector molecules like detergents,[189-190] substrate

and cofactors,[191] salts,[192] multivalent ions,[193] and molecular chaperones.[194] The effector molecules either stabilize some transient intermediates[189, 194] or bind to the non-native structure and prevent wrong interactions.[192, 195]

In the vast majority of in vitro studies, folding experiments are typically initiated with 1M-6M Guanidium Hydrochloride (GdmCl) or 1M-8M urea denatured proteins. In the cases of disulfide proteins, native disulfide bonds are usually kept intact (disulfide intact) in the denatured state. GdmCl (6 M)-denatured proteins are generally considered fully unfolded or extensively unfolded. Forty years ago, Tanford[196] showed that 6 M GdmCl-denatured proteins were essentially structureless. However, subsequent research from various groups using more sophisticated techniques has shown that residual structures do persist in many proteins even under strongly denaturing conditions (e.g., 7.5 M GdmCl)[197-204]. NMR and circular dichroism techniques have proven to be particularly useful in comprehensive structural characterization of denatured proteins[205-207]. Denatured structures of barnase [208], protein L variant [197], Drosophila melanogaster [209], protein G [210], 434 repressor [198], ferricytochrome c [211], staphylococcal nuclease [200], R-lactalbumin [212-215], antichymotrypsin [214], SH3 domain [215], and fatty acid binding protein [216] were reported. A common conclusion obtained from these studies is the persistence of residual hydrophobic clusters and native like secondary structures in the denatured state of proteins [199, 202, 204].

The structure of 1 M-6 M GdmCl-denatured protein is relevant to the study of protein folding because there is always concern regarding the conformational heterogeneity of the starting materials and whether they still possess residual secondary structures or hydrophobic clusters. These remaining structures may skew

the observation of the early folding mechanism, which is the most crucial event in understanding how protein folding is started[217-220] and in defining the model of protein folding.[221-223] Therefore, the structural heterogeneity of GdmCl-denatured proteins is critically important to the interpretation of the metalloprotein folding pathway and mechanism.

An important branch of protein active site design is the design and engineering of new metal-binding sites into native proteins with characteristic scaffolds. Metal ions add new functionality to proteins and help catalyze some of the most difficult biological reactions. Protein reactivity is finely tuned by using different metal ions, different redox states of the same metal ion, or different ligands and geometric arrangements. Probably for these reasons, metalbinding sites are found in about 1/3 of structurally characterized proteins and in about 1/2 of all proteins.[224] Therefore, designing and engineering novel binding sites in proteins is an important test of our ability to design proteins. Another advantage of choosing metal-binding sites as targets for protein design is the rich spectroscopy available for evaluating the design process. At this early stage of protein design, one can learn just as much from a failed design as from a successful one, as long as the site is properly analyzed.

The problem of metalloprotein folding can be studied by the preparation of peptides crafted using first principles in the hope of generating "functionally active" biomolecules.[225-226] This design strategy involves the construction of a peptide intended to fold into a precisely defined three-dimensional structure, with a sequence that is not derived from that of any natural protein.[227] For the most part, de novo design has followed a minimalist approach to design the peptidic scaffold.[228-229] The advantage of this approach is that specific structure types can be ascertained without

the complication of deconvoluting the behavior of multiple alternate folding domains present in natural systems.

In general, there is still a serious lack of knowledge describing the relationship between the peptidic backbone sequence, its secondary and tertiary structures, and the functional properties of the protein. A survey of the literature suggests that reports detailing metal-induced protein folding are sparse. This observation is remarkable given that it is estimated that one-third of proteins contain metals which are indispensable for proper function. Significant attention has focused on engineering metal binding sites in de novo designed peptides because of the importance of metals in biology. The rate of research in the field of metallopeptide design has seen a tremendous jump in the past few years resulting in the emergence of very distinct approaches.

Many excellent reviews on metalloprotein design have appeared [230-234] in order to obtain a broader overview of the metalloprotein design field and attempt to focus on methodology used in the design and engineering of novel metal-binding sites in native proteins with characteristic scaffolds. Because the focus of the review is on new metal-binding sites, many interesting works on refining the properties of the existing sites such as binding affinity or substrate binding specificity.

The binding of metals to de novo designed peptides has been discussed under the following categories: (1) metal assisted folding of unstructured/partially structured de novo designed α-helices, (a) enhancement of α-helical character in partially folded peptides, (b) metal induced folding of random coils to generate α-helices;(2) metal binding to folded de novo designed proteins/peptides, (a) metal binding to folded α-helical peptides, (b)metal binding to β-turns and β-sheets.

Alkaline phosphatase (AP) is a homodimeric metalloprotein containing two intramolecular disulfide bonds. The active dimer contains four tightly bound zinc atoms. The two zinc atoms are critical for the catalytic activity of the enzyme, the two being thought necessary for structural integrity of the molecule[235]. In addition, two magnesium atoms are important both for catalysis and for stabilizing the active conformation of the molecule [236].

Generally, the enzyme is denatured by exposure to low pH or to increasing concentrations of urea or guanidine hydrochloride (GdnCl). The subunits prepared in these ways have intact S–S bonds [237-238], a prerequisite for stable folding of the monomers [239]. The unfolded subunits refold readily upon removal of the denaturant and dimerize spontaneously to form active protein[240].

Ronald et al. introduced a method for the design of an oxygen transport protein, akin to human neuroglobin. Beginning with a simple unnatural helix-forming sequence with histidines to bis-histidine ligate haems, and exploited helical rotation of glutamate towards on haem binding to introduce distal histidine strain and facilitate O_2 binding. O_2 affinities and exchange timescales match natural globins with distal histidines, with the remarkable exception that O_2 binds tighter than CO.[241].

Okrasa et al. designed a manganese substituted carbonic anhyrase for epoxidation reaction. Carbonic anhydrase is a zinc metalloenzyme that catalyzes the hydration of carbondioxide to bicarbonate. Replacing the active-site zinc with manganese yielded manganese-substituted carbonic anhydrase (CA[Mn]), which shows peroxidase activity with a bicarbonate-dependent mechanism. The active-site zinc removed from carbonic anhydrase by dialysis against a zinc chelator, 2,6-pyridinedicarboxylate,removed 90–95% of the active-site zinc. Subsequent dialysis

against manganese(ii) yielded manganese-substituted carbonic anhydrase (CA[Mn]).[242]

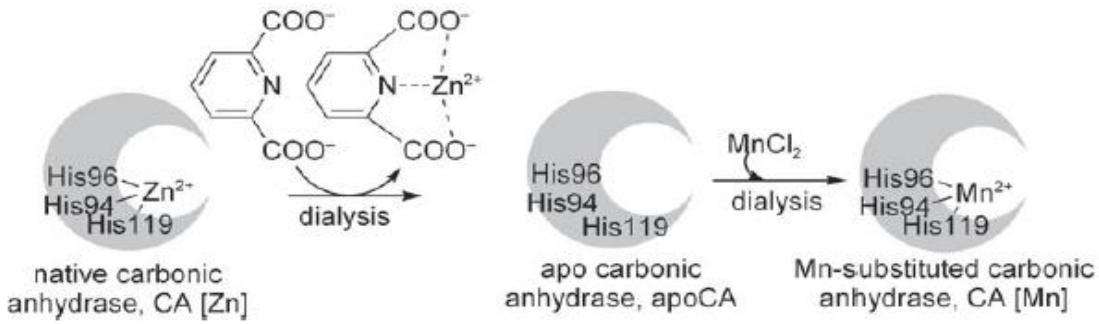

Fig. 1.12 Mn-substituted carbonic anhydrase (CA[Mn]) from carbonic anhydrase

Rhodanase (thiosulfate sulfur transferase) consists of a single polypeptide chain folded into two domains. The first time completely reversible unfolding was achieved using guanidinium chloride-denatured with a systematically defined protocol.[243] Mettalothionene (MT) is a 61 amino-acid polypeptide that has no α-helix or β-sheet, but wraps 6–7 divalent heavy metal ions at highly conserved with 20 cysteines. The reversible defolding achieved and in addition to adapted to metal substitution of metal-containing enzymes in refolding process.[244]

1.20. Aim and outline of this thesis

This thesis also deals with the studies to improve enzyme activity, stability and reusability, using silica materials as carriers for enzyme immobilization, varying immobilization methods, altering the porosity properties of the carrier, etc., but always with strong background knowledge of the material properties. Creating a novel enzyme molecule from existing protein molecules is a major challenge in protein engineering which one is attempted using reversible denaturation followed by renaturation in presence of metal ions.

First chapter introduces the protein chemistry for globular structure, function of the enzyme with the various classification catalytic groups. The enzyme causes the natural biochemical functions in various living systems for different diagnostic applications. The various immobilization techniques for improving of an enzyme artificially with retention of catalytic function often stabilizes the structure. Immobilization of enzymes on Meso Porous silica's (MPS's) could help in their economic reuse and in the development of continuous bioprocesses in industries. Protein engineering, involves the use of chemical techniques to modify the structure of a protein, thereby altering its structural function activity for catalytic application.

In **Chapter 2**, synthesis of highly ordered porous SBA-15 and MCF, as carrier for alkaline serine endo peptidase immobilization, was performed. Functionalization of silica's followed by covalent binding of enzyme molecule on surface by amide linkage were obtained. The influence of the pore size properties on the loading of alkaline serine endo peptidase during immobilization and on the enzyme activity, stability and reusability of the immobilized enzyme was studied.

A strategy for chemical binding of cellulase on surface functionalized MCF is presented in **Chapter 3**. The amination followed by glutaration of MCF, cellulase was immobilized by imine bond formation, which could be reduced to amine group using $NaBH_4$. The influence of the amount of enzyme loading, activity, stability and reusability was investigated.

Chapter 4 focuses on reversible denaturation of alkaline protease using increased amount of Gdn-HCl and renturation in refolding buffer in presence of cobalt metal ion for designing towards the nitrile hydratase. A systematic characterization of structural changes upon denaturation followed by renaturation was studied using various spectra-chemical techniques. Furthermore, the nitrile hydratase kinetic study was also discussed using 3-cyanopyridine as a substrate.

Chapter 5 gives a summary of the main results and conclusions of the study and outline suggestions for future work. In particular it will address how the biomolecules such as enzyme, antibodies, DNA, RNA and lipids can be immobilized on functionalized ordered mesoporous silica surfaces and their diverse utilities. The protein engineering recent research has focused on the effects of metal binding on the overall secondary and tertiary conformations of unstructured peptides/proteins towards the designing of novel enzyme molecules.

Finally, **Appendices** gives the total enzyme concentration standard curves. Standard product curves were obtained from known concentration. An overview of the porosity properties of the synthesized SBA-15 and MCF from SEM and TEM is also included.

1.21. References

[1] D.L. Nelson, M.M. Cox, Principles of Biochemistry 4th Edition Book (2004), 190-193.

[2] A. Bairoch, *Nucleic Acids Res.* 28 (2000) 304–305.

[3] D. Lilley. *Curr. Opin. Struct. Biol.* 15 (2005): 313–23.

[4] T. Cech, *Science* 289 (2000) 878–879.

[5] J.T. Groves, *Nature* 389 (1997) 329–30.

[6] J. Dubos, *Trends Biotechnol.* 13 (1995) 511–515.

[7] Nobel Laureate Biography of Eduard Buchner at http://nobelprize.org

[8] C.C. Blake, D.F. Koenig, G.A. Mair, A.C. North, D.C. Phillips, V.R. Sarma, *Nature* 22 (1965)757–761.

[9] C.B. Anfinsen, *Science* 181 (1973) 223–230.

[10] D. Dunaway-Mariano, *Structure* 16 (2008) 1599–600.

[11] K.E. Jaeger, T. Eggert, *Curr Opin Biotechnol.* 15 (2004) 305–313.

[12] A. Warshel, P.K. Sharma, M. Kato, Y. Xiang, H. Liu, M.H. Olsson. *Chem. Rev.* 106 (2006) 3210–3235.

[13] E.Z. Eisenmesser, D.A. Bosco, M. Akke, D. Kern, *Science* 295 (2002) 1520–1523.

[14] E.Z. Eisenmesser, O. Millet, W. Labeikovsky, *Nature* 438 (2005) 117–121.

[15] L.W. Yang, I. Bahar, *Structure* 13 (2005) 893–904.

[16] P.K. Agarwal, A. Geist, A. Gorin, *Biochemistry* 43 (2004) 10605–10618.

[17] A. Tousignant, J.N. Pelletier, *Chem. Biol.* 11 (2004) 1037–42.

[18] E. Fischer, *Ber. Dt.* Chem. Ges. *27* (1894) *2985–2993. http://gallica.bnf.fr/ark:/12148/bpt6k90736r/f364.chemindefer*.

[19] D.E. Koshland, *Proc. Natl. Acad. Sci.* 44 (1958) 98–104.

[20] Boyer, Rodney, (2002) *Concepts in Biochemistry* (2nd ed.). New York,: John Wiley & Sons, Inc.. pp.137–8.

[21] V. Henri, *Compt. Rend. Hebd. Acad. Sci. Paris* 135 (1902) 916–919.

[22] P.L. Sørensen, *Biochem. Z.* 21 (1909) 131–304.

[23] L. Michaelis, M. Menten, *Biochem. Z.* 49 (1913) 333–369.

[24] G.E. Briggs, J.B.S. Haldane, *Biochem. J.* 19 (1925) 339–339.

[25] H. Theorell, J.S. McKee, Nature 192 (1961) 47-50.

[26] S.A. Cetinus, H.N. Oztop, *Enzyme Microb. Technol.*, 32 (2003) 889-894.

[27] R. Light, M. Macgregor, P. Luchsinger, W. Ball, Ann. Intern. Med., 77 (1972) 507-513.

[28] S. Bork, M. Okamura, S. Boonchit, H. Hirata, N. Yokoyama, I. Igarashi, *Mol. Biochem. Parasitol.* 136 (2004) 165-172.

[29] R.A. Mustati, M. Kollarova, N. Mernik, D. Mikullasova, Gen. Physio. Biophy., 17 (1998) 193-210.

[30] S. Hsieh, T. Shih, C. Yeh, C. Lin, Y. Chou, Y. Lee, *Proteomics* 6 (2006) 5322-5331.

[31] G.L. Prosise, H. Luecke, J. Mol. Biol., 326 (2003) 517-527.

[32] J.R.A. Pich, A. Grantzdorffer, A. Schierhorn, K.P. Rucknagel, J.R. Andersen, A. Pich, J. Bio. Chem., 274 (1999) 8445-8454.

[33] A. Dinopoulos, S. Kure, G. Chuck, K. Sato, D.L. Gilbert, Y. Matsubara, T. Degrauw, *Neurology* 64 (2005) 1255-1257.

[34] J. Li, S. Tong, H.B. Lee, A.L. Perdigoto, H.C. Spangenberg, J.R. Wands, *J. Virol*.78 (2004) 1873-1881.

[35] J.R. Seckl, Front. Neuroendocrinol. 18 (1997) 49-99.

[36] J.W. Tomlinson, *Minerva Endocrinol.,* 30 (2005) 37-46.

[37] S.J. Gould, S. Subramani, Anal. Biochem., 175 (1998) 5-13.

[38] H.J. Chen, T. Shimada, A.D. Moulton, A. Cline, R.K. Humphries, J. Maizel, A.W. Nienhuis, J. Biol. Chem., 259 (1984) 3933-3943.

[39] B. Roth, E. Bliss, C.R. Beddell, *Top. Mol. Struct. Biol*. 3 (1983) 363-393.

[40] T. Shimakata, R.K. Stumpf, Arch. Biochem. Biophys., 218 (1982) 77-91.

[41] K. Karmodiya, N. Surolia, *FEBS J*. 273 (2006) 4093-4103.

[42] W. Richmond, Clin. Chem. 19 (1973) 1350-1356.

[43] J.M. Petrash, Cell. Mol. life Sci. 61 (2004) 737-749.

[44] J. Dudka, J. Jodynis-Liebert, E, Korobowicz, F. Burdan, A. Korobowicz, J. Szumilo, E. Tokarska, R. Klepacz, M. Murias, *Basic Clin. Pharmacol. Toxicol*. 97 (2005) 74-79.

[45] I.F. Durr, H. Rudney, J. Biol. Chem., 235 (1960) 2572-2578.

[46] H.L. Zhao, P.C. Tong, F.M. Lai, B. Tomlinson, J.C. Chan, *Diabetes*. 53 (2004) 2984-2991.

[47] G. Gaetani, A. Ferraris, M. Rolfo, R. Mangerini, S. Arona, H. Kirkman, Blood 87 (1996) 1595-1599.

[48] P. Chelikani, I. Fita, Cell. Mol. Life Sci 61 (2004) 192-208.

[49] E. Adams, A. Gold stone, J. Biol. Chem., 235 (1960) 3499-3503.

[50] J. Cheng, W.L. Zhu, J.J. Dao, S.Q. Li, Y. Li, *Biomed. Environ. Sci*. 18 (2005) 58-64.

[51] V. Yankovskaya, R. Horsefield, S. Tornroth, Science 299 (2003) 700-704.

[52] J. Pandhare, S.K. Cooper, J.M. Phang, *J. Biol. Chem*. 281 (2006) 2044-2052.

[53] H.R. Mahlet, J. Biol. Chem., 206 (1954) 13-26.

[54] Y. Du, C.M. Miller, T.S. Kern, *Free Radic Biol Med*., 35 (2003) 1491-149.

[55] S. Thiele, U. Hoppe, P.M. Holterhus, O. Hiorr, Eur. J. Endocrinol., 152 (2005) 875-880.

[56] M.A. Kurian, L. Hartley, Z. Zolkipli, M.A. Little, D. Costigan, E.R. Naughten, S. Olpin, F. Muntoni, M.D. King, *Neuropediatrics*. 35 (2004) 312-316.

[57] S. Elzanaty, Y.L. Giwercman, A. Giwercman, *Int. J. Androl*. 29 (2006) 414-420.

[58] J.M. Torres, E. Ortega, *Endocr Res*. 30 (2004) 149-157.

[59] J. Raba, H.A. Mottola, Crit. Rev. Analyt. Chem., 25 (1995) 1-42.

[60] D. Keilin, E.F. Hartree, Biochem. J., 50 (1952) 331-341.

[61] K. Pollegioni, L. Piubelli, S. Sacchi, M.S. Pilone, G. Molla, Cell. Mol. Life Sci., 64 (2007) 1373-1394.

[62] M.S. Pilone, *Cell. Mol. Life Sci.* 57 (2000) 1732-1747.

[63] M. Maekawa, T. Okamura, N. Kasai, Y. Hori, K.H. Summer, R. Konno, *Chem Res Toxicol.* 18 (2005) 1678-1682.

[64] G.W. Haywood, P.I. Large, Biochem. J. 199 (1981) 187-201.

[65] L. Gouya, H. Puy, A.M. Robreau, S. Lyoumi, J. Lamoril, V. Da Silva, B. Grandchamp, J.C. Deybach, *Hum Genet.* 114 (2004) 256-262.

[66] K. Csiszar, Prog. Nucleic acid Res. Mol. Biol., 70 (2001) 1-32.

[67] C.J. Diaz, J. Perianes, E. Arjona, L. Lorente, M. Aguirre, *Bull Inst Med Res Univ Madr*. 3 (1950) 229-233.

[68] K. Fujita, Y. Sasaki, Curr. Drug. Metab., 8 (2007) 554-562.

[69] G.M. Gilad, H.M. Kagan, V.H. Gilad, *Neurosci Lett*. 376 (2005) 210-214.

[70] F. Ramos, J.M. Wiame, Eur. J. Biochem. 123 (1982) 571-576.

[71] D. Simon, J. Hoshino, H. Kroger, Biochim. Biophys. Acta. 321 (1973) 361-368.

[72] D.C. MacLaren, C.M. Oconnor, Y.R. Xia, M. Mehrabian, I. Klisak, R.S. Sparkes, S. Clarke, A.J. Lusis, Genomics 14 (1993) 852-856.

[73] V.L. Mohler, D.M. Heithoff, M.J. Mahan, K.H. Walker, M.A. Hornitzky, L.W. Shum, K.J. Makin, J.K. House, *Vaccine*. 26(2008):1751-1758.

[74] W.J. Williams, J. Litwin, C.B. Thorne, J. Biol. Chem., 212 (1955) 427-438.

[75] H. Zhu, W. Yang, W. Lu, J. Zhang, G.M. Shaw, E.J. Lammer, R.H. Finnell, *Mol. Genet. Metab*. 87 (2006) 66-70.

[76] T. Noguchi, E. Okune, Y. Takada, Y. Minatogawa, K. Okai, R. Kido, Biochem. J., 169 (1978) 113-122.

[77] L.A. Vasconcelos, E.A. de Almeida, L.F. Bachur. *Arq Bras Cardiol*. 88 (2007) 590-595.

[78] A. Faulkner, J.M. Turner, Biochem. Soc. Trans., 2 (1974) 133-136.

[79] Y. Liu, M.C. Ekambaram, P.S. Blum, C.D. Stimbert, H.M. Jernigan, *Exp. Eye Res*. 67 (1998) 193-202.

[80] N.J. Schönbrunner, E.H. Fiss, O. Budker, S. Stoffel, C.L. Sigua, D.H. Gelfand, T.W. Myers. *Biochemistry*. 45 (2006) 12786-12795.

[81] J.L. Pope, J.C. McPherson, H.C. Tidwell, J. Biol. Chem., 241 (1966) 2306-2310.

[82] G. Labar, C. Bauvois, G.G. Muccioli, J. Wouters, D.M. Lambert, *Chembiochem* 8 (2007) 1293-1297.

[83] J.P. Jost, R.M. Bock, J. Biol. Chem., 244 (1969) 5866-5873.

[84] G. Das, U. Varshney, *Microbiology* 152 (2006) 2191-2195.

[85] Berg, J. Mark, J.L. Tymoczke, Lubert stryer (2002) "Glycolysis and Gluconeogenesis' in susan moran (ed.). Biochemistry (5 th Edition ed.). 41 Madison Avenue, New York, W.H. Freeman and Company.

[86] P.D. Van Poelje, Q. Dang, M.D Erion, *Curr. Opin. Drug Discov. Devel*. 10 (2007) 430-437.

[87] S.Y. Jung, J.H. Suh, H.J. Park, K.M. Jung, M.Y. Kim, D.S. Na, D.K. Kim, J. Neurochem., 75 (2000) 1004-1014.

[88] A. Soloviev, E.M. Schwarz, M. Darowish, R.J. O'Keefe, *J. Orthop. Res.* 23 (2005) 1258-1265.

[89] N.F. Krynetskaia, E.Y. Krynetski, W.E. Evans, Mol. Pharma Col., 56 (1999) 841-848.

[90] X. Tang, I.J. Dmochowski, *Angew. Chem*. 45 (2006) 3523-3526.

[91] C.G. Takada, K. Gardiner, T. Marsh, N. Pace, S. Altman, Cell 35 (1983) 849-857.

[92] A.F. Kilani, P. Trang, S. Jo, A. Hsu, J. Kim, E. Nepomuceno, K. Liou, F. Liu, *J. Biol. Chem.* 275 (2000) 10611-10622.

[93] P.S. Eder, R. Kekuda, V. Stolc, S. Altman, *Proc Natl Acad Sci U S A*. 94 (1997) 1101-1106.

[94] S.A. Costa, *Enzyme Microb. Technol.* 30 (2002) 387-391.

[95] M. Matsumoto, *J. Chem.Technol. Biotechnol.*, 70 (1997) 188-192.

[96] C. OFagain, *Enzyme Microb. Technol.* 33(2003) 137-149

[97] K. Khajeh, *Biochim. Biophys. Acta — Protein Struct. Mol. Enzymol.*, 1548 (2001) 229-237.

[98] J. Minshull, *Methods*, 32 (2004) 416-427.

[99] Z. Bilkova, *J. Chromatogr. A*, 852 (1999) 141-149.

[100] C.O. Fagain, *Biochim. Biophys. Acta*, 1252 (1995)1-14.

[101] V.P. Torchilin, *Adv. Drug Del. Rev.*, 1 (1987) 41-86.

[102] Kennedy, J.F., Handbook of enzyme technology, in *Principles of Immobilization of Enzymes*, 3rd ed., Wiseman, A., Ed., Prentice Hall Ellis Harwood, New York, 1995, p. 235

[103] G.F. Bickerstaff. Immobilization of enzymes and cells: methods in biotechnology, vol. 1. Totowa: Humana Press; 1997.

[104] I. Chibata, T. Tosa, T Sato, *J. Mol. Catal*. 37 (1986)1–24.

[105] E. Katchalski-Katzir, *Trends Biotechnol*. 11(1993) 471–8.

[106] P.S.J. Cheetham. *Trends Biotechnol.*, 11(1993) 478–488.

[107] C. Mateo, J.M. Palomo, M. Fuentes, L. Betancor, V. Grazu, F. L´opez-Gallego, *Enzyme Microb Technol*. 39(2006) 274–280.

[108] R.M. Blanco, J.J. Calvete, J.M. Guis´an, *Enzyme Microb. Technol*. 11 (1988) 353–359.

[109] E. Katchalski-Katzir, D.M. Kraemer. *J. Mol Catal B: Enzym*. 10 (2000)157–176.

[110] V. Graz´u, L. Betancor, T. Montes, F. Lopez-Gallego, J.M. Guisan, R. Fernandez-Lafuente, *Enzyme Microb. Technol*. 38 (2006) 960–966.

[111] C. Mateo, O. Abian, M. Bernedo, E. Cuenca, M. Fuentes, G. Fernandez-Lorente, *Enzyme Microb. Technol*. 37 (2005) 456–462.

[112] L. Betancor, F. L´opez-Gallego, A. Hidalgo, N. Alonso-Morales, G. Dellamora-Ortiz, J.M. Guis´an, *J. Biotechnol*. 121 (2006) 284–289.

[113] F. Lopez-Gallego, L. Betancor, A. Hidalgo, N. Alonso, G. Fernandez-Lorente, J.M. Guisan, *Enzyme Microb. Technol*. 37 (2005) 750–756.

[114] N. Alonso, F. Lopez-Gallego, L. Betancor, A. Hidalgo, C. Mateo, J.M. Guisan, *J. Mol. Catal B: Enzym*. 35 (2005) 57–61.

[115] I. Migneault, *Biotechniques* 37 (2004) 790–802.

[116] L. Betancor, F. Lopez-Gallego, A. Hidalgo, N. Alonso-Morales, G. Dellamora-Ortiz, C. Mateo, *Enzyme Microb. Technol*. 39 (2006) 877–882.

[117] I. Migneault, C. Dartiguenave, J. Vinh, M.J. Bertrand, K.C. Waldron, *Electrophoresis* 25 (2004) 1367–1378.

[118] F. Lopez-Gallego, L. Betancor, C. Mateo, A. Hidalgo, N. Alonso-Morales, G. Dellamora-Ortiz, *J. Biotechnol*. 119 (2005) 70–75.

[119] A.S. Bommarius, A. Karau, *Biotechnol. Prog*. 21 (2005) 1663–1672.

[120] M. Caussette, A. Gaunand, H. Planche, B. Lindet, *Proc. Biotechnol*. 15 (1998) 393–398.

[121] M. Caussette, A. Gaunand, H. Planche, S. Colombie, P. Monsan, B. Lindet, *Enzyme Microb. Technol*. 24 (1999) 412–418.

[122] S. Colombie, A. Gaunand, B. Lindet, *J. Mol. Catal B: Enzym*. 11 (2001) 559–565.

[123] T. Bes, C. Gomez-Moreno, J.M. Guis´an, R. Fern´andez-Lafuente, *J. Mol. Catal*. 98 (1995)161–169.

[124] J.M. Bolivar, L. Wilson, S.A. Ferrarotti, R. Fernandez-Lafuente, J.M. Guisan, C. Mateo, *Biomacromolecules* 7 (2006) 669–673.

[125] S.C. Tsang, C.H. Yu, X. Gao, K. Tam. *J. Phys. Chem B*; 110 (2006) 16914–16922.

[126] L. Zeng, K.K. Luo, Y.F. Gong, *J. Mol. Catal B: Enzym*. 38 (2006) 24–30.

[127] G.M. Qiu, B.K. Zhu, Y.Y Xu, *J. Appl. Polym. Sci*. 95 (2005) 328– 335.

[128] L. Betancor, M. Fuentes, G. Dellamora-Ortiz, F. L´opez-Gallego, A. Hidalgo, N. Alonso-Morales, *J. Mol. Catal B: Enzym*. 32 (2005) 97–101.

[129] K. Flodstrom, C. V. Teixeira, H. Amenitsch, V. Alfredsson, M. Linden, *Langmuir*, 20 (2004) 4885-4891.

[130] X. Liu, B. Tian, C. Yu, F. Gao, S. Xie, B. Tu, R. Che, L. M. Peng, D. Zhao, *Angew. Chem., Int. Ed*., 41 (2002) 3876-3878.

[131] J. Fan, C. Yu, F. Gao, J. Lei, B. Tian, L. Wang, Q. Luo, B. Tu, W. Zhou, D. Zhao, *Angew. Chem., Int. Ed.*, 42 (2003) 3146-3150.

[132] D.Y. Zhao, J.L. Feng, Q.S. Huo, N. Melosh, G.H. Fredrickson, B.F. Chmelka, G.D. Stucky, *Science*, 279 (1998) 548-552.

[133] D.Y. Zhao, Q.S. Huo, J.L. Feng, B.F. Chmelka and G. D. Stucky, *J. Am. Chem. Soc.*, 120 (1998) 6024-6036.

[134] A. Thommes, in Nanoporous Materials—Science and Engineering, ed. G. Q. Lu, X. S. Zhao, Imperial College Press, London, 2004, p. 317.

[135] F. Ehrburger-Dolle, I. Morfin, E. Geissler, F. Bley, F. Livet, C. Vix-Guterl, S. Saadallah, J. Parmentier, M. Reda, J. Patarin, M. Iliescu, J. Werckmann, *Langmuir*, 19 (2003) 4303-4308.

[136] J.W. Zhao, F. Gao, Y.L. Fu, W. Jin, P.Y. Yang, D.Y. Zhao, *Chem. Commun*., 7 (2002) 752-753.

[137] A. Katiyar, L. Ji, P. Smirniotis, N.G. Pinto, *J. Chromatogr. A*., 1069 (2005) 119-126.

[138] A. Vinu, C. Streb, V. Murugesan, M. Hartmann, *J. Phys. Chem. B*, 107 (2003) 8297-8299.

[139] P.M. Price, J.H. Clark, D.J. Macquarrie, J. Chem. Soc., *Dalton Trans*., (2000) 101-110.

[140] D.J. Macquarrie, D.B. Jackson, J.E.G. Mdoe, J.H. Clark, *New J. Chem*., 23 (1999) 539-544.

[141] A. Stein, B.J. Melde, R.C. Schroden, *Adv. Mater*., 12 (2000) 1403-1419.

[142] M.H. Lim, A. Stein, *Chem. Mater*., 11 (1999) 3285-3295.

[143] Y.J. Han, G.D. Stucky, A. Butler, *J. Am. Chem. Soc*., 121 (1999) 9897-9898.

[144] H.H. Weetall, *Appl. Biochem. Biotechnol*., 41 (1993) 157-188.

[145] J.F. Dıaz, K.J. Balkus, Jr., *J. Mol. Catal B: Enzym*., 2 (1996) 115-126.

[146] X.F. Li, J. He, R.Y. Ma, X. Duan, *Acta Chim. Sinica*, 58 (2000) 167-172.

[147] A.M. Tope, N. Srinivas, S.J. Kulkarni, K. Jamil, *J. Mol. Catal. B: Enzym*., 16 (2001) 17-26.

[148] H.H.P. Yiu, P.A. Wright, N.P. Botting, *Microporous Mesoporous Mater*., 44 (2001) 763-768.

[149] G. Carrea, S. Riva, *Angew. Chem., Int. Ed*., 39 (2000) 2226-2254.

[150] S. Colonna, N. Gaggero, C. Richelmi, P. Pasta, *Trends Biotechnol*., 17 (1999) 163-168.

[151] H. Takahashi, B. Li, T. Sasaki, C. Miyazaki, T. Kajino, S. Inagaki, *Chem. Mater*., 12 (2000) 3301-3305.

[152] B. Li, H. Takahashi, *Biotechnol. Lett*., 22 (2000) 1953-1958.

[153] Z.Z. Chen, Y.M. Li, X. Peng, F.R. Huang, Y.F. Zhao, *J. Mol. Catal B: Enzym.*, 18 (2002) 243-249.

[154] R.J. Tweddell, S. Kermasha, D. Combes, A. Marty, *Biocatal. Biotransform*., 16 (1999) 411-426.

[155] Z. Dai, S. Liu, H. Ju, H. Chen, *Biosens. Bioelectron*., 19 (2004) 861-867.

[156] Z. Dai, X. Xu, H. Ju, *Anal. Biochem*., 332 (2004) 23-31.

[157] X. Xu, B.Z. Tian, S. Zhang, J.L. Kong, D.Y. Zhao, B.H. Liu, *Anal. Chim. Acta*, 519 (2004) 31-38.

[158] T.J. Su, R.J. Green, Y. Wang, E.F. Murphy, J.R. Lu, R. Ivkov, S.K. Satija, *Langmuir*, 16 (2000) 4999-5007.

[159] T.J. Su, J.R. Lu, R.K. Thomas, Z.F. Cui, J. Penfold, *J. Colloid Interface Sci*., 203 (1998) 419-429.

[160] H.H.P. Yiu, C.H. Botting, N.P. Botting, P. A. Wright, *Phys. Chem. Chem. Phys.*, 3 (2001) 2983-2985.

[161] J. Lei, J. Fan, C. Yu, L. Zhang, S. Jiang, B. Tu, D. Zhao, *Microporous Mesoporous Mater*, 73 (2004) 121-128.

[162] A. Vinu, V. Murugesan, M. Hartmann, *J. Phys. Chem. B*, 108 (2004) 7323-7330.

[163] L.F. Atyaksheva, E.E. Knyazeva, O.M. Poltorak, E.S. Chukhrai, A.S. Khomich, A.V. Medvedko, *Russ. J. Phys. Chem*., 78 (2004) 1849-1853.

[164] J. He, X. Li, D. G. Evans, X. Duan, C. Li, *J. Mol. Catal. B: Enzym*., 11 (2000) 45-53.

[165] H. Ma, J. He, D. G. Evans, X. Duan, *J. Mol. Catal. B: Enzym*., 30 (2004) 209-217.

[166] Y.J. Wang, F. Caruso, *Chem. Mater*., 17 (2005) 953-961.

[167] H.R. Luckarift, J.C. Spain, R.R. Naik, M.O. Stone, *Nat. Biotechnol*., 22 (2004) 211.

[168] H.H.P. Yiu, P.A. Wright, N.P. Botting, *J. Mol. Catal B: Enzym*., 15 (2001) 81-92.

[169] C. Lei, Y. Shin, J. Liu, E.J. Ankerman, *J. Am. Chem. Soc*., 124 (2002) 11242-11243.

[170] P. Wang, S. Dai, S.D. Waezsada, A.Y. Tsao, B.H. Davison, *Biotechnol. Bioeng.*, 74 (2001) 249-255.

[171] S.S. Wong, Chemistry of Protein Conjugation and Cross-linking, CRC Press, Boca Raton, 1993.

[172] R. Takeuchi, N. Sato, *J. Organomet. Chem*., 393 (1990) 1-10.

[173] G.E. Meister Winter, A. Butler, *Biochemistry*, 35(1996) 11805-11811.

[174] P.H. Pandya, R.V. Jasra, B.L. Newalkar, P.N. Bhatt, *Microporous Mesoporous Mater*., 77 (2005) 67-77.

[175] X. Zhang, R.F. Guan, D.Q. Wu, K.Y. Chan, *J. Mol. Catal. B: Enzym*., 33 (2005) 43-50. (b) A.B. Jarzebski, K. Szymanska, J. Bryjak, J. Mrowiec-Białon, *Catal. Today* 124 (2007) 2–10.

[176] L. Washmon-Kriel, V.L. Jimenez, K.J. Balkus, Jr., *J. Mol.Catal B: Enzym*., 10 (2000) 453-469.

[177] E.L. Pires, E.A. Miranda, G.P. Valenca, *Appl. Biochem. Biotechnol*., 98 (2002) 963-976.

[178] J.M. Gomez, J. Deere, D. Goradia, J. Cooney, E. Magner, B.K. Hodnett, *React. Kinet. Catal. Lett*., 88 (2003) 183-191.

[179] N.W. Fadnavis, V. Bhaskar, M.L. Kantam, B.M. Choudary, *Biotechnol. Prog.*, 19 (2003) 346-351.

[180] M.C.R. Hernandez, J.E.M. Wejebe, J. I .V. Alcantara, R.M. Ruvalcaba, L.A. Garcıa Serrano, J.T. Ferrara, *Micropor. Mesopor. Mater*., 80 (2005) 25-31.

[181] Y.J. Wang, F. Caruso, *Chem. Commun*., 13 (2004) 1528-1529.

[182] A.S.M. Chong, X.S. Zhao, *Appl. Surf. Sci*., 237 (2004) 398-404.

[183] B. Kuhlman, G. Dantas, G.C. Ireton, G. Varani, B.L. Stoddard, D. Baker, *Science* 302 (2003)1364–1368.

[184] C. Pabo, C. *Nature*, 301 (1983) 200-200.

[185] C. Anfinsen, *Science* 181 (1973) 223-230.

[186] U. Nath, J.B. Udgaonkar, *Curr. Sci*. 72 (1997) 180-191.

[187] H.M. Wilks, J.J. Holbrook, *Curr. Opin. Struct. Biol*. 2 (1991) 561-567.

[188] P.S. Kim, *Annu. Rev. Biochem.* 59 (1990) 631–660.

[189] S. Tandon, P.M. Horowitz, *J. Biol. Chem.* 262, (1987) 4486–4491.

[190] S. Tandon, P.M. Horowitz, *J. Biol. Chem.* 261, (1986) 15615–15618.

[191] C. Ghelis, J. Yon, (1982) *in* Protein Folding, Academic Press, New York. pp. 471–479.

[192] A.L. Fink, L.J. Calciano, Y. Goto, D.R. Palleros, (1990) Techniques, Structure and Function (Villafranca, J. J., Ed.), Academic Press, New York, pp. 417–424.

[193] Y. Goto, N. Okamura, S. Aimoto, *J. Biochem.* 109 (1991) 746–750.

[194] R.J. Ellis, *Annu. Rev. Biochem.* 60 (1991) 321–347.

[195] J. Martin, T. Langer, R. Boteva, A. Schramel, A.L. Horwich, F.U. Hartl, *Nature* 352 (1991) 36–42.

[196] C. Tanford, *Adv. Protein Chem*. 24 (1970) 1–95.

[197] Q. Yi, M.L. Scalley-Kim, E.J. Alm, D. Baker, *J. Mol. Biol*. 299 (2000) 1341–1351.

[198] D. Neri, M. Billeter, G. Wider, K. Wuthrich, *Science* 257 (1992) 1559–1563.

[199] E.R. McCarney, J.E. Kohn, K.W. Plaxco, *Crit. Rev. Biochem. Mol. Biol*. 40 (2005) 181–189.

[200] D. Shortle, C. Abeygunawardana, *Structure* 1 (1993) 121–134.

[201] B.N. Hammack, C.R. Smith, B.E. Bowler, *J. Mol. Biol*. 311 (2001) 1091–1104.

[202] L. J. Smith, K.M. Fiebig, H. Schwalbe, C.M. Dobson, Folding Des. 1 (1996) R95–R106.

[203] B.M. Gorovits, J.W Seale, P.M. Horowitz , *Biochemistry* 34 (1995) 13928–13933.

[204] D. Shortle, M.S. Ackerman, *Science* 293 (2001) 487–489.

[205] S.W. Englander, L. Mayne, *Annu. Rev. Biophys. Biomol. Struct*. 21(1992) 243–265.

[206] D.R. Shortle, *Curr. Opin. Struct. Biol*. 6 (1996) 24–30.

[207] H. J. Dyson, P.E. Wright, *Chem. Rev*. 104 (2004) 3607–3622.

[208] K.B. Wong, J. Clarke, C.J. Bond, J.L. Neira, S.M. Freund, A.R. Fersht, V. Daggett, *J. Mol. Biol*. 296 (2000) 1257–1282.

[209] T.L. Religa, J.S. Markson, U. Mayor, S.M. Freund, A.R. Fersht, *Nature* 437 (2005) 1053–1056.

[210] N. Sari, P. Alexander, P.N. Bryan, J. Orban, *Biochemistry* 39 (2000) 965–977.

[211] B.S. Russell, R. Melenkivitz, K.L. Bren. *Proc. Natl. Acad. Sci. U.S.A*. 97 (2000) 8312–8317.

[212] J. Wirmer, H. Berk, R. Ugolini, C. Redfield, H. Schwalbe, *Protein Sci*. 15 (2006) 1397–1407.

[213] A.T. Alexandrescu, P.A. Evans, M. Pitkeathly, J. Baum, C.M. Dobson, *Biochemistry* 32 (1993) 1707–1718.

[214] M.C. Pearce, L.D. Cabrita, H. Rubin, M.G. Gore, S.P. Bottomley, *Biochem. Biophys. Res. Commun*. 324 (2004) 729–735.

[215] J.A. Marsh, C. Neale, F.E Jack, W.Y. Choy, A.Y. Lee, K.A. Crowhurst, J.D. Forman-Kay, *J. Mol. Biol*. 367 (2007) 1494–1510.

[216] I.J. Ropson, J.A. Boyer, P.M. Dalessio, *Biochemistry* 45 (2006) 2608–2617.

[217] C. Magg, J. Kubelka, G. Holtermann, E. Haas, F.X. Schmid, *J. Mol. Biol*. 360 (2006) 1067–1080.

[218] E. Welker, K. Maki, M.C. Shastry, D. Juminaga, R. Bhat, H.A. Scheraga, H. Roder, *A. Proc. Natl. Acad. Sci. U.S.A*. 101 (2004) 17681–17686.

[219] V.R. Agashe, M.C. Shastry, J.B. Udgaonkar, *Nature* 377 (1995) 754–757.

[220] C. Camilloni, L. Sutto, D. Provasi, G. Tiana, R.A. Broglia, *Protein Sci*. 17 (2008) 1424–1433.

[221] D.J. Felitsky, M.A. Lietzow, H.J. Dyson, P.E. Wright, *Proc. Natl. Acad. Sci. U.S.A.* 105 (2008) 6278–6283.

[222] O. Bilsel, C.R. Matthews, *Curr. Opin. Struct. Biol*. 16 (2006) 86–93.

[223] T. Kimura, S. Akiyama, T. Uzawa, K. Ishimori, I, Morishima, T. Fujisawa, S. Takahashi, *J. Mol. Biol*. 350 (2005) 349–362.

[224] A.J. Thomson, H.B. Gray, *Curr. Opin. Chem. Biol. 2* (1998) 155-158.

[225] R.B. Hill, D.P. Raleigh, A. Lombardi, W.F. DeGrado, *Acc. Chem.Res.*, 33 (2000) 745-754.

[226] F. Nastri, A. Lombardi, V. Pavone, *Chem. Rev.*, 101 (2001) 3165-3189.

[227] W.F. DeGrado, C.M. Summa, V. Pavone, F. Nastri, A. Lombardi, *Annu. Rev. Biochem.*, 68 (1999) 779-819.

[228] W.F DeGrado, Z.R. Wasserman, J.D. Lear, *Science*, 243 (1989) 622-628.

[229] J.W. Bryson, S.F. Betz, Z.X. Lu, D.J. Suich, H.X. Zhou, *Science*, 270 (1995) 935-941.

[230] L. Regan, *Trends Biochem. Sci., 20 (*1995) 280-285.

[231] H.W. Hellinga, In *Protein Engineering*; Cleland, J. L., Craik,C. S., Eds.; Wiley-Liss: New York, 1996; pp 369-398.

[232] H.W. Hellinga, *Curr. Opin. Biotechnol. 7 (*1996) 437-441.

[233] L. Regan, *Adv. Mol. Cell Biol. 22A (*1997) 51-80.

[234] H.W. Hellinga,. *Folding Des. 3 (*1998) R1-R8.

[235] D.E. Benson, M.S. Wisz, H.W. Hellinga, *Curr. Opin.Biotechnol., 9 (*1998) 370-376.

[236] J.E. Coleman, *Annu. Rev. Biophys. Biomol. Struct.* 21 (1992) 441–483.

[237] X. Xu, E.R. Kantrowitz, *Biochemistry* 32 (1993) 10683–10691.

[238] M.J. Schlesinger, K. Barrett, *J. Biol. Chem.* 240 (1965) 4284–4292.

[239] C. Tanford, *Adv. Protein Chem.* 24 (1970) 1–95.

[240] M.J. Schlesinger, *Brookhaven Symp. Biol.* 17 (1964) 66.

[241] R.L. Koder, J. L. Ross Anderson, L. A. Solomon, K.S. Reddy, C. C. Moser, P.L. Dutton, Nature 458 (2009) 305–309.

[242] K. Okrasa, R.J. Kazlauskas Chem. Eur. J., 12 (2006) 1587–1596.

[243] S. Tandon, P.M. Horowitz, *J. Biol. Chem.* 264 (1989) 9859-9866.

[244] Y.L. Liu, H.T. Lee, C.C. Chang, L.S. Kan, Biochem. Biophys. Res. Commun., 306 (2003) 59–63.

Chapter 2

Immobilization of Alkaline Serine Endopeptidase from Bacillus Licheniformis on Mesoporous Silica Materials SBA-15 and MCF by Surface Covalent Binding

2.1. Introduction

Alkaline proteases are important enzymes having diverse applications in a wide variety of industries such as food, pharmaceutical, detergent, leather, silk, diagnostics, and for the recovery of silver from used X-ray films.[1-4] Alkaline serine endopeptidase from selected strain of Bacillus Licheniformis, which hydrolyses casein, plays a vital role in dairy industries. Casein is a slowly digesting protein which is essential in building muscles in human body and is a major component of milk, whey and soy.[5] The industrial application of this enzyme requires specificity, stability at higher pH and temperature and reusability. Numerous techniques have been used for immobilization of free enzymes on solid support to obtain efficient biocatalysts.[6]

Mesoporous silica's (MPSs) obtained by different templating methods demonstrate high potential as solid supports for enzyme immobilization.[7-22] These supports are environmentally acceptable, structurally more stable, and resistant to microbial attack. MPSs have a large specific surface area (~ 1000 m^2/g) and pore diameter, in the range of 2-50 nm, which can be tuned to host the enzymes of varied size. As such, the enzymes have considerable affinity towards the MPSs surfaces.[7-14] Besides, the MPSs surface can be modified with various anchor groups to covalently bind the enzyme molecules, which could reduce the enzyme leaching from the support during the recycling of the catalyst.[14-22] The uniform distribution of pores in MPSs favors the uniform loading of enzyme as well as facile diffusion of the substrate and product molecules inside the channels. The loading of an enzyme and its activity depends upon the surface area and pore size of the MPSs.[17-22]

Among the MPSs, SBA-15 and MCF have been shown to be efficient supports for covalent immobilization of α-amylase, trypsin, chloroperoxidase, penicillin G acylase, organophosphorus hydrolase, glucose oxidase, glucoamylase, and invertase.[8, 9-11, 14, 19-22] SBA-15 and MCF have pore sizes in the range of 9–25 nm and possess 600-800 m^2/g surface area, which make them suitable to host the alkaline endopeptidase comfortably and also allows substrate and product molecule's facile diffusion towards and from the active site of the enzyme.[18, 21] The average size of the alkaline endopeptidase is 4.7 nm as shown in Fig. 2.1, produced using Chem3D Pro 10.0 from the Research Collaboratory for Structural Bioinformatics (RCSB) enzyme data base.[23]

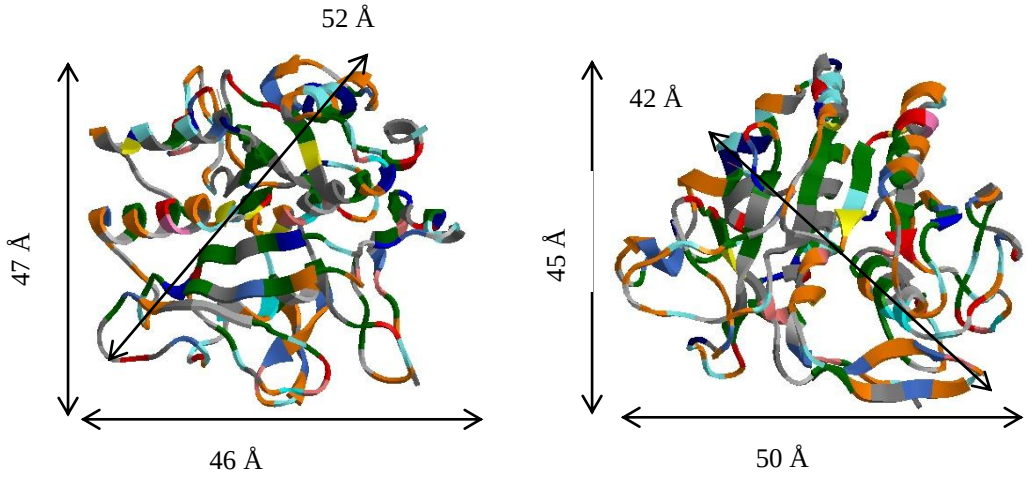

Fig. 2.1 Alkaline serine endopeptidase structure from RCSB protein data base

Alkaline endopeptidase immobilized on polymeric support has been evaluated for stability, activity and reusability with reference to free enzyme.[24-26] In this chapter, covalent immobilization of alkaline serine endopeptidase has been done through amide bond formation on modified SBA-15 and MCF. Surface modification of MPSs was done with 3-aminopropyltriethoxy silane followed by succinic anhydride. The specific activity of the immobilized enzyme was studied using casein as a substrate.

2.2. Experimental section

2.2.1. Materials

Tetraethoxysilane (98%, TEOS), Triblock poly(ethylene oxide)-block-poly(propylene oxide)-block-poly(ethylene oxide) copolymer (Pluronic P123, M_w = 5,800), Bradford reagent (B6916), Na_2HPO_4 (99%, A.R) were from Aldrich (USA). 3-aminopropyl triethoxy silane (98%, APTES), 1-[3-(dimethylamino)propyl]-3-ethyl carbodiimide hydrochloride (EDAC) were purchased from Fluka (USA). Bacterial Alkaline Protease (E.C.3.4.21.62) from Bacillus Licheniformis was donated by Genencor International, Netherlands. Trichloroacetic acid (98%, A.R) was procured from Merck, Germany. 4-N,N-dimethylaminopyridine AR (98%, DMAP), 1,3,5-trimethylbenzene (98%, TMB), Soluble casein A.R, $NaH_2PO_4.2H_2O$ (99% A.R), Na_2CO_3 (98%, A.R) $NaHCO_3$ (98%, A.R) were purchased from s.d Fine Chemical, India. Glycine (98%, A.R), NaOH (98%, A.R) were from Qualigens Fine Chemicals, India. These chemicals were used in MPSs synthesis, surface functionalization and kinetic studies of enzymes.

2.2.2 Synthesis of SBA-15

Highly ordered mesoporous SBA-15 was synthesized[27] using Pluronic P123 triblock copolymer (EO20-PO70-EO20, BASF) as a template and TEOS as a silica source in acidic conditions. In a typical synthesis, 12 g of triblock P123 was dissolved in 90 g of de-ionized water and 360 g of 2 M HCl was added under stirring at ambient temperature (25–30 ^oC) for 90 min. TEOS, 27 g was added to the homogeneous surfactant solution and the mixture was stirred at 40 ^oC for 24 h. Then, it was allowed to stand for crystallization under static hydrothermal conditions at 110 ^oC for 48 h in a

Teflon lined autoclave reactor. The crystallized product was filtered, washed with de-ionized water and dried. Finally, it was calcined at 550 ^{o}C in air for 6 h to remove the template.

2.2.3 Synthesis of MCF

Siliceous MCF syntheses are reported in the literature.[28-33] However, in the present work, MCF was synthesized using the procedure reported by Lettow et al. [29] In a typical synthesis, 4 g of Pluronic P123 triblock copolymer (EO20-PO70-EO20, BASF) was dissolved in 150 mL of 1.6 M HCl followed by addition of 2 g of TMB to the polymer solution. The mixture was stirred for at least 90 min at 35–40 ^{o}C. 8.5 g of TEOS was added as the silica source to this homogeneous emulsion. This mixture was stirred for 24 h at 35–40 ^{o}C and aged for 24 h at 110 ^{o}C, the product was filtered, washed with de-ionized water and dried. Finally, it was calcined at 500 ^{o}C in air for 6 h to remove the template.

2.2.4 Surface modification of SBA–15 and MCF

The surfaces of MPSs were amino functionalized by refluxing 1 g of SBA-15 or MCF with 3 ml of APTES in 100 ml of dry toluene at 110 ^{o}C for 16 h with stirring under N_2 atmosphere. Product was separated by filtration, washed with toluene, dichloromethane and methanol. It was further Soxhlet-extracted using dichloromethane to remove excess APTES. APTES modified samples were labeled as SBA-A and MCF-A. The amino functionalized SBA-15 or MCF was succinylated typically, by adding 1 g into 0.4 g of succinic anhydride and a catalytic amount of DMAP in 100 ml of dry toluene at 60 ^{o}C for 16 h. The functionalization of SBA-15, MCF and immobilization of enzyme is shown in Fig. 2.2. The product was filtered,

washed with toluene and dichloromethane. The samples obtained after succinylation were designated as SBA-S and MCF-S.

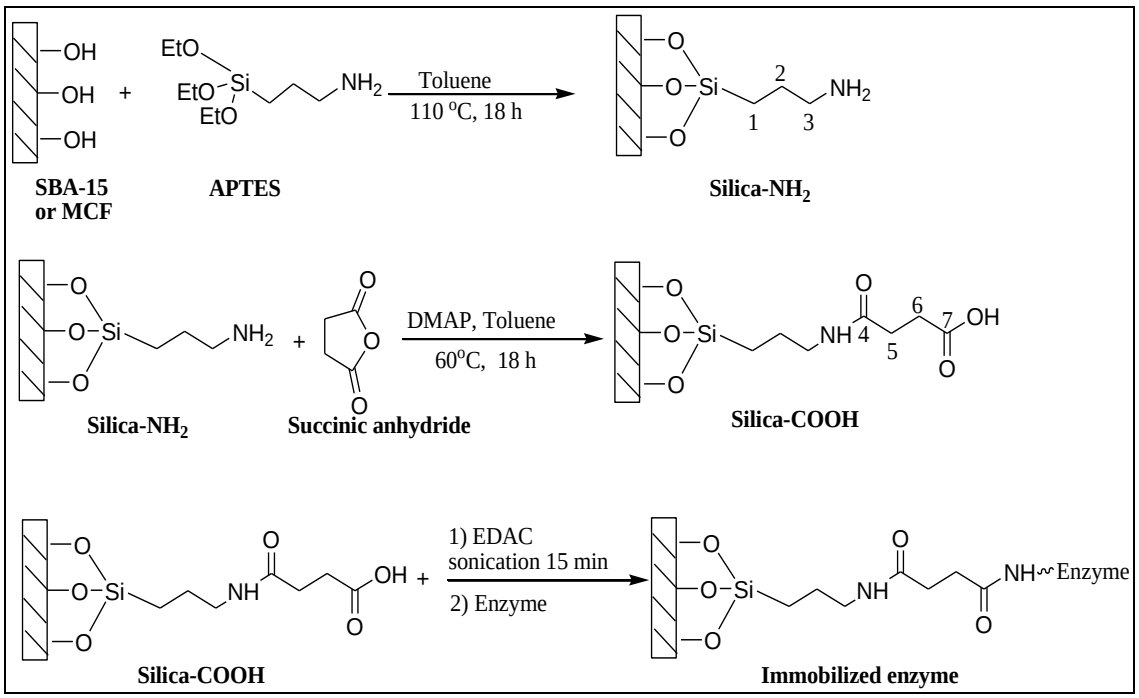

Fig. 2.2 Schematic functionalization of SBA-15, MCF and immobilization of Enzyme

2.2.5 Characterization

Powder X-ray diffraction patterns of calcined samples were recorded with a Philips X'Pert MPD system using Cu Kα X-ray radiations (λ= 1.54056 Å) in 2θ = 0.5° to 10° range in step size of 0.01 and a step time of 10 s. The textural parameters (surface area, S_{BET}; pore volume, V_p and pore diameter d_p) of calcined and surface modified MPSs were obtained from N_2 adsorption data measured at -195.6 °C using a volumetric adsorption set-up (Micromeritics ASAP 2010, USA). All the samples were degassed at 50 °C for 3 h prior to N_2 adsorption. The specific surface area of the sample was calculated by using the Brunauer-Emmett-Teller (BET) method in the relative pressure range (P/P_o) of 0.05–0.3. The pore size distribution was determined using the Barrett-Joyner-Halenda (BJH) method, and pore sizes were obtained from

the peak positions of the distribution curves. Thermogravimetric analysis of calcined, aminated and succinylated MPSs were carried out with a thermal analyzer (Mettler–Toledo TGA/SDTA 851e) up to 850 ^{o}C with a heating rate of 10 ^{o}C/min under N_2 flow (100 ml/min). Fourier transform infrared (FTIR) spectra were collected on a Perkin-Elmer Spectrum GX FT-IR instrument in the range of 400 cm^{-1} to 4000 cm^{-1}. CHN elemental analyses were performed on a Perkin-Elmer (CHNS/O, 2400) analyzer. ^{13}C-NMR solid-state magic-angle spinning (MAS) nuclear magnetic resonance (NMR) spectra were obtained on a Bruker DRX500 MHz with MAS speed of 8 kHZ.

2.2.6 Immobilization of enzyme

In a typical procedure, functionalized SBA-15 or MCF (100 mg) was dried at 100 ^{o}C in a vacuum oven for 30 min. To these dried samples, 25 mg of EDAC was added and the mixture ultrasonicated for 15 min. Alkaline serine endopeptidase (250 µl) diluted with an equal amount of buffer solution was added drop by drop into carboxyl activated SBA-15 or MCF and allowed to incubate for 30 min. The excess protein was removed by washing with excess of buffer and unbound enzyme was estimated by Bradford method.[34]

2.2.7 Activity assay of the enzyme

Activity of both free and immobilized enzyme was measured by incubating free (70 µl) or immobilized enzyme with 1 ml of casein (0.5 %) solution in 0.1 M bicarbonate buffer at pH 9.5, for exactly 20 min at 45 ^{o}C with a stirring speed of 150 rpm. The reaction was stopped by the addition of 3 ml of 10 w/v of trichloroacetic acid and the precipitate was removed by centrifugation. The absorbance due to the

amino acid produced during hydrolysis was measured at 280 nm using a UV-vis-NIR scanning spectrophotometer (CARY Varian 500 SCAN), with L-tyrosine as a standard. One unit of enzyme activity is defined as the amount of enzyme required to hydrolyse casein to increase one absorbance unit at 280 nm due to 1 µmol of tyrosine produced per min at 45 ^{o}C. The kinetic parameters of free and immobilized enzyme were evaluated by incubating with casein concentration of 0.1-0.65% and following the above described procedure.

2.2.8 Effect of pH and temperature on enzyme activity

The effects of temperature and pH on the activity of free and immobilized alkaline serine endopeptidase were investigated. The enzymes were incubated with casein in 0.1M bicarbonate buffer solution having a pH of 9.5 at temperatures ranging from 30 to 80 ^{o}C, and alternatively incubated at a fixed temperature of 45 ^{o}C with pH ranging from 7 to 12 (phosphate buffer, 7-8.5 ; bicarbonate 9-11 ; glycine-NaOH 11.5-12). The activity of alkaline serine endopeptidases at different pH and temperature were then measured according to a previously described (Section 2.2.7) method.

2.2.9 Reusability and deactivation stability of the immobilized enzyme

The initial activity of the immobilized enzyme was measured and then compared with the activity of the used enzyme obtained after its repeated use for 15 cycles with 3 cycles per day. After each cycle, the immobilized enzyme was immediately filtered, washed with buffer solution and stored at 5 ^{o}C. The deactivation stability of free and immobilized enzyme was studied by deactivating at

pH 11, holding for different time intervals at a temperature of 60 ^{o}C and comparing with the activity of fresh enzymes.

2.3. Results and discussion

2.3.1 Characterization of synthesized and surface modified silicas

X-ray diffraction patterns of the calcined SBA-15 and MCF samples are given in Fig. 2.3. The presence of the three reflection peaks corresponding to 100, 110, and 200 planes confirming the presence of the ordered hexagonal mesoporous structure of SBA-15. There was no significant peak observed for MCF.

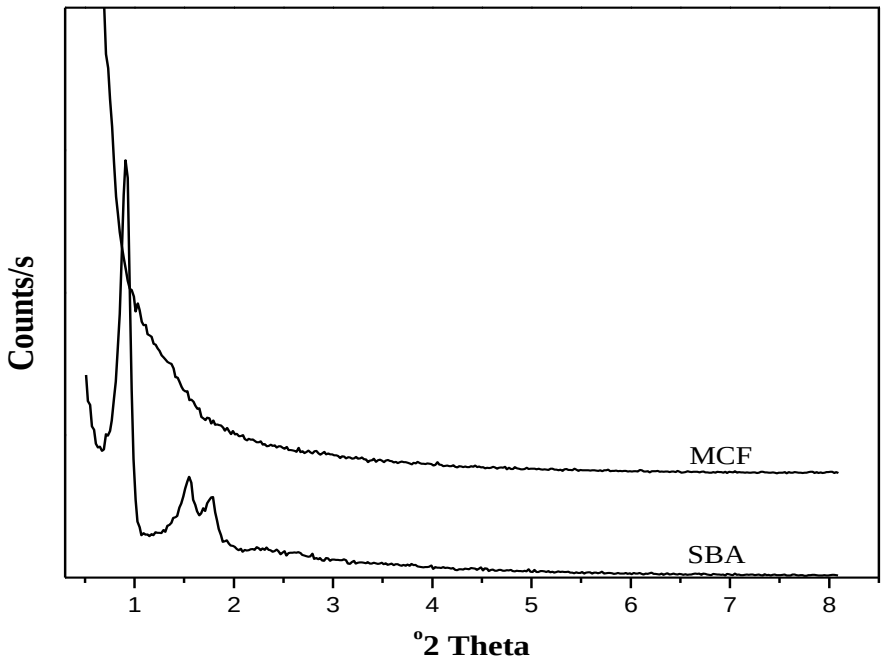

Fig. 2.3 Powder XRD pattern of calcined SBA-15 and MCF

Physico-chemical characterization data of calcined (SBA, MCF), aminated (SBA-A, MCF-A) and succinylated (SBA-S, MCF-S) are shown in Table 2.1. The synthesized and modified MPSs with organosilane followed by succinylation resulted in a decrease of all textural parameters like surface area, pore volume and pore diameter. The calcined samples are having higher BET surface area, pore volume and

pore diameter. On amination of SBA-15 and MCF, all the above parameters were observed to decrease sharply. N_2 adsorption-desorption isotherm and pore size distribution of calcined (SBA, MCF), aminated (SBA-A, MCF-A) and succinylated (SBA-S, MCF-S) is given in Fig. 2.4 and Fig.2.5. The sharp decrease in adsorbed volume at relative pressure (P/P_o) in the range of 0.2 to 0.9 is an indication of uniform functionalization on the surface.

Table 2.1 Physico-chemical characterization data of calcined (SBA, MCF), aminated (SBA-A, MCF-A) and succinylated (SBA-S, MCF-S)

Sample	N_2 adsorption			Elemental (CHN) analysis		
	Surface area S_{BET} (m^2/g)	Total pore volume $V_p N_2$ (cm^3/g)	Pore diameter d_m (Å)	%C	%H	%N
SBA	638	0.91	94	-	-	-
SBA-A	352	0.23	80	09.41	4.82	3.36
SBA-S	116	0.20	63	19.73	3.21	2.85
MCF	682	0.82	218	-	-	-
MCF-A	336	0.42	187	11.26	3.00	3.91
MCF-S	116	0.33	178	20.00	3.35	2.89

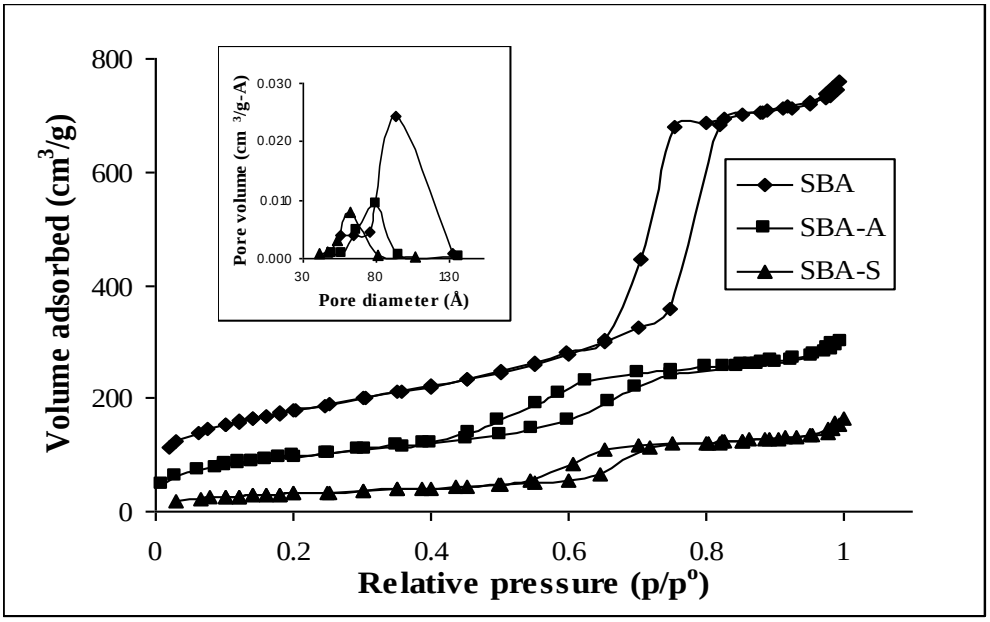

Fig. 2.4 N_2 adsorption-desorption isotherm and pore size distribution of SBA, SBA-A and SBA-S

However, succinylated MPSs were observed to have surface area (65.5%), pore volume (21.4%) and pore diameter (4.8%) decrease values compared to aminated MPSs. This shows that amination and then succinylation have occurred inside the pores as well as on the surfaces of the MPSs. The pore diameter values of succinylated SBA (63 Å) and MCF (178 Å) are large enough to host the alkaline serine endopeptidase inside their channels. However, the possibility of some enzyme molecules to be present on the external surface cannot be ruled out.

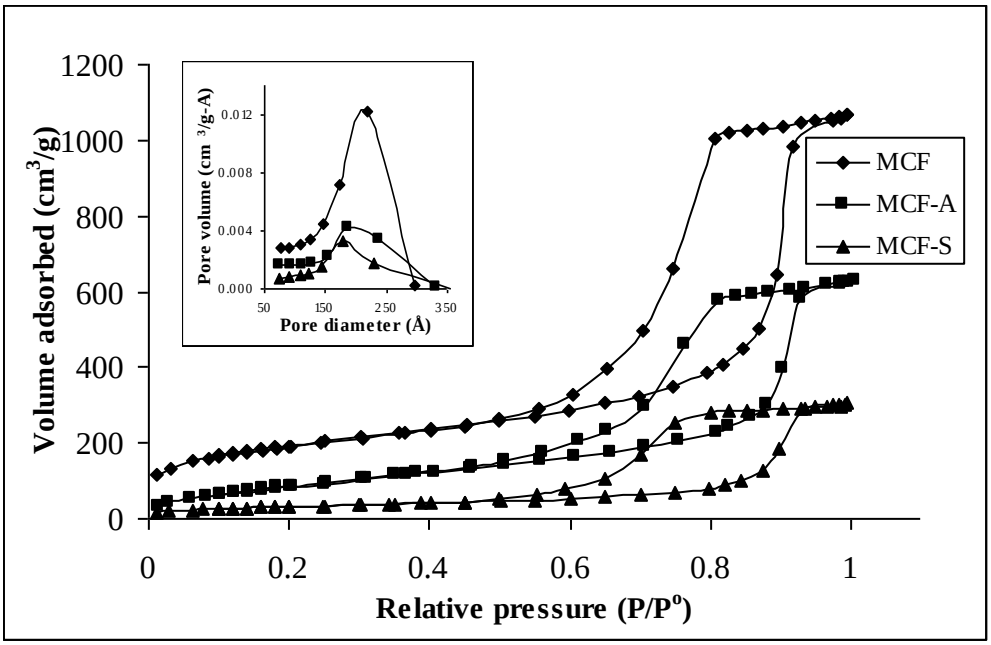

Fig. 2.5 N_2 adsorption-desorption isotherm and pore size distribution of MCF, MCF-A and MCF-S

The amino functionalization followed by succinylation of SBA-15 and MCF was analyzed by FTIR spectroscopy. Fig. 2.6 shows the FT-IR spectra for calcined SBA, SBA-A and SBA-S. FT-IR spectra for calcined MCF, MCF-A and MCF-S are given in Fig. 2.7. The broad band at 3600–3000 cm^{-1} for hydrogen bonded silanol[35-36] was appreciably reduced in the modified samples. The organosilane presence was identified by the absorbance of the band 2950-2850 cm^{-1} for the propyl chain [9] and the deformation bands at 1455-1410 cm^{-1}.[36] The N-H absorption band overlapped with O-H bands at 3300-3500 cm^{-1}.[9]

The presence of bands at 1710 cm $^{-1}$ (-C=O, acid), 1695-1650 cm^{-1} (-C=O amide I band), 1566-1561 (-NH amide II band) and 1415-1419 cm^{-1} (-C-N amide) confirmed that succinylation had taken place in MPSs.[37]

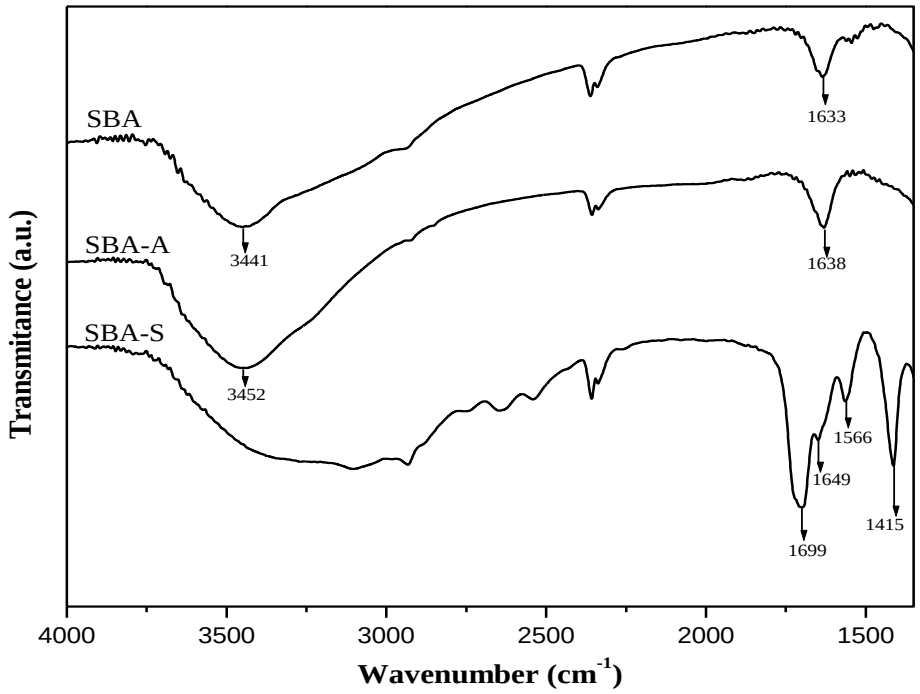

Fig. 2.6 IR spectra of calcined (SBA), aminated (SBA-A) and succinylated (SBA-S)

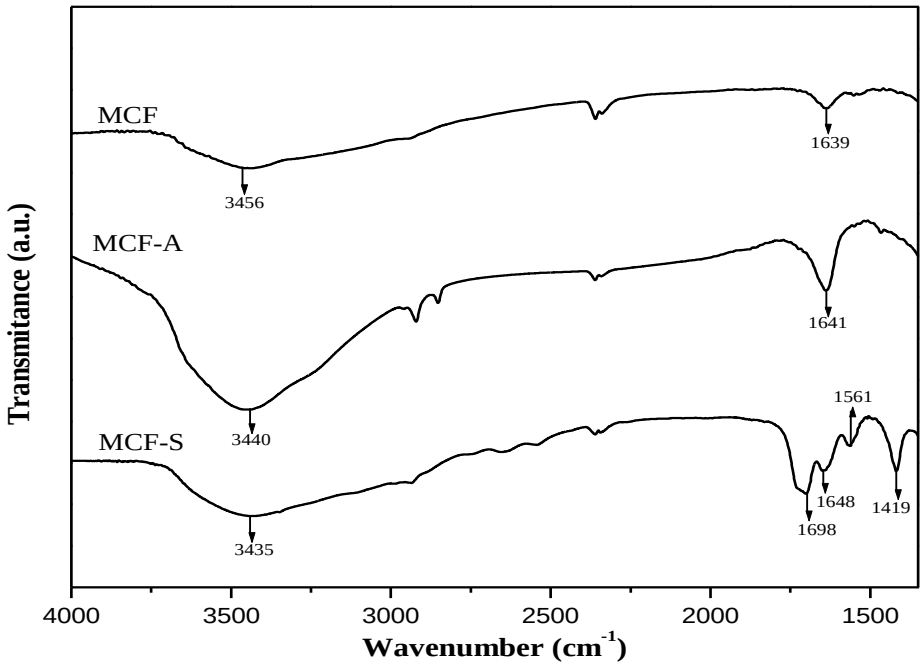

Fig. 2.7 IR spectra of calcined (MCF), aminated (MCF-A) and succinylated (MCF-S)

C,H and N are not observed in calcined SBA-15 and MCF. However, upon functionalization with APTES followed by succinylation, C, H and N were observed in modified MPS's (Table 2.1). On succinylation of aminated MPSs the overall %N is expected to decrease and the data indeed show this trend.

The data shown in Fig. 2.8 and Fig. 2.9 are TGA of calcined, aminated and succinylated SBA-15 and MCF samples, respectively. The TGA curves of pristine calcined samples showed no appreciable weight losses, aminated samples showed one sharp weight loss between 368 ^{o}C and 617 ^{o}C with 9% weight loss due to aminopropyl group decomposition. Succinylated samples gave two sharp weight losses, 123 ^{o}C to 226 ^{o}C with 8% weight loss due to succinyl and 436 ^{o}C to 587 ^{o}C with 3% weight loss due to aminopropyl decompositions on MPSs.

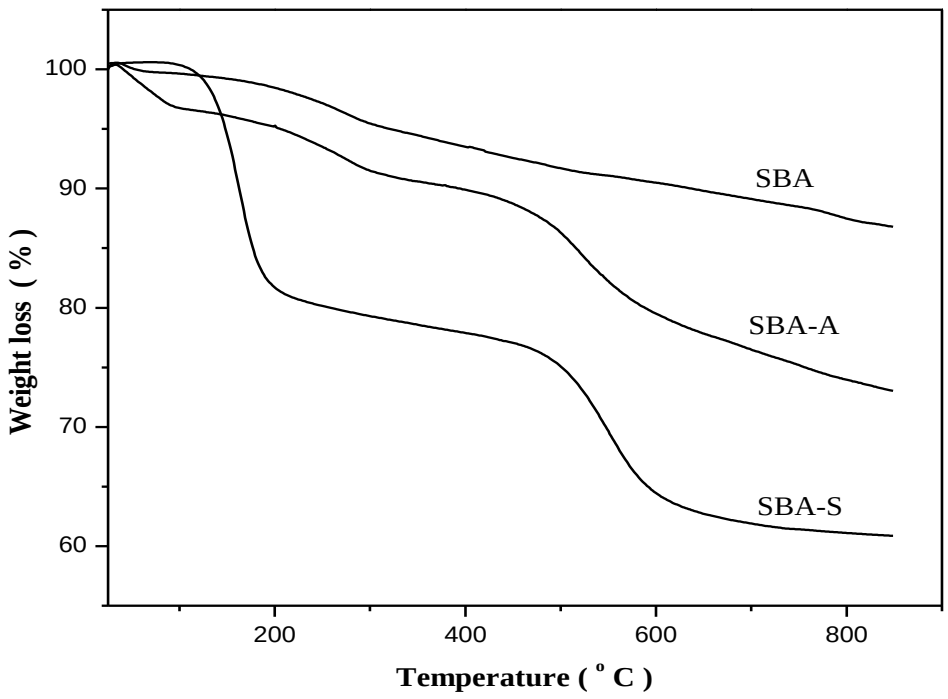

Fig. 2.8 TGA curve of calcined (SBA), aminated (SBA-A) and succinylated (SBA-S)

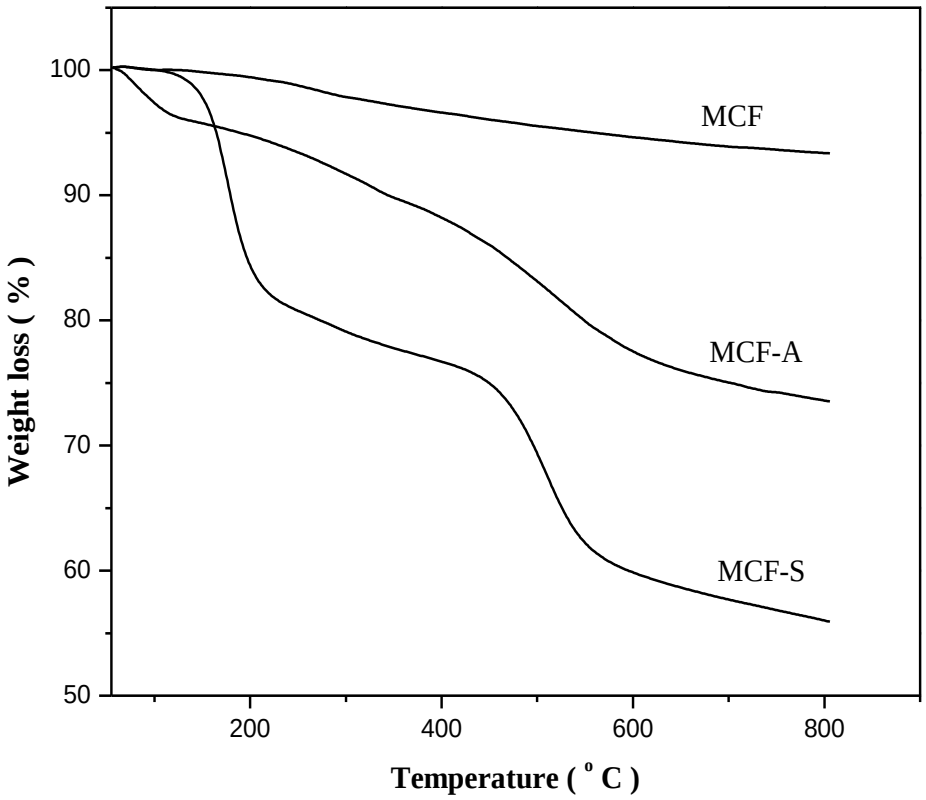

Fig. 2.9 TGA curve of calcined (MCF), aminated (MCF-A) and succinylated (MCF-S)

The amination[34] and succinylation of MPSs were further confirmed by solid state ^{13}C- MAS NMR spectroscopy. ^{13}C NMR spectra of aminated (SBA-A, MCF-A) and succinylated (SBA-S, MCF-S) are shown in Fig. 2.10. The SBA-A sample gave peak values at 7.51 (-C_1-), 19.13 (-C_2-) and 39.81 (-C_3-) ppm and the MCF-A sample at 7.27 (-C_1-), 19.04 (-C_2-) and 39.87 (-C_3-) ppm. The chemical shift values for the SBA-S methylene carbons were 7.08 (-C_1-), 19.85 (-C_2-), 39.76 (-C_3-), 25.53 (-C_5-) and 28.27 (-C_6-) and for the carbonyl carbons 174.71 (-(-C_4-, amide) and 177.31 (-C_7-, acid) ppm. In case of MCF-S methylene carbons were at 7.37 (-C_1-), 18.66 (-C_2-), 39.49 (-C_3-), 25.39 (-C_5-), 27.21 (-C_6-) and carbonyl carbons were at 174.40 (-C_4-, amide) and 177.24 (-C_7-, acid) ppm.

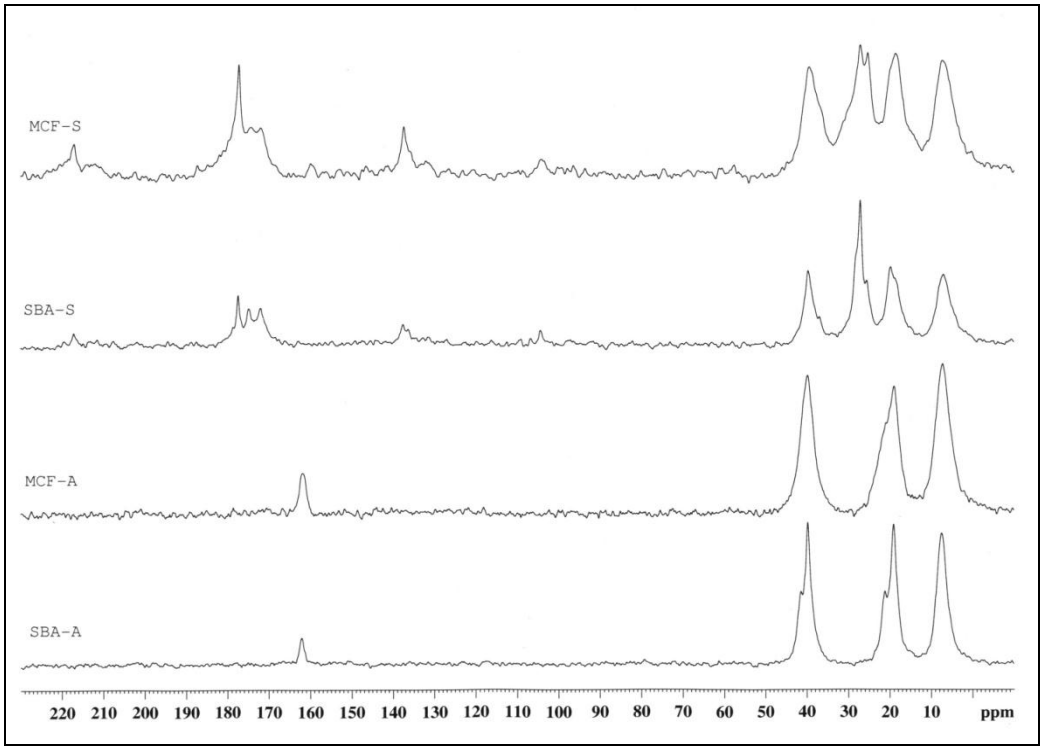

Fig. 2.10 Solid state ^{13}C-MAS NMR spectra of aminated (SBA-A, MCF-A) and succinylated (SBA-S, MCF-S)

2.3.2 Activity of the enzyme

The kinetic parameters of the Michaelis-Menten equation were determined for free and immobilized enzymes. Experiments were carried out by using various substrate concentrations 0.1% to 0.65% as shown in Table. 2.2 and Fig. 2.11. The MCF immobilized enzyme (MCF-Enz) shows higher specific activity than the SBA immobilized (SBA-Enz) and the free enzyme (Free-Enz).

Table 2.2 Experimental data of activity at different substrate (casein) concentration

MCF-Enz					
Conc. of Casein (%)	Enzyme amount (µl)	Product (g/L)	Rate of reaction x 10^{-7} (mol/min)	Enzyme activity x 10^{-8} (mol/sec)	Specific activity x10^{-2} (µ mol $mg^{-1}min^{-1}$)
0.05	123	0.103	4.737	8.53	64.79
0.10	108	0.106	4.875	8.78	75.94
0.20	97	0.109	5.013	9.02	86.94
0.30	101	0.148	6.807	12.3	113.37
0.50	94	0.185	8.509	15.3	152.27
0.65	106	0.232	10.670	19.2	169.34

SBA-Enz					
Conc. of Casein (%)	Enzyme amount (µl)	Product (g/L)	Rate of reaction x 10^{-7} (mol/min)	Enzyme activity x 10^{-8} (mol/sec)	Specific activity x10^{-2} (µ mol $mg^{-1}min^{-1}$)
0.05	124	0.0808	3.716	6.69	50.42
0.1	109	0.0897	4.126	7.43	63.67
0.3	107	0.128	5.887	10.6	92.56
0.5	93	0.172	7.911	14.2	143.09
0.65	94	0.190	8.739	15.7	156.39
Free-Enz					
Conc. of Casein (%)	Enzyme amount (µl)	Product (g/L)	Rate of reaction x 10^{-7} (mol/min)	Enzyme activity x 10^{-8} (mol/sec)	Specific activity x10^{-2} (µ mol $mg^{-1}min^{-1}$)
0.05	70	0.0403	1.854	3.34	44.54
0.1	70	0.0517	2.378	4.28	57.14
0.3	70	0.0859	3.950	7.11	94.92
0.5	70	0.120	5.519	9.93	132.63
0.65	70	0.136	6.255	11.3	150.32

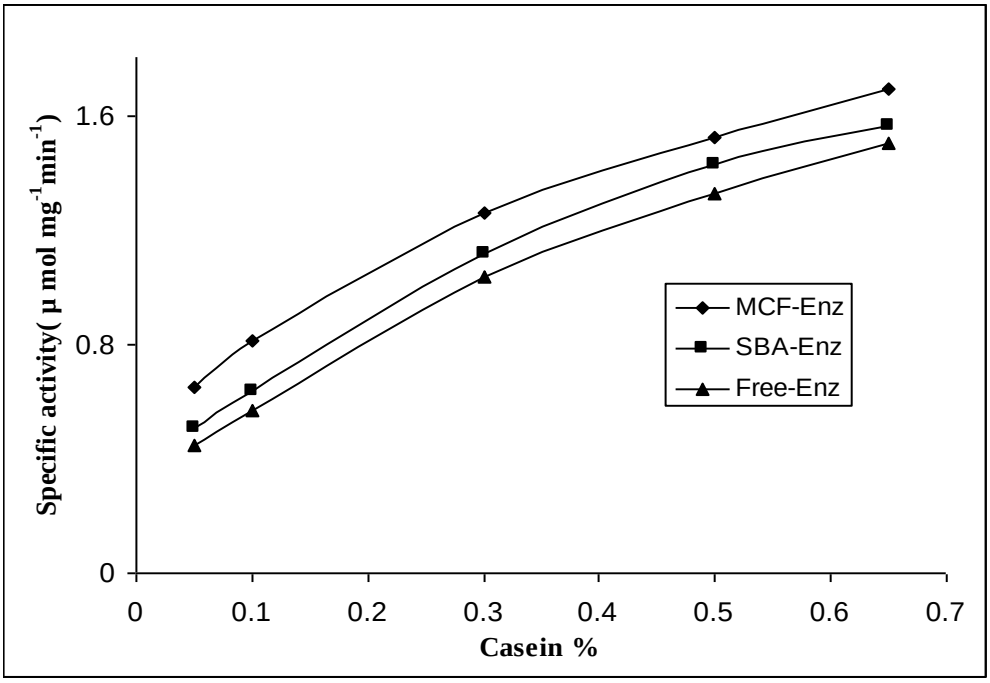

Fig. 2.11 Comparison of activity at different substrate (casein) concentration

The Michaelis-Menten constant (K_m) and the maximum reaction velocity (V_{max}) values were calculated from Lineweaver–Burk plots (Fig. 2.12) by the linear regression method with R^2 value of 0.95. K_m values were found to be 13.375, 11.956, and 8.698 x 10^{-4} mg/ for free, SBA-15 immobilized, and MCF immobilized enzymes respectively. V_{max} values were calculated as 0.156, 0.163 and 0.17 x 10^{-3} U/mg for free, SBA-15 immobilized, and MCF immobilized enzymes respectively. Km value of both MPSs immobilized enzymes were lower than free enzyme, which reveals lower affinity of enzyme to the substrate.

Table 2.3 Calculated 1/S and 1/V values for Lineweaver–Burk plot

MCF-Enzyme			
S x 10^{-3} (mg/ml)	1/S (ml/mg)	Specific activity x10^{-2} (μ mol$mg^{-1}min^{-1}$)	1/V (min/U)
0.5	2000	64.79	15434.6
1.0	1000	81.20	12315.2
3.0	333.3	125.90	7942.8
5.0	200.0	152.27	6567.2
6.5	153.8	169.34	5905.3
SBA-Enzyme			
S x 10^{-3} (mg/ml)	1/S (ml/mg)	Specific activity x10^{-2} (μ mol $mg^{-1}min^{-1}$)	1/V (min/U)
0.5	2000	50.42	19835.2
1.0	1000	63.67	15705.8
3.0	333.3	11.17	8952.6
5.0	200.0	143.09	6988.4
6.5	153.8	156.39	6394.4
Free Enzyme			
S x 10^{-3} (mg/ml)	1/S (ml/mg)	Specific activity x 10^{-2} (μ mol $mg^{-1}min^{-1}$)	1/V (min/U)
0.5	2000	44.54	22450.2
1.0	1000	57.14	17499.8
3.0	333.3	103.50	9661.8
5.0	200.0	132.63	7539.5
6.5	153.8	150.32	6652.5

For immobilized enzymes, the calculated V_{max} value was found to be higher than that of the free enzyme. The calculated V_{max} value for MCF immobilized enzyme was higher than that of the SBA-15 immobilized enzyme, though the loading of the enzyme was the same. The observed increase in the kinetic parameters could be due to the increase in diffusion of substrate and product molecules in SBA-15 and MCF. No significant structural changes of the enzyme upon immobilization on SBA-15 and MCF are expected as enzyme activity is higher than the free enzyme.

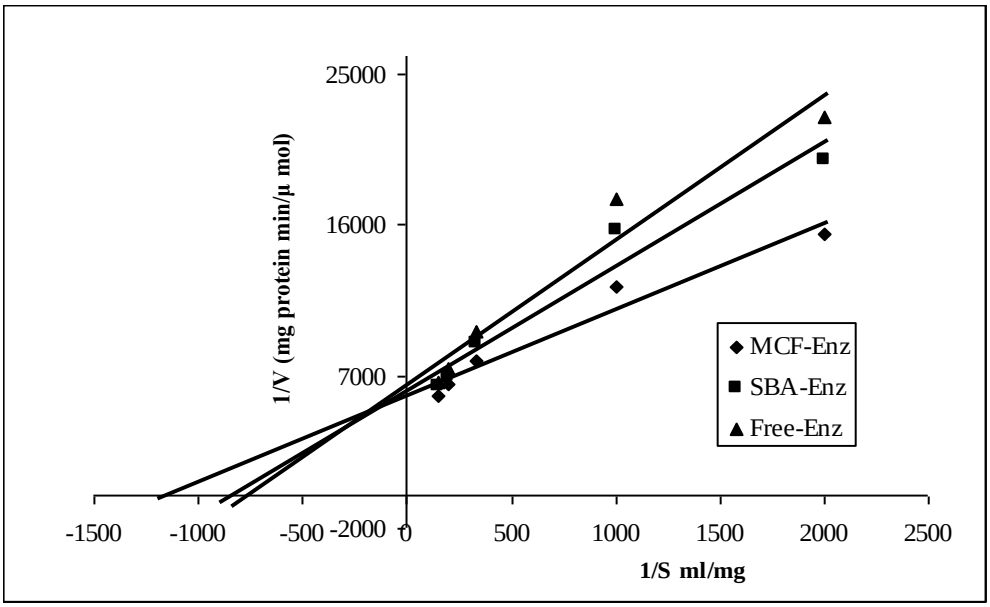

Fig. 2.12 L-B plot for kinetic parameters of free and immobilized enzymes

The specific activity of MCF (218 Å) immobilized enzyme was higher than that of SBA (94 Å) immobilized enzyme, which implies that larger pore diameter facilitates the diffusion of the casein (dimension ~ 50 Å, M.W= ~ 30 kD) towards the active sites of the enzyme where it is gets hydrolyzed.[8] This increased activity could also be due to the easy accessibility of substrate molecules to active sites of covalently attached enzyme particularly with the eight atom long chain carrier inside the pore as well as on the external surface of the MPSs.

Table 2.4 Experimental data of effect of pH on free and immobilized enzymes activities

MCF-Enz					
pH	Enzyme amount (µl)	Product (g/L)	Rate of reaction x 10^{-8} (mol/min)	Enzyme activity x 10^{-8} (mol/sec)	Specific activity x 10^{-2} (µ mol $mg^{-1}min^{-1}$)
7.0	98	0.165	75.887	13.660	130.27
7.5	91	0.159	73.128	13.163	135.19
8.0	92	0.163	74.967	13.494	137.08
8.5	94	0.168	77.267	13.908	138.28
9.0	124	0.233	107.162	19.289	145.38
9.5	94	0.185	85.085	15.315	152.27
10.0	99	0.204	93.824	16.888	159.43
10.5	114	0.231	106.242	19.124	156.78
11.0	103	0.201	92.444	16.640	150.98
11.5	91	0.174	80.027	14.405	147.94
12.0	93	0.171	78.647	14.156	142.26
SBA-Enz					
pH	Enzyme amount (µl)	Product (g/L)	Rate of reaction x 10^{-8} (mol/min)	Enzyme activity x 10^{-8} (mol/sec)	Specific activity x 10^{-2} (µ mol $mg^{-1}min^{-1}$)
7.0	92	0.148	68.069	12.252	124.47
7.5	97	0.159	73.128	13.163	126.82
8.0	89	0.151	69.448	12.501	131.27
8.5	97	0.171	78.647	14.156	136.40
9.0	108	0.194	89.225	16.061	138.98
9.5	93	0.172	79.107	14.239	143.09
10.0	98	0.186	85.546	15.398	146.85
10.5	113	0.209	96.124	17.302	143.10
11.0	108	0.195	89.685	16.143	139.70
11.5	101	0.179	82.326	14.819	137.12
12.0	91	0.154	70.828	12.749	130.93
Free- Enz					
pH	Enzyme amount (µl)	Product (g/L)	Rate of reaction x 10^{-8} (mol/min)	Enzyme activity x 10^{-8} (mol/sec)	Specific activity x10^{-2} (µ mol $mg^{-1}min^{-1}$)
7.0	70	0.109	50.132	9.024	120.48
7.5	70	0.112	51.511	9.272	123.79
8.0	70	0.114	52.431	9.438	126.00
8.5	70	0.116	53.351	9.603	128.21
9.0	70	0.119	54.731	9.852	131.53
9.5	70	0.121	55.651	10.017	133.74
10.0	70	0.119	54.731	9.852	131.53
10.5	70	0.116	53.351	9.603	128.21
11.0	70	0.110	50.592	9.107	121.58
11.5	70	0.109	50.132	9.024	120.48
12.0	70	0.107	49.212	8.858	118.27

The experimental data of Table 2.4, Table 2.5 and Fig.2.13 show the relative specific activity of the free enzyme and the immobilized enzymes at pH values ranging from 7 to 12. In the free enzyme, the specific activity increased with increasing pH upto a pH of 9.5, after that the activity started to decrease. In case of SBA and MCF immobilized enzymes, the optimum pH was found to be 10 beyond which a decrease in specific activity was seen.

Table 2.5 Calculated relative activities at various pH

	MCF-Enz		SBA-Enz		Free Enz	
pH	Specific Activity x 10^{-2}	Relative activity (%)	Specific Activity x 10^{-2}	Relative activity (%)	Specific Activity x 10^{-2}	Relative activity (%)
7.0	130.27	81.71	124.47	78.07	120.48	75.57
7.5	135.19	84.79	126.82	79.55	123.79	77.65
8.0	137.08	85.98	131.27	82.34	126.00	79.03
8.5	138.28	87.80	136.40	85.55	128.21	80.42
9.0	145.38	91.19	138.98	87.17	131.53	82.50
9.5	152.27	95.51	143.09	89.75	133.74	83.89
10.0	159.43	100	146.85	92.11	131.53	82.50
10.5	156.78	98.34	143.10	89.76	128.21	80.42
11.0	150.98	94.70	139.70	87.62	121.58	76.26
11.5	147.94	92.79	137.12	86.01	120.48	75.57
12.0	142.26	89.23	130.93	82.13	118.27	74.18

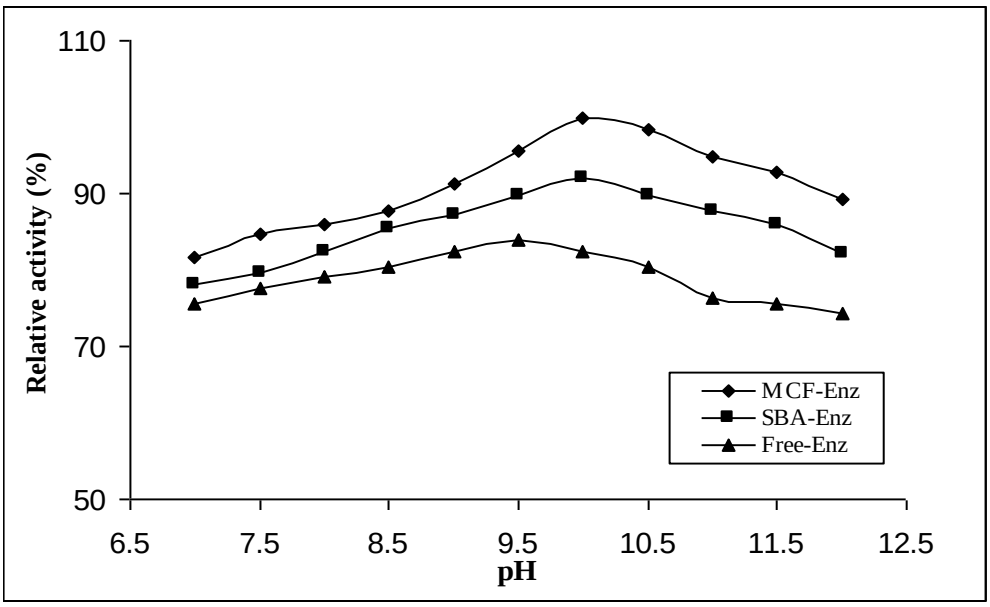

Fig. 2.13 Effect of pH on free and immobilized enzymes activities

Table 2.6 Experimental data of temperature on free and immobilized enzymes

MCF-Enz					
Temp. (°C)	Enzyme amount (µl)	Product (g/L)	Rate of reaction x 10^{-8} (mol/min)	Enzyme activity x 10^{-8} (moles/sec)	Specific activity x10^{-2} (µ mol $mg^{-1}min^{-1}$)
35	113	0.201	92.44	16.64	137.62
40	99	0.181	83.25	14.98	141.45
45	94	0.185	85.09	15.32	152.27
50	114	0.239	10.99	19.79	162.21
55	96	0.245	11.27	20.28	197.46
60	98	0.26	11.96	21.52	205.27
65	102	0.241	11.08	19.95	182.81
70	118	0.239	10.99	19.79	156.71
85	91	0.165	75.89	13.66	140.29
80	93	0.159	73.13	13.16	132.28
SBA-Enz					
Temp. (°C)	Enzyme amount (µl)	Product (g/L)	Rate of reaction x 10^{-8} (mol/min)	Enzyme activity x 10^{-8} (mol/sec)	Specific activity x10^{-2} (µ mol $mg^{-1}min^{-1}$)
35	103	0.166	76.35	13.74	124.69
40	99	0.171	78.65	14.16	133.64
45	93	0.173	79.57	14.32	143.93
50	118	0.230	105.78	19.04	150.81
55	99	0.237	109.00	19.62	185.22
60	100	0.256	117.74	21.19	198.07
65	105	0.231	106.24	19.12	170.21
70	122	0.221	101.64	18.30	140.15
75	101	0.171	78.65	14.16	130.99
80	116	0.185	85.09	15.32	123.39
Free-Enz					
Temp. (°C)	Enzyme amount (µl)	Product (g/L)	Rate of reaction x 10^{-8} (mol/min)	Enzyme activity x 10^{-8} (mol/sec)	Specific activity x 10^{-2} (µ mol $mg^{-1}min^{-1}$)
35	70	0.108	49.67	8.94	119.37
40	70	0.110	50.59	9.11	121.58
45	70	0.117	53.81	9.69	129.32
50	70	0.132	60.71	10.93	145.90
55	70	0.161	74.05	13.33	177.95
60	70	0.155	71.29	12.83	171.32
65	70	0.143	65.77	11.84	158.06
70	70	0.115	52.89	9.52	127.11
75	70	0.109	50.13	9.02	120.48
80	70	0.104	47.83	8.61	114.95

The experimental data in Table 2.6, Table 2.7 and Fig. 2.14 shows the relative specific activity of the enzyme at different temperatures. In the free enzyme, the specific activity increased with increasing temperature, but beyond 55 ^{o}C the activity showed a sharp decrease. But in the case of SBA and MCF immobilized enzymes, the optimum temperature was found to be 60 ^{o}C and the specific activity decreased gradually at temperatures higher than that.

Table 2.7 Calculated Relative activities at various temperatures

	MCF-Enz		SBA-Enz		Free Enz	
Temp. (°C)	Specific Activity x 10^{-2}	Relative activity (%)	Specific Activity x 10^{-2}	Relative activity (%)	Specific Activity x 10^{-2}	Relative activity (%)
35	137.62	67.04	124.69	60.74	119.37	58.15
40	141.45	68.91	133.64	65.11	121.58	59.23
45	152.27	74.18	143.93	70.12	129.32	63.00
50	162.21	79.02	156.81	76.39	145.90	71.08
55	197.45	96.19	185.22	90.23	177.95	86.69
60	205.27	100	198.07	96.49	171.32	83.46
65	182.81	89.06	170.21	82.92	158.06	77.00
70	156.71	76.34	140.15	68.28	127.11	61.92
75	140.29	68.34	130.99	63.81	120.48	58.69
80	132.28	64.44	123.39	60.11	114.95	56.00

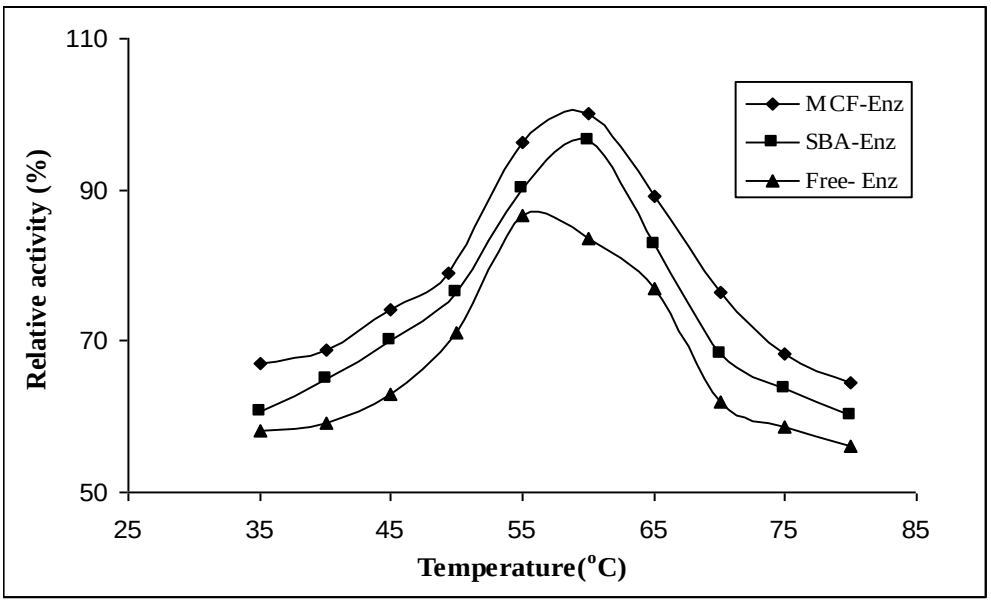

Fig. 2.14. Effect of temperature on free and immobilized enzymes activities

The reusability data of SBA and MCF immobilized enzyme are shown in Table 2.8 and Fig.2.15.

Table 2.8 Reusability data of SBA-15 and MCF immobilized enzyme

MCF-Enz				SBA-Enz		
Cycles	Enzyme Activity x 10^{-2}	Relative activity (%)		Cycles	Enzyme Activity x 10^{-2}	Relative activity (%)
1	122.52	100		1	108.45	100
2	112.59	91.89		2	98.52	90.84
3	113.42	92.57		3	99.34	91.60
4	111.76	91.22		4	96.03	88.55
5	110.11	89.86		5	93.55	86.26
6	105.97	86.49		6	91.89	84.73
7	106.79	87.16		7	93.55	86.26
8	104.31	85.14		8	90.24	83.21
9	101.00	82.43		9	88.58	81.68
10	102.66	83.78		10	86.10	79.39
11	99.34	81.08		11	84.44	77.86
12	96.03	78.38		12	81.96	75.57
13	94.38	77.03		13	77.82	71.76
14	91.97	75.06		14	71.85	66.25
15	94.09	76.79		15	69.54	64.12

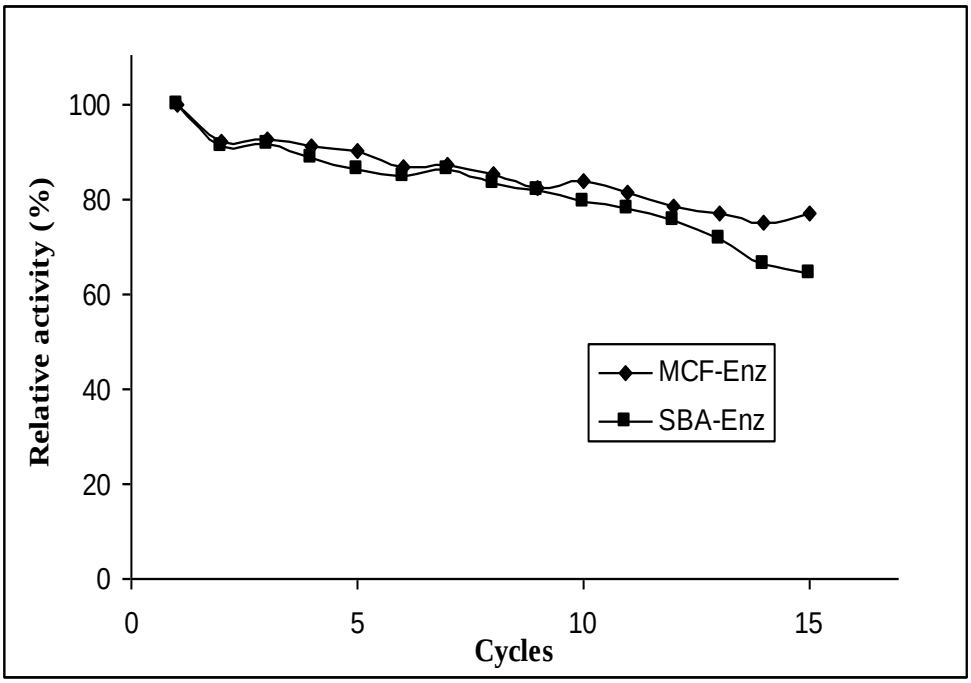

Fig. 2.15 Effect of reuse number on the enzymes activities

The relative activity of MCF immobilized enzyme was higher than that of the SBA immobilized enzyme. Initially, there was a rapid decrease which could be due to the leaching of ionic immobilized and encapsulated enzyme.

Table 2.9 Data of deactivation of free and immobilized enzymes activities

MCF-Enz					
Time	Enzyme amount (µl)	Product (g/L)	Rate of reaction x 10^{-8} (mol/min)	Enzyme activity x 10^{-8} (mol/sec)	Specific activity x 10^{-2} (µ mol $mg^{-1}min^{-1}$)
30	81	0.221	67.76	12.2	140.73
45	83	0.248	50.69	9.12	102.75
60	97	0.291	44.61	8.03	77.37
90	101	0.297	30.36	5.46	50.56
120	84	0.288	22.08	3.97	44.21
180	97	0.341	17.43	3.13	30.22
SBA-Enz					
Time	Enzyme amount (µl)	Product (g/L)	Rate of reaction x 10^{-8} (mol/min)	Enzyme activity x 10^{-8} (mol/sec)	Specific activity x 10^{-2} (µ mol $mg^{-1}min^{-1}$)
30	83	0.198	60.71	10.9	123.05
45	106	0.264	53.96	9.71	85.64
60	92	0.224	34.34	6.18	62.79
90	94	0.237	24.22	4.36	43.35
120	97	0.299	22.92	4.13	39.75
180	102	0.296	15.13	2.72	24.95
Free Enz					
Time	Enzyme amount (µl)	Product (g/L)	Rate of reaction x 10^{-8} (mol/min)	Enzyme activity x 10^{-8} (mol/sec)	Specific activity x 10^{-2} (µ mol $mg^{-1}min^{-1}$)
30	70	0.183	56.11	10.1	134.85
45	70	0.186	38.02	6.84	91.37
60	70	0.191	29.28	5.27	70.37
90	70	0.194	19.83	3.57	47.65
120	70	0.201	15.41	2.77	37.03
180	70	0.226	11.55	2.08	27.76

The activity was found to decrease after every cycle because of loss of small amount of enzyme immobilized MPSs in each cycle. The relative specific activity of deactivation studies at different time intervals is shown in Table 2.9 and Fig. 2.16.

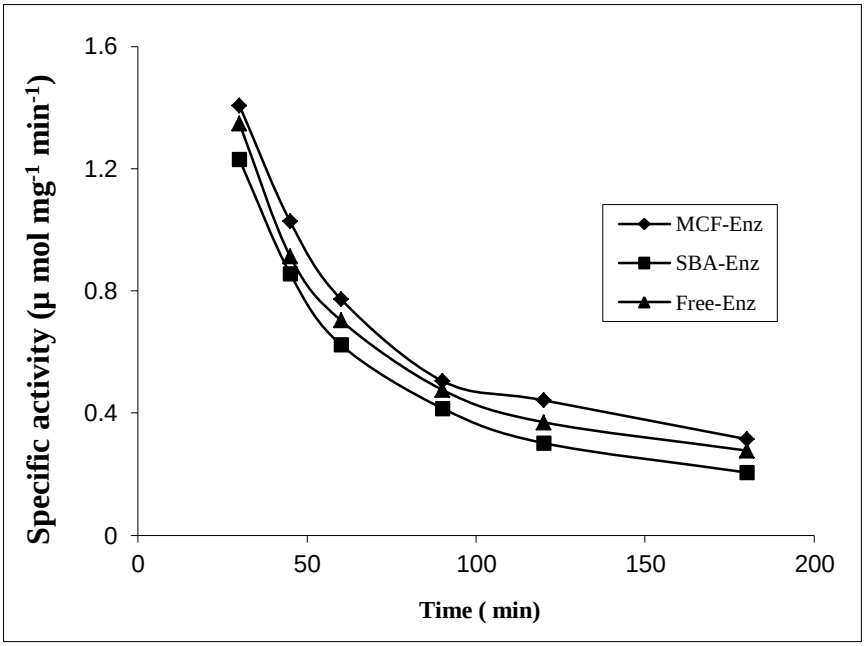

Fig. 2.16 Effect of deactivation of free and immobilized enzymes activities

The specific activities of free and immobilized enzymes decrease with increasing time. However, the MCF immobilized enzymes showed higher specific activity than the SBA-15 immobilized and free enzyme. The multi point covalent attachment of enzyme on surface functionalized MPSs rigidify the enzyme's globular structure to some extent, later the enzyme structure get denature due to the higher temperature and pH of reaction condition. Hence the SBA-15 and MCF immobilized alkaline serine endo peptidase are given better operational stability than the free enzyme.

2.4 References:

[1] Cowan D, *Trends Biotechnol*. 14 (1996)177–188.

[2] C.G. Kumar, H. Takagi, *Biotechnol. Adv*. 17 (1999) 561–594.

[3] L. Hedstrom, *Chem. Rev*. 102 (2002) 4501-4523.

[4] A. Anwar, M. Saleemuddin, *Biotechnol. Appl. Biochem*. 31 (2000) 85–89.

[5] E. Bramanti, C. Sortino, G. Raspi, R.E. Synovec, *Analyst* 126 (2001) 995–1000.

[6] K. Buchholz, V. Kasche, U.T. Bornscheuer, Biocatalysts and Enzyme Technology, Wiley–VCH, Weinheim, 2005.

[7] J.F. Diaz, K.J. Balkus Jr, *J. Mol. Catal. B* 2 (1996) 115-126.

[8] P.H. Pandaya, R.V. Jasra, B.L. Newalker, P.N. Bhatt, *Microporous Mesoporous Mater*. 77 (2005) 67-77.

[9] A.B. Jarzębski, K. Szymańska, J. Bryjak, J. Mrowiec-Białoń., *Catal.Today* 124 (2007) 2–10.

[10] S. Jang, D. Kim, J. Choi, K. Row, W. Ahn, *J. Porous Mater*. 13 (2006) 385-391.

[11] H.H.P. Yiu, P.A. Wright, N.P. Botting, *J. Mol. Catal. B* 15 (2001) 81-92.

[12] H.H.P. Yiu, P.A. Wright, N.P. Botting, *Microporous Mesoporous Mater*. 44–45 (2001) 763-768.

[13] H. Takahashi, B. Li, T. Sasaki, C. Miyazaki, T. Kajino, S. Inagaki, Microporous Mesoporous Mater. 44–45 (2001) 755-762.

[14] Y.J. Han, T. Watson, G.D. Stucky, A. Butler, J. Mol. Catal. B 17 (2002) 1–8.

[15] J. Deere, E. Manger, J.G. Wall, B.K. Hodnett, Catal. Lett. 85 (2003) 19-23.

[16] A.Vima, V. Mangesan, O. Tangerman, M. Hartman, Chem. Mater. 16 (2004) 3056-3065.

[17] D. Goradia, J. Cooney, B.K. Hodnett, E. Manger, J. Mol. Catal. B 32 (2005) 231-239.

[18] Y. Wang, F. Caruso, Chem. Mater. 17 (2005) 953-961.

[19] A.S. Maria Chong, X.S. Zhao, Catal. Today 93–95 (2004) 293-299.

[20] C. Lei, Y. Shin, J. Liu, E.J. Ackerman, J. Am. Chem. Soc. 124 (2002) 11242-11243.

[21] X. Zhang, R.F. Guan, D.Q. Wu, K.-Y. Chan, J. Mol. Catal. B 33 (2005) 43-50.

[22] K. Szyman´ska, J. Bryjak, J. Mrowiec-Białon´, A.B. Jarzebski, Microporous Mesoporous Mater. 99 (2007) 167-175.

[23] http://www.rcsb.org/pdb/explore/explore.do?structureId=1SCA

[24] C.J.S.M. Silva , Q. Zhang, J. Shen , A.Cavaco-Paulo, Enzyme Microb. Technol. 39 (2006) 634–640.

[25] A.Tanksale, P. M.Chandra, M.Rao,V. Deshpande, Biotechnol. Lett. 23 (2001) 51-54.

[26] S. Kiatkamjornwong, N. Siwarungson, A. Nganbunsri, J. Appl. Poly. Sci. 73 (1999) 2273-2291.

[27] D.Zhao, J. Am. Chem. Soc. 120 (1998) 6024-6036.

[28] P. Schmidt-Winkel,W.W. Luckens, D. Zhao, P. Yang, B.E. Chmelka, G.D.Stucky, J. Am. Chem. Soc. 121 (1999) 254-255.

[29] J.S. Lettow, Y.J. Han, P. Schmidt-Winkel, P. Yang, D. Zhao, G.D. Stucky, J.Y. Ying, Langmuir 16 (2000) 8291-8295.

[30] A. Ungureanu, D. Trong On, E. Dumitriu, S. Kaliaguine, Appl. Catal. A 254 (2003) 203-223.

[31] N.V. Maksimchuk, M.S. Melgunov, J. Mrowiec-Białon´ , A.B. Jarzebski, O.A. Kholdeeva, J. Catal. 235 (2005) 175-183.

[32] S. Krompiec, N. Kuz´nik, R. Penczek, J. Rzepa, J. Mrowiec-Białon´, J. Mol. Catal. A 219 (2004) 29-40.

[33] M.M. Bradford, Anal. Biochem. 72 (1976) 248-254.

[34] A. S. M. Chong, X. S. Zhao, J. Phys. Chem. B 107 (2003) 12650-12657.

[35] I. Diaz, C. Marquez-Alvarez, F. Mahino, J. Perez-Periente, E. Sastre, J. Catal. 193 (2000) 283-294.

[36] B.H. Wouters, T. Chen, M. Dewilde, P.J. Grobet, Microporous Mesoporous Mater. 44–45 (2001) 453-457.

[37] J. Aburto, M. Ayala, I.Bustos-Jaimes, C. Montiel, E. Terrés, J. M. Domínguez, E.Torres, Microporous Mesoporous Mater. 83 (2005) 193–200.

Chapter 3

Catalytic hydrolysis of carboxy methyl cellulose using cellulase immobilized on functionalized meso cellular foam

3.1. Introduction

The abundance and relatively low cost of lignocellulosic materials make them attractive feedstock for the production of ethanol from renewable resources. [1-5] Ethanol is a potential future fuel having reduced net greenhouse gas emission. The enzymatic process has the potential to convert the lignocellulosic materials to ethanol with a high yield and low production cost.[6-7] However, the recalcitrance of the lignocellulosic matrix to enzymatic attack necessitates pretreatment of the material in order to enhance the accessibility of the substrate to the enzyme.

High-pressure steam treatment with small amount of acid catalyst such as sulphuric acid or sulphur dioxide, reduces the cellulose crystallinity.[8-11] Though, there have been efforts to reduce cellulase enzyme cost (http://eere.energy.gov/), yet the production cost of enzymes is still too high. Immobilization of enzyme is one of the methods to reduce the cost by reusing same enzyme while retaining its specificity and stability. Therefore, research efforts have been directed to immobilize enzyme using inorganic, organic and hybrid supports.[15] Moreover, immobilized enzymes can also be used in fixed bed type reactor, which can operate in a continuous mode.

Mesoporous silicas (MPSs) have emerged as potential solid supports for enzyme immobilization.[12] These supports are environmentally acceptable, structurally stable, and resistant to microbial attack. Besides, the MPSs surface can be modified with various anchor groups to covalently bind the enzyme molecules, which could reduce the enzyme leaching from the support during the recycling of the catalyst.[13–15]

The uniform distribution of pores in MPSs favors the uniform loading of enzyme as well as facile diffusion of the substrate and product molecules inside the channels. Among the MPSs, MCF has been shown to be efficient support for covalent immobilization of α-amylase, protease, trypsin, chloroperoxidase, glucose oxidase, glucoamylase, and invertase.[13-24] Because of MCFs large pore size (~25 nm) and higher surface area (~800 m^2/g), it is suited to host the cellulase (~ 5 nm) molecules comfortably.[25] The diagonal measurement, lengthwise of the cellulase was produced using Chem3D Pro 10.0 from the Research Collaboratory for Structural Bioinformatics (RCSB) enzyme data base is shown in Fig. 3.1.

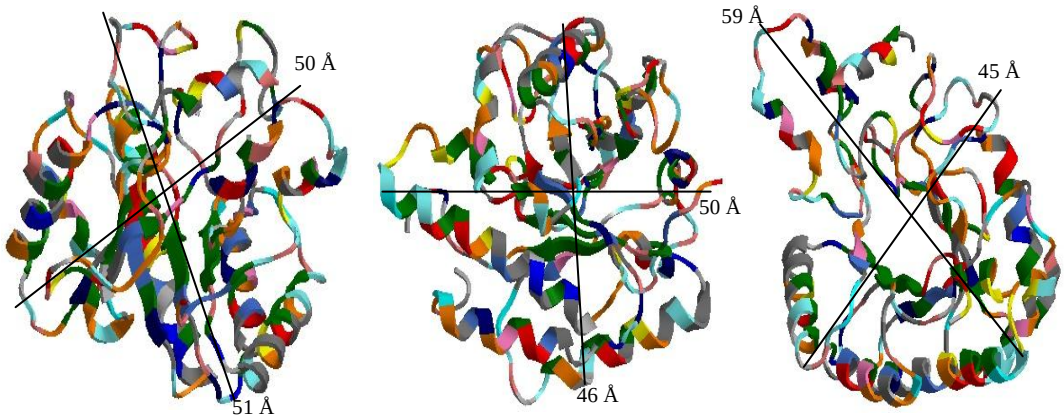

Fig. 3.1 Cellulase structure from RCSB protein data base

Cellulase has been immobilized on various supports[26–31] and evaluated for the stability, activity and reusability with reference to free enzyme. In the present study, covalent immobilization of cellulase has been done through Schiff base reaction on functionalized MCF followed by reduction with $NaBH_4$. Surface modification of MPSs was done with 3-aminopropyltriethoxy silane (APTES) followed by glutaraldehyde reaction with APTES. The specific activity of the immobilized enzymes was studied for hydrolysis of CMC.

3.2. Experimental section

3.2.1. Materials

D-(+) Glucose anhydrous (98%), 3-Aminopropyl triethoxy silane (98%, APTES) were procured from Fluka (USA). Tetraethoxysilane (98%, TEOS), Triblock poly(ethyleneoxide)-block-poly(propyleneoxide)-block-poly(ethyleneoxide) copolymer (Pluronic P123, M.W. = 5800), Bradford reagent (B6916), Glutaraldehyde in H_2O 25%(wt/v), Na_2HPO_4 (99%, A.R.), $NaH_2PO_4 \cdot 2H_2O$ (99% A.R.), were purchased from Aldrich (USA). Bacterial cellulase (E.C.3.4.21.62) from Penicillium funiculosum was donated by Genencor International, The Netherlands. 1,3,5-trimethylbenzene (98%, A.R., TMB), soluble carboxymethyl cellulose (200-400 cps, CMC, DS = ~0.8), 3,5-Dinitro salicylic acid (98%, A.R.), Phenol (98%, A.R.), Na-K tartarate (99%, A.R), CH_3COONa (98%, A.R), CH_3COOH, Na metabisulfite were purchased from s.d. Fine Chemical, India. $NaBH_4$ (98%, A.R.), NaOH (98%, A.R.) were obtained from Qualigens Fine Chemicals, India. DNS reagent was prepared by dissolving 3,5-Dinitro salicylic acid (5.3 g), NaOH (9.9 g) into distilled water (708 ml) followed by addition of Na,K tartarate (153 g), Phenol (3.8 ml at 50 ˚C) and Na Metabisulfite (4.15 g) in that order. These chemicals were used in material synthesis, functionalization of MCF and enzyme kinetic studies.

3.2.2. Synthesis of MCF

Siliceous MCF was synthesized using the procedure reported by Lettow et al. [26] The detailed synthesis of MCF was described in earlier section 2.2.3.

3.2.3. Surface modification of MCF

The amino functionalization was described previously in Section 2.2.4. APTES modified sample was labeled as MCF-A. The amino functionalized MCF was glutarated by adding 0.5 g into 0.3 g of glutaraldehyde in 75 ml of methanol for 1 h. The systematic surface functionalization of MCF and cellulase immobilization is shown in Fig. 3.2. The product was filtered, washed with excess of water till excess of glutaraldehyde was completely removed. The sample obtained after glutaration designated as MCF-AG. The requisite amount of $NaBH_4$ (11 mg) needed to reduce imine bonds selectively in MCF-AG-Enz were determined by reduction of MCF-AG separately. The reduced MCF-AG sample was designated as MCF-AGR.

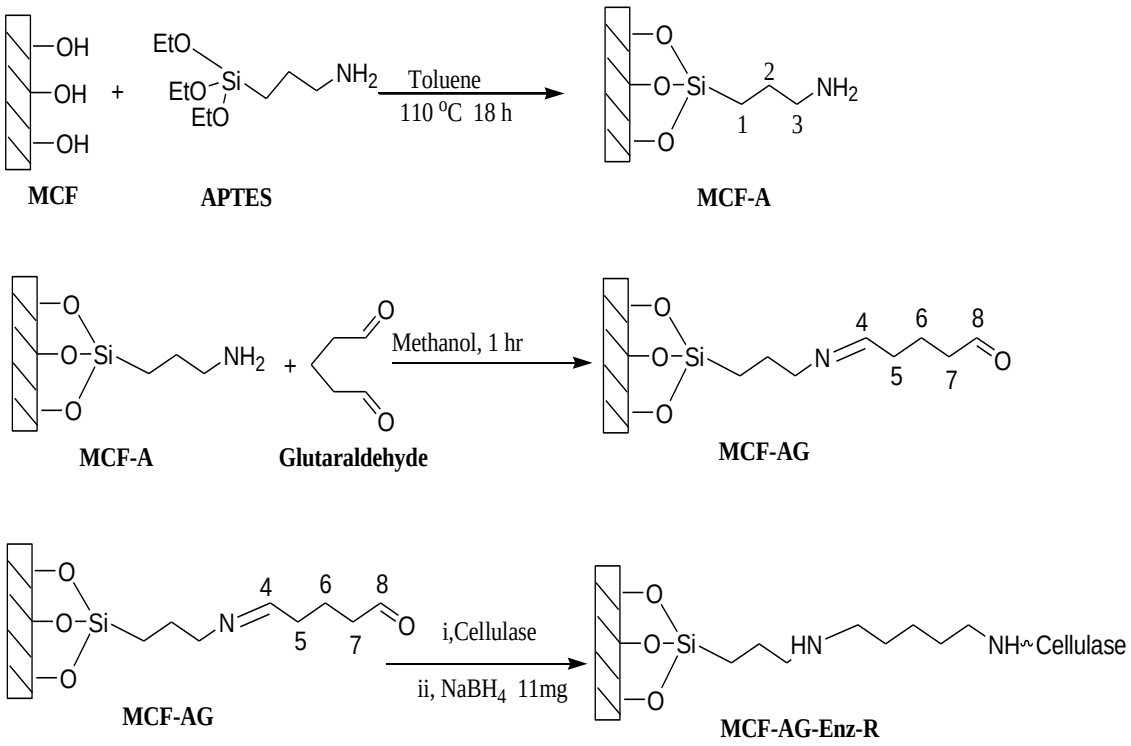

Fig. 3.2 Schematic surface functionalization of MCF and cellulase immobilization

3.2.4. Characterization

The physico chemical characterization of calcined (MCF), aminated (MCF-A), glutarated (MCF-AG), reduced (MCF-AGR) and enzyme immobilized (MCF-AG-Enz-R) was described in previous section 2.2.5.

3.2.5. Adsorption isotherm and immobilization of Cellulase

Cellulase solutions of 0.025, 0.05, 0.075, 0.1, 0.125, 0.15, 0.175 and 0.2 ml were diluted to 0.5 ml using phosphate buffer (pH=5). These enzyme solutions were slowly added on to 100 mg of MCF and MCF-AG in 0.5 ml at room temperature (~ 30 °C) separately and kept for 4 h (optimized by measuring adsorption kinetics) with constant shaking to achieve equilibrium adsorption. Cellulase was immobilized on MCF-AG surface through covalent bonding between –CHO of MCF-AG with $–NH_2$ group of enzyme by adding 0.2 ml of cellulase into 100 mg of MCF-AG in 0.5 ml buffer (pH=5) with regular shaking. Finally, $NaBH_4$ (11 mg) was slowly added and kept in cool (~5 ˚C) for 15 min (MCF-AG-Enz-R). During both adsorption isotherm and immobilization studies the excess enzyme was removed by washing with excess of acetate buffer and unbound enzyme was estimated by Bradford method. [33]

3.2.6. Activity assay of the enzyme

Activity of free and immobilized enzyme was measured by incubating free (150 µl, 519 U) or immobilized enzyme in 2 ml of acetate buffer (0.1M, pH=5) with 1 ml of carboxymethyl cellulose (2 mg/ml solution) for exactly 30 min at 50 ˚C. The reaction was stopped by putting the reaction tube into the boiling water bath for 3 min and the precipitate was removed by centrifugation. The hydrolysis products of CMC

include glucose as well as unconverted carboxymethyl cellulose. To this 1.5 ml filtrate, 3 ml of DNS reagent was added and kept in boiling water bath for 5 min then brought down to room (~28 ˚C) temperature.[34] The absorbance due to the amount of glucose produced was measured at 540 nm using a UV–vis–NIR scanning spectrophotometer (CARY Varian 500 SCAN).

One unit of cellulase activity is defined by the amount of enzyme, which produced 1.0 μmol of reducing sugar from the substrate per minute. The kinetic parameters of free and immobilized enzyme were evaluated by incubating with CMC solution having the concentration of 0.25–3 (mg/ml) and applying above described procedure.

Specific activity of cellulase was determined using the equation:

$$\text{Specific activity of cellulase (} \mu \text{ mol/ ml mg min)} = \frac{1000\ w}{M\ \nu A\ t}$$

Where, w is the amount of produced glucose, M the molecular weight of glucose, ν the volume of the measured sample, A is the amount of enzyme (mg) and t is the reaction time, respectively.[26]

The relative activity of immobilized cellulase is the ratio of the specific activity of the immobilized enzyme to that of the free enzyme under the same conditions according to the following equation:

$$\text{Relative activity} = \frac{\text{Specific activity of immobilized cellulase}}{\text{Specific activity of free cellulase}} \text{ X } 100\%$$

3.2.7 Effect of temperature and pH on enzyme activity

The enzymes were incubated with CMC in 0.1M acetate buffer solution having a pH of 5 at temperatures from 30 to 70 ˚C, and alternatively incubated at a fixed temperature of 50 ˚C at pH ranging from 3 to 7. The activity of cellulase at different pH and temperature was then measured as per previously described (Section 3.2.6) method.

3.2.8 Reusability and operational stability

The initial activity of the immobilized enzyme was measured and then compared with activity of the enzyme obtained after its use for 15 cycles. After each cycle the immobilized enzyme was immediately filtered, washed with buffer solution and stored at ~5 ˚C. The operational stability of free and immobilized enzyme was studied by deactivating at pH of 5, holding for different time intervals at a temperature of 85 ˚C and comparing the activities with the fresh enzymes activity.

3.3. Results and discussion

3.3.1. Characterization of synthesized and surface modified MCF

Physico-chemical characterization data of calcined (MCF), aminated (MCF-A), glutarated (MCF-AG), reduced (MCF-AGR) and enzyme immobilized (MCF-AG-Enz-R) samples are shown in Table 3.1. MCF sample after modification with APTES followed by glutaration resulted a decrease in BET surface area, pore volume and pore diameter values. Calcined MCF has higher textural parameter values than the aminated MCF.

Table 3.1 Physico-chemical characterization data of calcined (MCF), aminated (MCF-A), glutarated (MCF-AG) reduced (MCF-AGR) and enzyme immobilized (MCF-AG-Enz-R).

Sample	N_2 adsorption			Elemental (CHN) analysis		
	Surface area S_{BET} (m^2/g)	Total pore volume $V_p N_2$ (cm^3/g)	Pore diameter d_m (Å)	%C	%H	%N
MCF	682	0.82	218	-	-	-
MCF-A	336	0.42	187	09.41	4.82	3.36
MCF-AG	299	0.14	108	12.86	2.25	2.15
MCF-AGR	265	0.12	107	12.59	2.20	1.50
MCF-AG-Enz-R	171	0.014	91	14.14	2.28	3.04

The nitrogen adsorption isotherm of calcined (MCF), aminated (MCF-A), glutarated (MCF-AG), reduced (MCF-AGR) and enzyme immobilized (MCF-AG-Enz-R) samples are shown in Fig. 3.3. The observed decreases in pore volume of MCF on immobilization clearly show that celllulase is immobilized inside the pores of MCF. The sharp decrease in adsorbed volume at relative pressure (P/P_o) in the range of 0.2–0.9 is an indication of uniform functionalization on the surface of MCF.

In glutarated and reduced MCFs were observed to have slightly lower textural parameter values compared to aminated MCF. This shows that amination and then glutaration have occurred on the surface of the MCF. However, the pore diameter values of reduced MCF (108 Å) are large enough to host the cellulase inside their channels. Though, the possibility of some enzyme molecules to be present on the external surface cannot be ruled out. In case of enzyme immobilized MCF, lower surface area (171 m^2/g) and pore diameter (91 Å) is expectedly observed.

On glutaration followed by enzyme immobilization of aminated MCF the overall N% is expected to decrease then increase and the data indeed show this trend (Table. 3.1). In MCF-AG sample higher number –N=CH- groups are present. These get reduced to $–NH-CH_2-$ groups in MCF-AGR and thereby the amount of hydrogen increases resulting into decrease in the net content of nitrogen in CHN analysis. CHN data also support that enzyme immobilization has occurred on functionalized MCF.

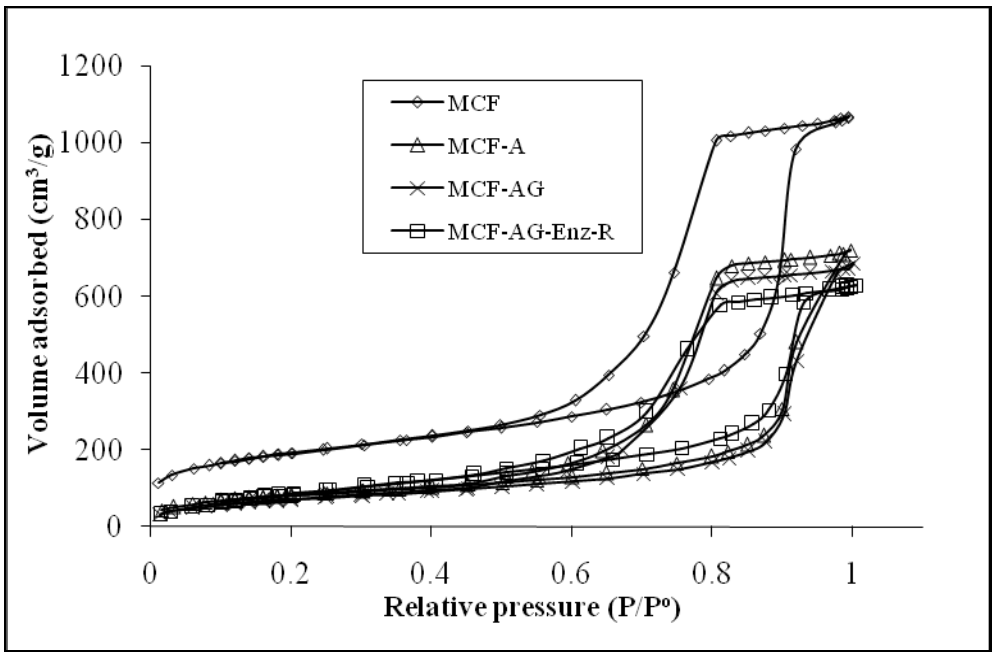

Fig. 3.3 Nitrogen adsorption isotherm of calcined (MCF), aminated (MCF-A), glutarated (MCF-AG), reduced (MCF-AGR) and enzyme immobilized (MCF-AG-Enz-R)

FT-IR spectra for of calcined (MCF), aminated (MCF-A), glutarated (MCF-AG), reduced (MCF-AGR) and enzyme immobilized (MCF-AG-Enz-R) samples are given in Fig. 3.4. The broad band at 3600–3000 cm^{-1} for hydrogen bonded silanol[13-15] was observed to appreciably reduce in the modified samples.

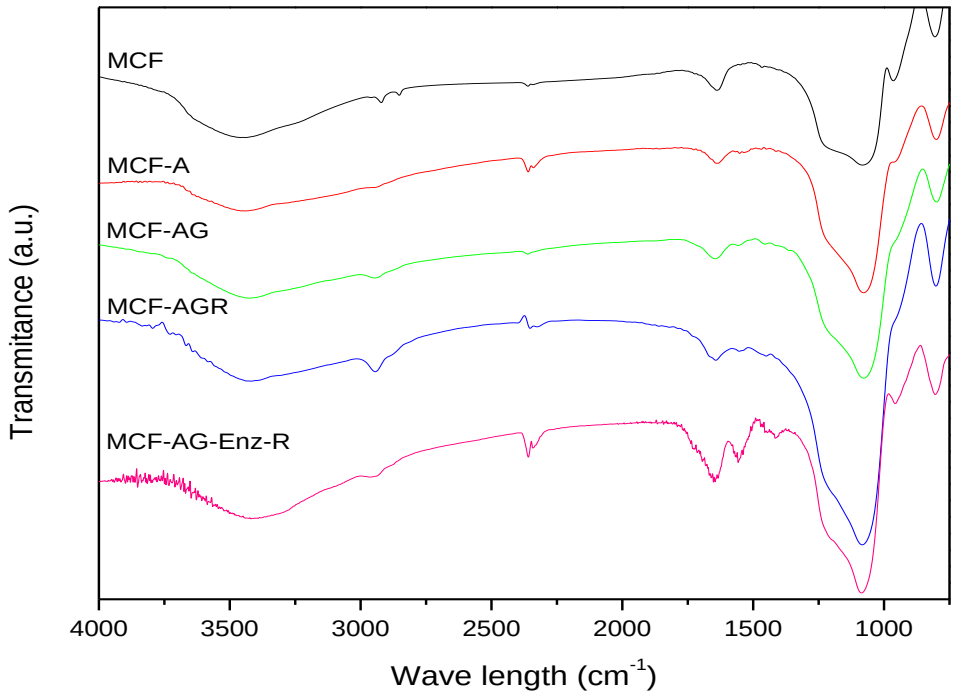

Fig. 3.4 IR spectra of calcined (MCF), aminated (MCF-A), glutarated (MCF-AG), reduced (MCF-AGR) and enzyme immobilized (MCF-AG-Enz-R)

The organosilane presence was identified by the absorbance of the band 2950–2850 cm^{-1} for the propyl chain and the deformation bands at 1455–1410 cm^{-1}. N-H absorption band was observed overlap with O-H bands at 3300–3500 cm^{-1}. On glutaraldehyde loading, free $–NH_2$ group of APTES binds to one –CHO group of glutaraldehyde molecule and some of end –CHO may bind with near $–NH_2$ group. Bands between 1690-1630 cm^{-1} and 1718-1730 cm^{-1} have been shown for –CH=N- and carbonyl of –CHO group. Presence of band at 1668 cm^{-1} (-CH=N-) and 1723 cm^{-1} (–CHO) reveals that the glutaration has occurred, which was also confirmed by testing with Tollen's reagent. After reduction of MCF immobilized enzyme (MCF-AG-Enz-R) with calculated amount $NaBH_4$, the peak value at 1730 cm^{-1} for –COOH and 1646 cm^{-1} for amide in enzyme was observed.

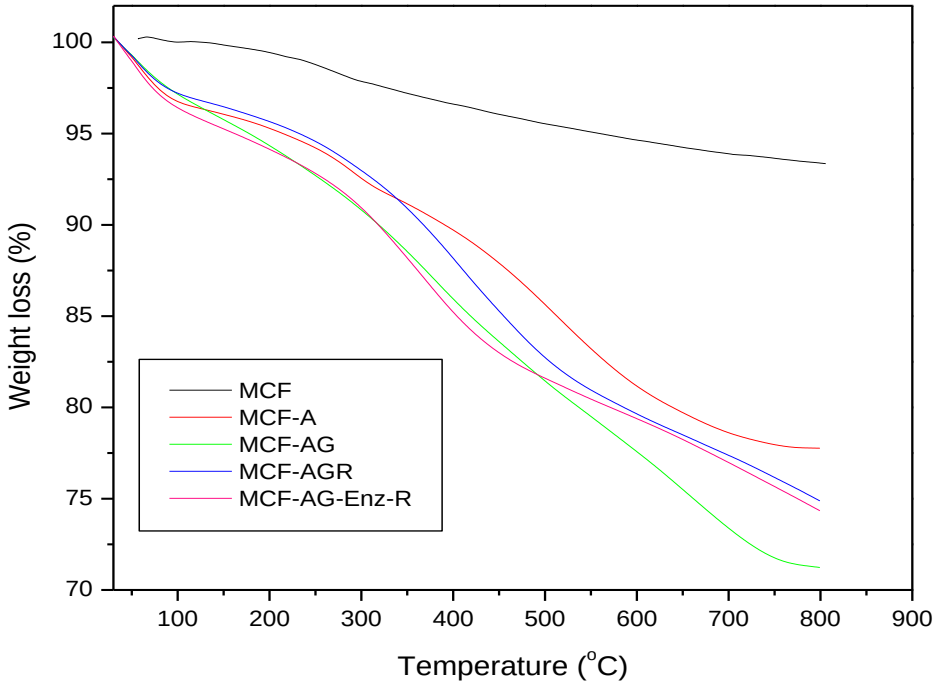

Fig. 3.5 TGA curve of calcined (MCF), aminated (MCF-A), glutarated (MCF-AG), reduced (MCF-AGR) and enzyme immobilized (MCF-AG-Enz-R)

TGA curve of calcined (MCF), aminated (MCF-A), glutarated (MCF-AG), reduced (MCF-AGR) and enzyme immobilized (MCF-AG-Enz-R) samples are given in Fig. 3.5. The calcined sample showed no appreciable weight losses; Aminated samples showed 13.4% weight loss between 473 and 763 ˚C due to amino propyl group decomposition. Glutarated sample gave 15% weight loss between 132–471 ˚C due to glutaryl and 7.9% weight loss at 473–750 ˚C due to amino propyl decompositions from MCF. However, the reduced MCF showed higher stability as seen by shift of decomposition of glutaryl to 132–522 ˚C with 16% weight loss, and of amino propyl group to 524–784 ˚C with 4% loss. This is due to the reduction of –CH=N- to $–CH_2$-NH- groups. The MCF-AG-Enz-R shows likewise 14.1% and 6.2% loss with enzyme loading of 16.4 wt%.

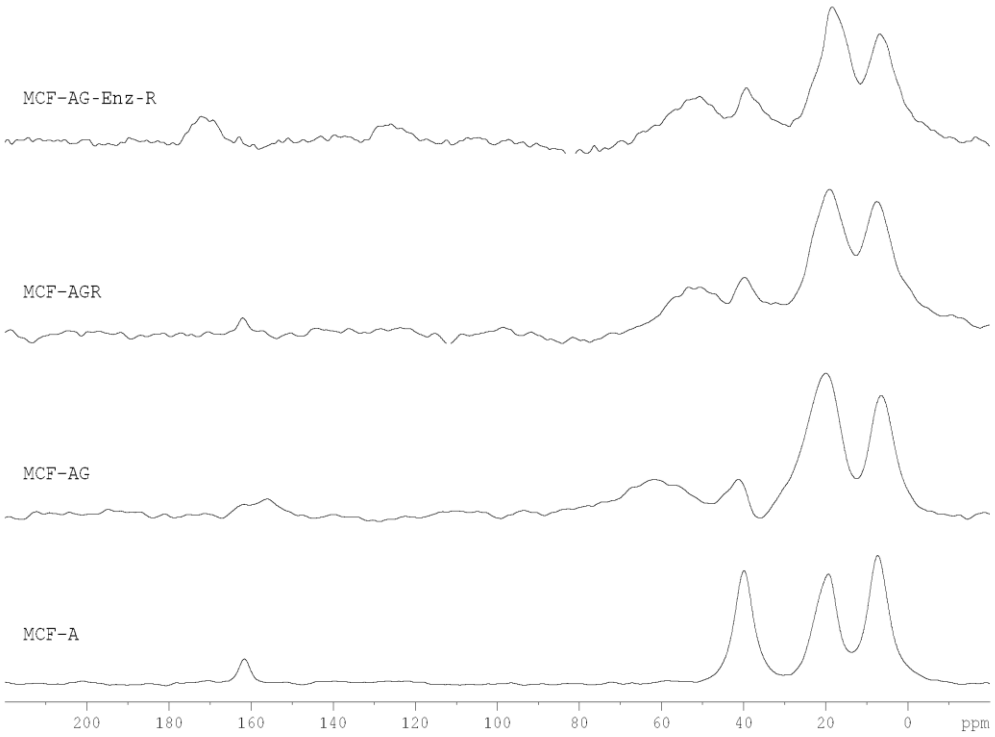

Fig. 3.6 Solid state ^{13}C-MAS NMR spectra of aminated (MCF-A) glutarated (MCF-AG), reduced (MCF-AGR) and enzyme immobilized (MCF-AG-Enz-R)

The amination[35] and glutaration of MCF were further confirmed by solid state ^{13}CMAS–NMR spectroscopy as shown in Fig. 3.6. The MCF-A sample gave chemical shift values at 7.27 (–C_1–), 19.04 (–C_2–) and 39.87 (–C_3–) ppm. The chemical shift values for the MCF-AG methylene carbons were 15.91 (–C_1–), 29.02 (–C_2–), 48.92 (–C_6–), 63.51 (–C_5–), 68.68 (–C_7–) and 73.60 (–C_3–) and for the double bond carbons 158.70 (–C_4–, imine) and 162.7 (–C_8–, aldehyde) ppm. In case of MCF–AGR chemical shifts values for methylene carbons were at 6.54 (–C_1–), 18.28 (–C_6–), 39.52 (–C_2–), 47.2 (–C_5–), 50.16 (–C_7–), 53.42 (–C_4–), 56.8 (–C_3–) and 161.4 (–C_8–, aldehyde) ppm. There was no peak value for imine bonded carbon, which appeared as a methylene peak with chemical shift value of 53.42 (-C_4-) ppm. It was confirmed that 30 mg $NaBH_4$ was enough to reduce the imine bonds in 0.5 g of glutarated MCF. MCF–AG-Enz-R methylene carbons showed chemical shift values at 6.82 (–C_1–),

18.39 (–C_6–), 39.30 (–C_2–), 45.2 (–C_5–), 49.5 (–C_7–), 52.9 (–C_4–), 56.7 (–C_3–), 125.97 and 129.3 (aromatic carbon in enzyme), 162.4 (phenolic) and 172.19 (-COOH carbon) ppm. These data further confirmed that cellulase was covalently immobilized on functionalized MCF.

3.3.2. Adsorption isotherm and activity of the enzymes

The adsorption isotherms of cellulase on MCF and MCF-AG are shown in Table 3.2 and Fig. 3.7. The point of zero charge for mesoporous silica is in the range 2-3.7. Therefore, in the pH range 3.7-7.0, the surface silanol groups of mesoporous silicas will be ionized to carry negative charges while cellulase will carry positive charges. To achieve electrostatic interactions between cellulase and MCF, pH=5 of the enzyme solution was used for celllulase adsorption isotherm. The surface modified MCF-AG has higher adsorption capacity than the MCF. This is due to the fact that the surface modified MCF-AG has higher interaction with cellulase enzyme molecules.

Table 3.2 Cellulase adsorbtion isotherm experiment data at ~30 °C

Cellulase (mg/ml)	Cellulase adsorbed on MCF (mg/mg)	Cellulase adsorbed on MCF-AG (mg/mg)
0.0275	0.143	0.198
0.0550	0.418	0.506
0.0825	0.649	0.748
0.1100	0.726	0.924
0.1375	0.759	1.034
0.1650	0.792	1.111
0.1925	0.803	1.122
0.2200	0.814	1.133

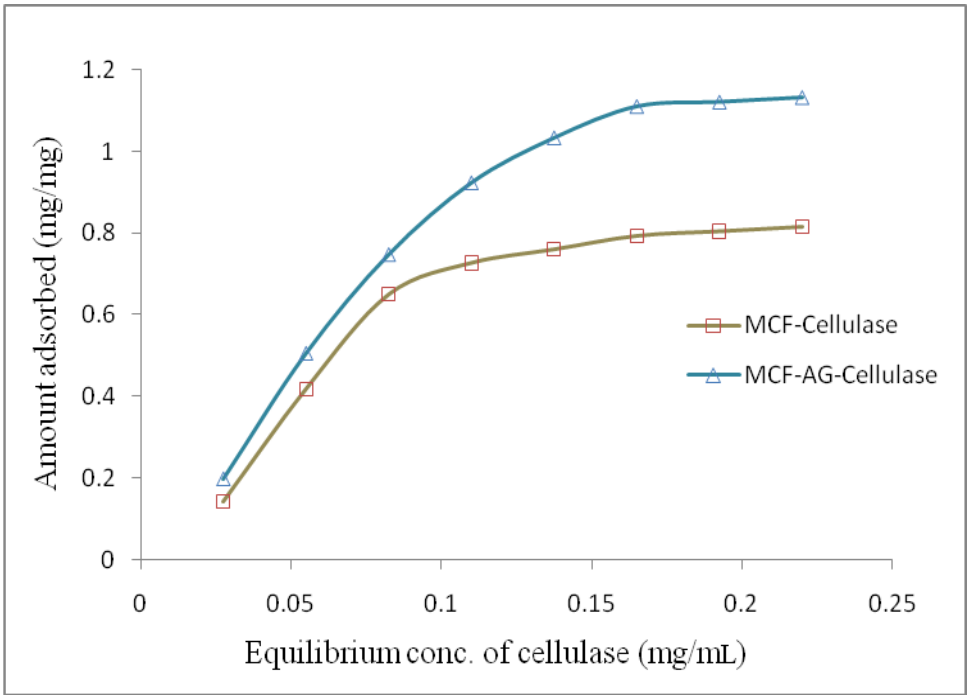

Fig. 3.7 The cellulase adsorption isotherms on MCF and MCF-AG at ~30 °C

The kinetic parameters of the Michaelis–Menten equation were determined for free and immobilized enzymes. Experiments were carried out by using different substrate CMC concentrations (0.25–2 % Wt/v). The comparative activity at different substrate (soluble CMC) concentration of free, MCF immobilized cellulase and functionalized MCF are given in Table 3.3 and Fig. 3.8. The MCF immobilized enzyme shows higher specific activity than the free enzyme.

Table 3.3 Experimental data of different substrate (soluble CMC) concentration

MCF-AG-Enz-R					
Conc. of Cellulose (mg/ml)	Absorb. at 540 nm	Product (mg/ml)	Enzyme activity x 10^{-6} (mol/sec)	Enzyme amount (ml)	Specific activity x 10^{-2} (μ mol $mg^{-1}min^{-1}$)
0.25	0.265	0.689	85.00	0.087	88.82
0.5	0.547	1.383	170.54	0.094	164.93
1	1.105	2.822	348.05	0.109	290.28
1.5	1.286	3.316	409.01	0.100	371.82
2	1.529	4.028	496.78	0.099	456.18
2.5	1.590	4.218	520.30	0.098	482.66
3	1.605	4.270	526.69	0.100	478.81

Free Enzyme					
Conc. of Cellulose (mg/ml)	Absorb. at 540 nm	Product (mg/ml)	Enzyme activity x 10^{-5} (mol/sec)	Enzyme amount (ml)	Specific activity x 10^{-2} (μ mol $mg^{-1}min^{-1}$)
0.25	0.246	0.660	8.14	0.15	49.34
0.5	0.420	1.045	12.89	0.15	78.12
1	0.738	1.845	22.76	0.15	137.92
1.5	1.051	2.677	33.02	0.15	200.12
2	1.329	3.430	42.31	0.15	256.41
2.5	1.541	4.056	50.03	0.15	303.22
3	1.619	4.299	53.03	0.15	321.37

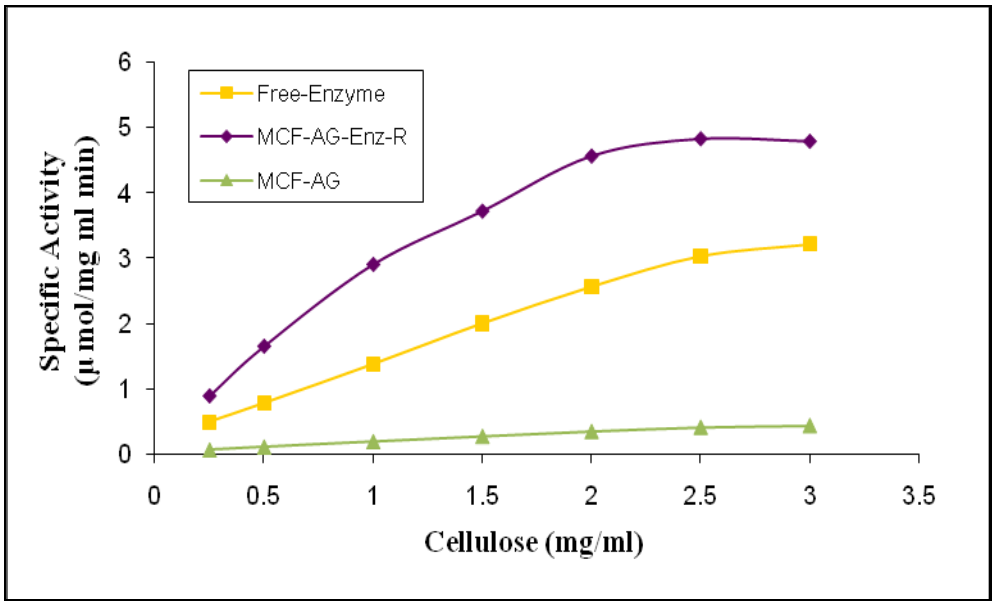

Fig. 3.8 Comparison of activity at different substrate (soluble CMC) concentration

Lineweaver–Burk plot calculation of 1/S and 1/V is given in Table 3.4. The Michaelis–Menten constant (*K*m) and the maximum reaction velocity (*V*max) values were calculated from Lineweaver–Burk plots (Fig. 3.9) by the linear regression method with R^2 value of 0.99. *K*m = 0.025 and 0.024 $\times 10^{-2}$ mg/ml and *V*max = 5.327 and 9.794 $\times 10^{-3}$ U/mg were observed for the free and MCF immobilized enzymes, respectively. For MCF immobilized enzyme, the calculated *V*max value was found to be higher than that of the free enzyme, may be due to the higher number of polar groups (-OH, -NH-) on the surface of the MCF.

Table 3.4 Lineweaver–Burk plot calculation of 1/S and 1/V

		MCF-AG-Enz-R		Free enzyme	
S x 10^{-3} (mg/ml)	1/S (ml/mg)	Specific activity x 10^{-2} (μ molmg^{-1}min^{-1})	1/V (min/U)	Specific activity x 10^{-2} (μ mol mg^{-1}min^{-1})	1/V (min/U)
0.0025	400	88.82	15434.6	49.34	22450.2
0.0050	200	164.93	12315.2	78.12	17499.8
0.0100	100	290.28	7942.8	137.92	9661.8
0.0150	66.67	371.82	6567.2	200.12	7539.5
0.0200	50	456.18	5905.3	256.41	6652.5

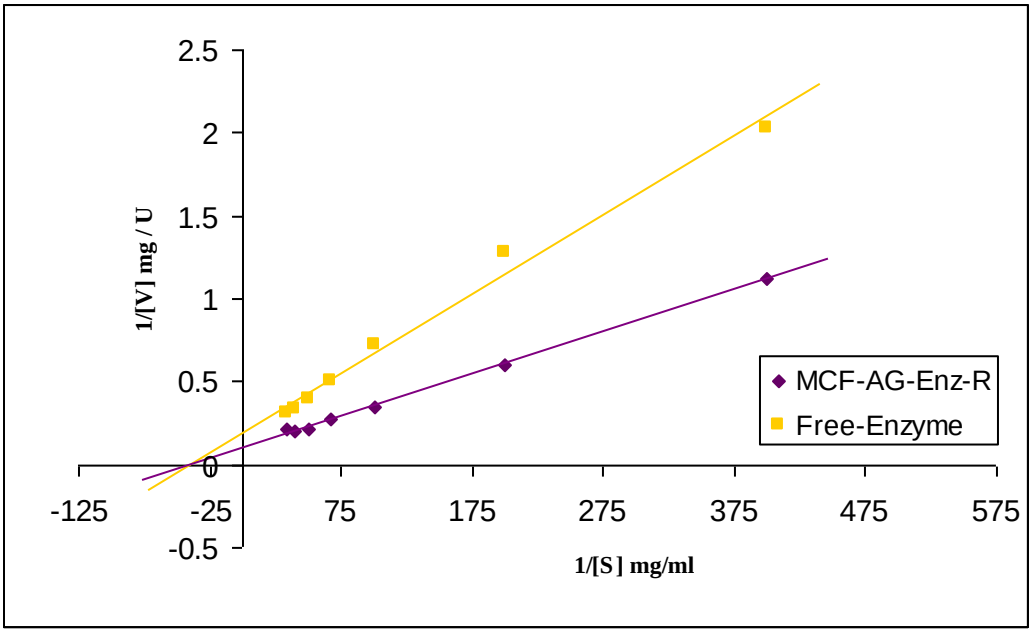

Fig. 3.9 L-B plot for kinetic parameters of free and immobilized enzymes

Cellulase molecule could bind on hydrated MCF surface through electrostatic, hydrogen bonding and Van Der Waals interactions, which stabilize the enzyme on surface. Moreover, the availability of large pore size is sufficient to host the enzyme molecules and facilitate the diffusion of the substrate molecules into active sites of the enzyme covalently attached with the 9-atom long space arm on MCF. Multi point covalent attachment of cellulase with carrier rigidified the enzyme and the availability of polar groups (-NH-, -OH). This could be electrostatically stabilizing the cellulase

on surface as well as inside the pores of surface modified MCF during hydrolysis of soluble carboxymethyl cellulose. Surface modified MCF-AG's active functional groups are also involved in the hydrolysis of soluble carboxymethyl cellulose to some extent leading to higher activity of MCF immobilized cellulase. There is possibility of reduction of disulphide bond (-S-S-) between the peptide chain to –SH during hydrogenation with $NaBH_4$. The higher activity for immobilized enzyme observed in this study shows that such a reduction is checked. This could be due to steric effects inside the pores of support or even if –S-S- bonds reduces to –SH groups, enzyme structure does not collapse on immobilization.

3.3.3. Optimum Temperature and pH

The experimental data of effect of temperature on free and MCF-AG-Enz-R enzymes and calculated relative activities are given in Table 3.5, Table 3.6. The optimum temperature of both free and MCF immobilized enzyme was observed to be 55 °C.

Table 3.5 Experimental data of effect of temperature on free and immobilized enzymes activities

MCF-AG-Enz-R					
Temp. (°C)	Absorb. at 540 nm	Product (g/L)	Enzyme activity x 10^{-2} (mol/sec)	Enzyme amount (ml)	Specific activity x 10^{-2} (μ mol $mg^{-1}min^{-1}$)
30	0.982	3.104	38.29	0.143	243.42
35	1.207	3.104	38.29	0.140	248.64
40	1.242	3.206	39.54	0.133	270.27
45	1.244	3.230	39.84	0.124	292.05
50	1.274	3.318	40.92	0.119	312.62
55	1.183	3.294	40.63	0.116	318.38
60	1.041	2.670	32.93	0.102	293.46
65	1.224	2.544	31.38	0.104	274.30
70	1.157	2.464	30.39	0.101	273.55

Free-Enzyme					
Temp. (°C)	Absorb. at 540 nm	Product (g/L)	Enzyme activity x 10^{-2} (mol/sec)	Enzyme amount (ml)	Specific activity x 10^{-2} (μ mol $mg^{-1}min^{-1}$)
30	1.185	3.04	37.50	0.15	227.27
35	1.202	3.08	37.96	0.15	230.06
40	1.239	3.16	38.95	0.15	236.05
45	1.288	3.34	41.25	0.15	250.01
50	1.329	3.45	42.55	0.15	257.91
55	1.365	3.57	44.08	0.15	267.16
60	1.340	3.49	43.03	0.15	260.78
65	1.326	3.45	42.50	0.15	257.59
70	1.309	3.38	41.71	0.15	252.80

Table 3.6 Calculated relative activity at various temperatures

MCF-AG-Enz-R			Free Enzyme		
Temp. (°C)	Specific Activity x 10^{-2}	Relative activity (%)	Temp. (°C)	Specific Activity x 10^{-2}	Relative activity (%)
35	243.42	76.46	35	227.27	71.38
40	248.64	78.09	40	230.06	72.26
45	270.27	84.89	45	236.05	74.14
50	292.05	91.73	50	250.01	78.53
55	312.62	98.19	55	257.91	81.32
60	318.38	100	60	267.16	83.91
65	293.46	92.17	65	260.78	81.91
70	274.30	86.15	70	257.59	80.90

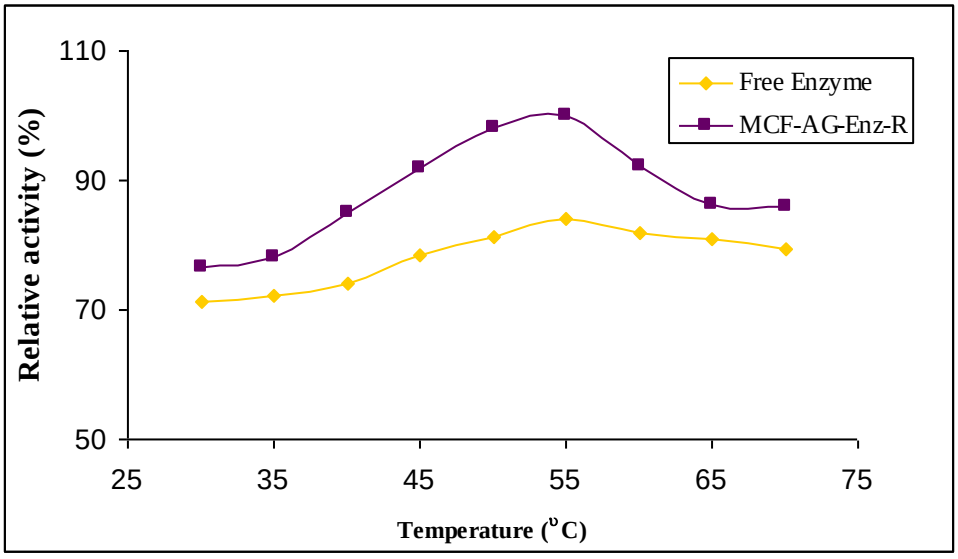

Fig. 3.10 Effect of temperature on free and immobilized enzymes activities

The specific activity of both free and MCF immobilized enzyme, increased with increasing temperature up to 55 °C beyond which the activity showed a decrease as shown in Fig. 3.10. Experimental data on the effect of pH on free and immobilized enzymes activities and calculated relative activity values ranging from 3 to 7 are given in Tables 3.7, 3.8 and Fig. 3.11. In the free enzyme, the specific activity increased with increasing pH value up to 4.5, after that the activity started to decrease.

Table 3.7 Experimental data on the effect of pH on free and immobilized enzymes activities

MCF-AG-Enz-R					
pH	Absorb. at 540 nm	Product (g/L)	Enzyme activity x 10^{-2} (mol/sec)	Enzyme amount (ml)	Specific activity x 10^{-2} (μ mol $mg^{-1}min^{-1}$)
3.0	0.982	2.509	30.95	0.105	267.98
3.5	1.103	2.832	34.93	0.111	286.10
4.0	1.243	3.200	39.47	0.113	317.58
4.5	1.244	3.230	39.84	0.106	341.65
5.0	1.274	3.318	40.92	0.105	354.30
5.5	1.285	3.294	40.63	0.114	323.97
6.0	1.041	2.669	32.93	0.106	282.39
6.5	1.000	2.544	31.38	0.110	259.33
7.0	0.980	2.464	30.39	0.108	255.82
Free Enzyme					
pH	Absorb. at 540 nm	Product (g/L)	Enzyme activity x 10^{-2} (mol/sec)	Enzyme amount (ml)	Specific activity x 10^{-2} (μ mol $mg^{-1}min^{-1}$)
3.0	1.238	3.184	39.28	0.15	238.05
3.5	1.276	3.296	40.66	0.15	246.42
4.0	1.311	3.422	42.21	0.15	255.79
4.5	1.444	3.806	46.94	0.15	284.51
5.0	1.329	3.454	42.60	0.15	258.18
5.5	1.285	3.312	40.86	0.15	247.62
6.0	1.243	3.198	39.44	0.15	239.04
6.5	1.226	3.136	38.68	0.15	234.45
7.0	1.202	3.088	38.09	0.15	230.86

Table 3.8 Calculated relative activity of free and MCF-AG-Enz-R at various pH

MCF-AG-Enz-R			Free Enzyme		
pH	Specific Activity x 10^{-2}	Relative activity (%)	pH	Specific Activity x 10^{-2}	Relative activity (%)
3.0	267.98	75.64	3.0	238.05	67.19
3.5	286.10	80.75	3.5	246.42	69.55
4.0	317.58	89.64	4.0	255.79	72.20
4.5	341.65	96.43	4.5	284.51	80.30
5.0	354.30	100	5.0	258.18	72.87
5.5	323.97	91.44	5.5	247.62	69.89
6.0	282.39	79.70	6.0	239.04	67.47
6.5	259.33	73.20	6.5	234.45	66.17
7.0	255.82	72.20	7.0	230.86	65.16

For MCF immobilized enzyme, the activity was observed to be higher than that of free enzyme. Electrostatic cellulase–surface interactions are likely to be the strongest, particularly when the reaction is performed at pH higher than 3, where the enzyme possesses a positive charge and the MCF carries negative charges. The sign of the overall charge on a surface can readily be predicted on the basis of the isoelectric point (the pH at which the overall charge is zero, for cellulase pI=4.5). This pI value of a protein molecule depends on the balance of surface functional groups (e.g. $–NH_2$, –OH) which may have opposite charges.[12]

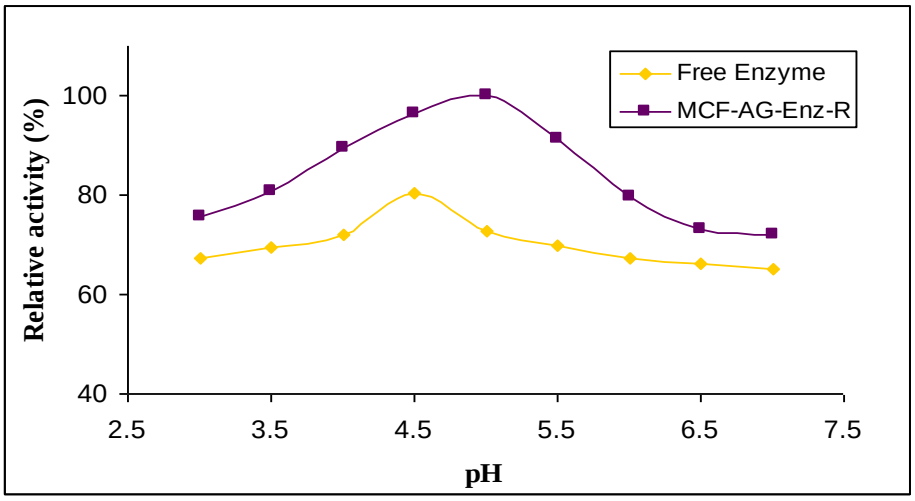

Fig. 3.11 Effect of pH on free and immobilized enzymes activities

However, MCF immobilized enzymes; the optimum pH was found to be 5 beyond which a decrease in specific activity was seen. It is observed that up to pH= 5, electrostatic interactions are maintained, however beyond that pH value, there is a decrease in these interactions which led to decrease in activity.

3.3.4. Reusability and operational stability

The reusability data of MCF immobilized enzyme and relative activity with reference to the initial activities are shown in Table 3.9 and Fig. 3.12. Initially, there was a rapid decrease which could be due to the leaching of external surface immobilized and encapsulated enzyme. The activity was found to decrease after every cycle because of loss of small amount of enzyme immobilized MCF in each cycle. The operational stability data and the calculated relative operational specific activity of free and MCF immobilized are given in Table 3.10 and Fig. 3.13.

Table 3.9 Reusability data of MCF immobilized (MCF-AG-Enz-R) enzyme

MCF-AG-Enz-R		
Cycles	Enzyme Activity x 10^{-2}	Relative activity (%)
1	122.52	100
2	112.59	91.89
3	113.42	92.57
4	111.76	91.22
5	110.11	89.86
6	105.97	86.49
7	106.79	87.16
8	104.31	85.13
9	101.00	82.43
10	102.66	83.78
11	99.34	81.08
12	96.03	78.38
13	94.38	77.03
14	91.96	75.06
15	94.09	76.79

The specific activity of free and immobilized enzymes decreased with increasing time. However, the MCF immobilized enzymes showed higher specific activity than the free enzyme.

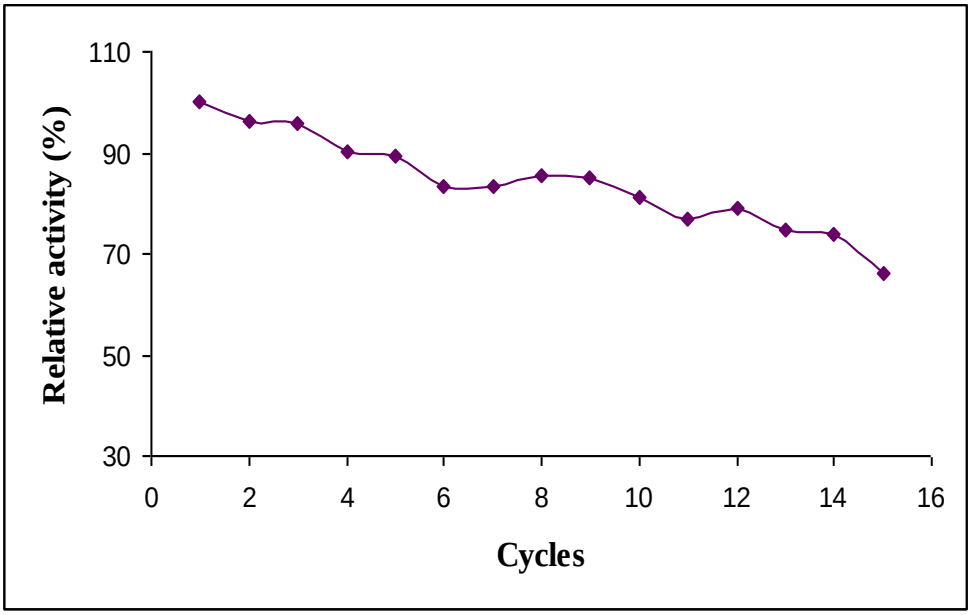

Fig. 3.12 Reusability of MCF immobilized (MCF-AG-Enz-R) enzyme

Table 3.10 Experimental value of operational stability of free and MCF-immobilized enzymes activities

MCF-AG-Enz-R					
Time	Absorb. at 540 nm	Product (g/L)	Enzyme activity x 10^{-2} (mol/sec)	Enzyme amount (ml)	Specific activity (µ mol $mg^{-1}min^{-1}$)
5	1.037	2.645	195.72	0.086	20.689
15	1.307	3.383	83.45	0.089	8.524
30	1.325	3.450	42.56	0.086	4.499
45	1.367	3.564	29.30	0.079	3.372
60	1.207	3.097	19.10	0.081	2.144
90	1.402	3.681	15.14	0.083	1.658
Free Enzyme					
Time	Absorb. at 540 nm	Product (g/L)	Enzyme activity x 10^{-2} (mol/sec)	Enzyme amount (ml)	Specific activity (µ mol $mg^{-1}min^{-1}$)
5	1.264	3.249	240.43	0.15	14.572
15	1.341	3.500	86.35	0.15	5.234
30	1.405	3.668	45.25	0.15	2.742
45	1.421	3.731	30.68	0.15	1.860
60	1.455	3.836	23.66	0.15	1.434
90	1.469	3.853	15.84	0.15	0.960

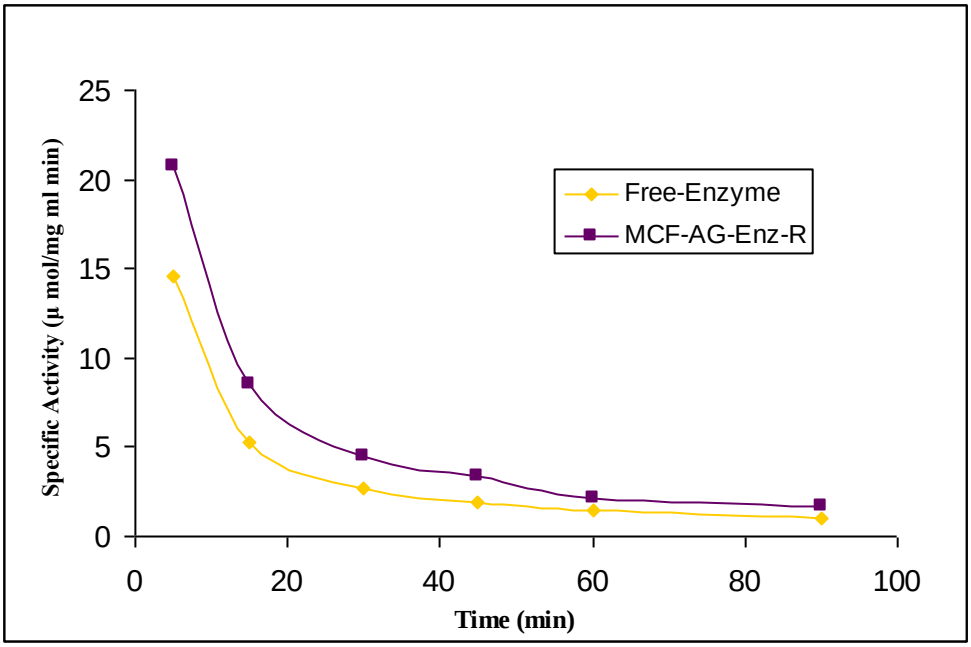

Fig. 3.13 Operational stability of free and immobilized enzymes

Multi point covalent attachment of cellulase with carrier rigidified the enzyme and the availability of polar groups (-NH-, -OH). This could be electrostatically stabilizing the cellulase on surface as well as inside the pores of surface modified MCF during hydrolysis of soluble carboxymethyl cellulose. These provides the rigidity to the cellulase enzyme globular structure to some extent, later get denatured due to higher temperature and pH of operational conditions. The large pore size MCF material was found to be good support for large enzyme and substrate molecules, which can facile the diffusion of substrate and product molecules into the active site of enzyme.

3.4. References:

[1] B. Hahn-Hägerdal, M. Galbe, M.F. Gorwa-Grauslund, G. Lidén, G. Zacchi, *Trends. Biotechnol*. 24 (2006) 549-556.

[2] P. Sassner, M. Galbe, G. Zacchi, *Biomass and Bioenergy* 32 (2008) 422-430.

[3] S.J.B. Duff, W.D. Murray, *Bioresour. Technol*. 55 (1996) 1-33.

[4] D.J Gregg, A. Boussaid, J.N. Saddler, *Bioresour. Technol*. 63 (1998) 7-12.

[5] M.V. Sivers, G. Zacchi, *Bioresour Technol* 56 (1996) 131-140.

[6] A. Wingren, M. Galbe, G. Zacchi, *Biotechnol. Prog*. 19 (2003) 1109-1117.

[7] M. Galbe, G. Zacchi, *Appl. Microbio. Biotechnol*. 59 (2002) 618-628.

[8] R. Eklund, M. Galbe, G. Zacchi, *Bioresour. Technol*. 52 (1995) 225-229.

[9] W.G. Glasser, R.S. Wright, *Biomass and Bioenergy* 14 (1998) 219-235.

[10] Ye Sun, J. Cheng, *Bioresour. Technol*. 83 (2002) 1-11.

[11] J. Soderstrom, L. Pilcher, M. Galbe, G. Zacchi, Appl. Biochem. Biotechnol. 98 (2002) 5-21.

[12] H.H.P. Yiu, P.A. Wright, J. Mater. Chem. 15 (2005) 3690-3700.

[13] P.H. Pandya, R.V. Jasra, B.L. Newalker, P.N. Bhatt, Micropor. Mesopor. Mater. 77 (2005) 67–77

[14] K. Kannan, R.V. Jasra, *J. Mol. Catal. B* 56 (2009) 34-40.

[15] C. Mateo, J.M. Palomo, G. Fernandez-Lorente, J.M. Guisan, R. Fernandez-Lafuente, *Enzyme Microb. Technol*. 40 (2007) 1451–1463.

[16] Y.J Han, T. Watson, G.D Stucky, A. Butler, *J. Mol. Catal. B* 17 (2002) 1–8.

[17] A.B. Jarzębski, K. Szymańska, J. Bryjak, J. Mrowiec-Białoń, *Catal. Today* 124 (2007) 2-10.

[18] M. Hartmann, Chem. Mater. 17 (2005) 4577-4593.

[19] D. Jung, C. Streb, M. Hartmann, *Int. J. Mol. Sci*. 11 (2010) 762-778.

[20] M. Hartmann, C. Streb, *J. Porous Mater*. 13 (2006) 347-352.

[21] A. Vinu, V. Murugesan, O. Tangermann, M. Hartmann, *Chem.Mater*., 16 (2004) 3056-3065.

[22] J. Deere, R. F. De Oliveira, B. Tomaszewski, S. Millar, A. Lalaouni, L. F. Solares, S. L. Flitsch, P.J. Halling, *Langmuir*, 24 (2008) 11762–11769.

[23] J. Deere, E. Magner, J. G. Wall, B. K. Hodnett, *Catal. Lett.* 88 (2003) 183-186.

[24] A. Vinu, M. Hartmann, *Stud. Surf. Sci. Catal*. 154 (2004) 2987-2994.

[25] http://www.rcsb.org/pdb/explore/explore.do?structureId=2BOE

[26] X. Yuan, N. Shan, J. Sheng, X. Wei, *J. Membr. Sci*. 155 (1999) 101-106.

[27] B. Afsahi, A. Kazemi, A. Kheirolomoom, S. Nejati, *Scientia Iranica* 14 (2007) 379-383

[28] L. Wu, X. Yuan, J. Sheng, *J. Membr. Sci*. 250 (2005) 167-173.

[29] A. Dinçer, A. Telefoncu, *J. Mol. Catal. B* 45 (2007) 10-14.

[30] M. Paljevac, M. Primožič, M. Habulin, Z. Novak,. Ž. Knez, J. Supercrit. Fluids. 43 (2007) 74-80.

[31] A.A.S. Sinegani, G. Emtiazi, H. Shariatmadari, *J. Colloid. Interface Sci*. 290 (2005) 39-44.

[32] J.S. Lettow, Y.J. Han, P. Schmidt-Winkel, P. Yang, D. Zhao, G.D. Stucky, J.Y. Ying, *Langmuir* 16 (2000) 8291–8295.

[33] M.M Bradford, *Anal. Biochem*. 72 (1976) 248–254.

[34] T.K. Ghose, *Pure. Appl. Chem*. 59 (1987) 257-268.

[35] A.S.M. Chong, X.S. Zhao, *J. Phys. Chem. B* 107 (2003) 12650–12657.

Chapter 4

De novo designing of Nitrile Hydratase from alkaline protease using reversible denaturation followed by renaturation in presence of cobalt metal ion

4.1. Introduction

Nitrile hydratases (NHases) are bacterial enzymes that catalyze the hydration of nitriles to the corresponding amides. NHases contain non-heme iron or non corrinoid cobalt at their active site. Iron-containing enzymes are the best known so far. Two of those, NHase from Chlororaphis B23 and NHase from Rhodococcus rhodochrous J1 are commonly used for industrial production of acrylamide and nicotinamide.[1] However, the wild strains still have some disadvantages, such as the poor thermo-stability, buffer ion inactivation of the NHase, and the accumulation of the by-product.[2] In order to overcome these obstacles, the heterogeneous cloning and expression of NHase in different recombinant strains had already been carried out by some researchers, but the results were not as good as expected.[3-5]

Recently, the crystal structures of NHase in the active and inactive states were determined at resolutions of 2.65 and 1.7 Å, respectively.[6-7] The structure of the catalytic center is very unusual; i.e. three cysteine sulfur atoms from KCys-109, KCys-112 and KCys-114 and two amide nitrogen atoms from KSer-113 and KCys-114 are coordinated to the Fe^{3+}. The crystal structure of the inactive enzyme revealed that two cysteine ligands, KCys-112 and KCys-114, are oxidized to a cysteine-sulfinic acid (Cys-SO_2H) and a cysteine-sulfenic acid (Cys-SOH), respectively.[7] Various spectroscopic studies revealed the metal ions of both Fe- and Co-type NHases existed as a low-spin trivalent state with similar ligand fields.[8-9] In all known NHases, metal centers are ligated by highly conserved sequence, Cys-X-Leu-Cys-Ser-Cys, where X=Ser for Fe-NHase and X=Tyr for Co-NHases.[10-11] Irrespective of the structural conservation between Fe- and Co-type NHases, there are some differences in the biochemical characteristics between them. The Co-type NHases do not exhibit the

photo reactivity, which is common among Fe-type NHases.[12-14] Fe-type NHase hydrates preferentially aliphatic small nitriles whereas the Co-type enzyme exhibits high affinity for aromatic nitriles.[15-17] Although the ion radii of Fe^{3+} (0.64 Å) and Co^{3+} (0.63) are similar and structures around their binding sites are conserved between Fe- and Co-type NHases, both enzymes specifically incorporate their own metals. The metal substitution of NHases is one of the best ways to understand the functions of the metal in metalloproteins.[18]

Chemical denaturants like urea and guanidine hydrochloride (GdnHCl) at their increased concentrations perturb protein structure by binding directly to peptide groups and weakening internal hydrogen bonds or by upsetting the hydrophobicity of the protein by changing the structure of water around hydrophobic groups.[19-22] There has been increased interest in the use of Gdn-HCl in the study of protein folding because of their high denaturing potential. Denaturation induced by these agents usually gives rise to the same unfolded state of proteins,[23-25] despite the difference in concentration required to give the same unfolded state.[26] However, some proteins, such as papain, cytochrome C551 and stem bromelain show different unfolded states with Gdn-HCl.[27-29] Carbonic anhydrase is a zinc metallo enzyme, replacing the active-site zinc with manganese yielded manganese-substituted carbonic anhydrase (CA[Mn]), which shows peroxidase activity.[30]

Bacterial alkaline proteases are the most important industrial enzymes which give their high activity at high pH, temperature with broad substrate specificity. There has been a renewed interest in the molecular study of these enzymes.[31] In this present work, de novo protein engineering of alkaline protease towards the nitrile hydratase

enzyme is discussed, with reference to catalytic conversion of 3-cyanopyridine to nicotinamide.

4.2. Experimental section

4.2.1 Materials

Guanidium Hydrochloride (Gdn-HCl, 99%, A.R.), Cobalt (III) fluoride (99%, A.R.), 3-Cyanopyridine (98%, A.R.), Nicotinic acid (98%, A.R.), Nicotinamide (98%, A.R.), Na_2HPO_4 (99%, A.R.), $NaH_2PO_4 \cdot 2H_2O$ (99% A.R.), were purchased from Sigma-Aldrich (USA). Alkaline Protease (E.C.3.4.21.62) from Bacillus Licheniformis was donated by Genencor International, The Netherlands. Fast spin dialyzer 2000 µl chamber, Cellulose acetate dialysis membrane MWCO= 1000 Da, were purchased from Harvard apparatus, Holliston, MA. Acetonitrile HPLC grade (98%, A.R.), Phosphoric acid (85%, A.R.) and Hydrochloric acid (35.4%, A.R.) were purchased from s.d. Fine Chemical, India. These chemicals were used for enzyme modification and their activities studies.

4.2.2 Cobalt centered new active site creation

1 ml of Guanidium Hydrochloride (3M to 6M) was added to the 1 ml of alkaline protease and mixed well and kept for 30 min at room temperature. To this solution 0.5 ml of CoF_3 (0.3 mM) solution was added and the resultant solution was transferred into double side fast spin dialyzer chamber having cellulose acetate membrane (MWCO=1000 Da). This was dialyzed in 12 ml CoF_3 and 100 ml phosphate buffer pH=7.5 twice and followed by dialysis with phosphate buffer pH=7.5 four times. This was finally transferred into 5 ml vessel and kept at ~4 °C for

10 h in a refrigerator to achieve rearranged globular structure. The native alkaline protease and 3-6M Gdn-HCl denatured enzymes are designated as AP-Blank, AP-3MGdn, AP-4MGdn, AP-5MGdn and AP-6MGdn respectively. The above denatured enzymes are renatured in presence of cobalt metal ion and designated as AP-3MGdn-Co, AP-4MGdn-Co, AP-5MGdn-Co and AP-6MGdn-Co respectively. The shematic creation of cobalt centered new active site is given in Fig. 4.1.

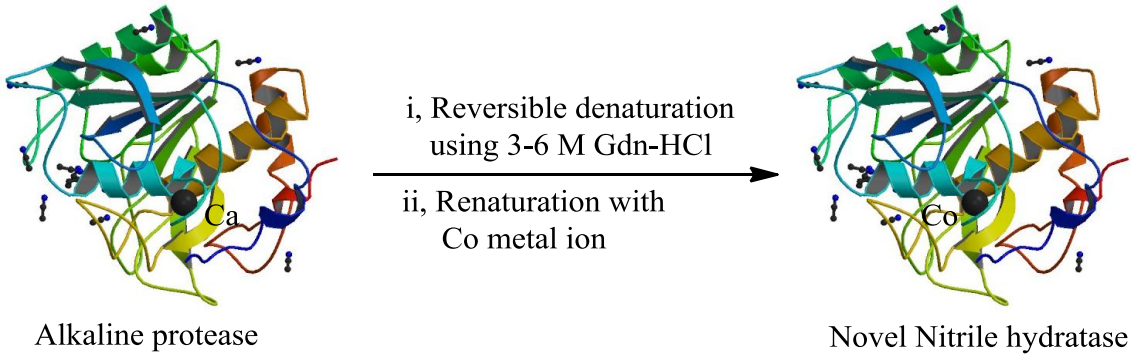

Fig. 4.1 Schematic creation of cobalt centered new active site

4.2.3 Fluorescence spectroscopy

The absorbance change due to the coordination of Co metal ion with peptide was measured using 2 mg/mL renatured novel enzyme solution with reference to the native alkaline protease in the range of 400-200 nm using a UV–vis–NIR scanning spectrophotometer (CARY, Varian 500 SCAN) to obtain excitation wavelength. The same concentration of cobalt active site centered novel enzyme solution was excited at 285 nm and the fluorescence spectra was collected from the 290-450 nm using model Fluorolog Horiba Jobin Yvon spectrofluorimeter at room temperature to measure the absorbance shift due to the cobalt metal ion in protein complex.

4.2.4 Inductive coupled plasma (ICP) analysis

Alkaline protease is a calcium having enzyme in its globular structure, the amount of calcium present in native enzyme was obtained by using as such (AP-Blank), in the instrument calcium detection limit of above 0.01 mg/L. The native was denatured using 3-6M Gdn-Hcl and then renatured by dialyzing in phosphate buffer with cobalt metal ion for the reason to check binding stability and the ability to replace the calcium by cobalt metal ions. The total amount of cobalt metal ion present in the new active site created enzyme solutions was determined in the detection range of 0.007 mg/L using the Inductively Coupled Plasma Optical Emission Spectrometry (ICP; Perkin Elmer, Optima 3300 RL) instrument.

4.2.5 Circular Dichroism (CD) Spectroscopy

Circular Dichroism (CD) spectra were typically measurements at 25 °C between 190 and 300 nm using a JASCO- 815 UV–Vis spectropolarimeter, equipped with a thermostat, in a 3-mL cuvette with 1-cm path length. Protein concentration was 0.1 mg/mL. Samples were scanned after 30 min incubation with the denaturant (3-6 M Gdn-HCl) in 0.1 M sodium phosphate buffer, pH 7.5. The ellipticity at 225 nm was used to measure the fraction of native structure remaining in each denaturing condition. Each spectrum was corrected for baseline. The molar mean residue ellipticity at wavelength λ, $[\theta]_{\lambda}^{25^{\circ}C}$ in degrees centimeter^2 decimole^{-1}, was obtained from

$$[\Theta]_{\lambda}^{25^{\circ}C} = \frac{\theta\ (MRW)}{10lc}$$

where θ= experimentally observed ellipticity in degrees at wavelength λ, l= path length in centimeters, c = protein concentration in grams per milliliter and MRW = mean residue weight of protein, 112 calculated from the amino acid composition in alkaline protease.

4.2.5.1 Secondary-Structure Analysis of Proteins

The secondary structures of denatured alkaline protease in 3-6 M Gdn-HCl and the renatured alkaline protease in presence of cobalt metal ion protein's components were assigned using the Define Secondary Structure of Proteins (DSSP) program [32]. The 3_{10}-helices were considered to be α- helices, the bends were treated as strands, and the single residues assigned as turns and bends were classified as unordered structures. Moreover, α-helices and β-strands were divided into regular (αR and βR) and distorted (αD and βD) classes, assuming that four residues per α-helix and two residues per β-strand were distorted [33]. Thus the protein structures were classified into six types: regular α-helix (αR), distorted α-helix (αD), regular β-strand (βR), distorted β-strand (βD), turn, and unordered structure.

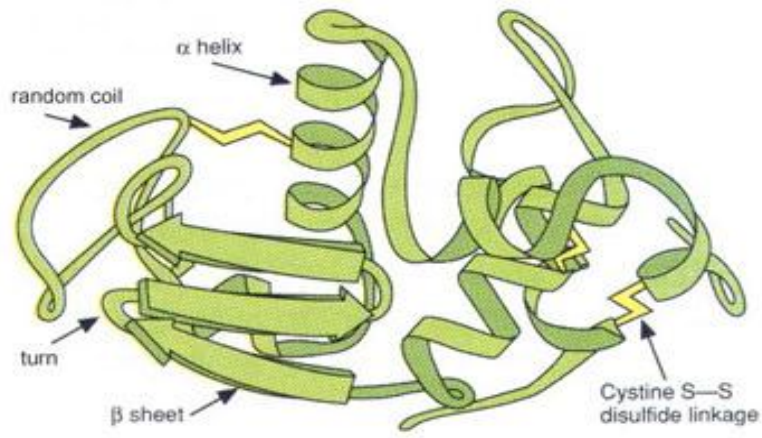

Fig. 4.2 Secondary structural component of the protein

4.2.4.2 CD analysis. The secondary structure fractions of the globular proteins from the CD spectrum of the denatured and renatured alkaline protease were analyzed using the reference set 4 in the member of the DICHROWEB online server. Two methods for analyzing protein CD spectra were used, as implemented in computer programs SELCON3 and CONTIN/LL. Only brief descriptions of the algorithms used in the two methods are given below. Detailed descriptions of these methods are available in the literature.

SELCON3. This is the latest version of the self-consistent method, SELCON [34], the spectrum of the protein analyzed is included in the matrix of CD spectral data, and an initial guess, the structure of the reference protein having the CD spectrum most similar to that of the protein analyzed, is made for the unknown secondary structure; the solution replaces the initial guess; and the process is iterated for convergence. The matrix equation relating the CD spectra to the secondary structure is solved by the singular-value decomposition algorithm and variable selection [35] in the locally linearized model [36]; solutions are obtained by varying the reference proteins and/or the SVD coefficients.

Acceptable solutions from the different variable selection combinations in the locally linearized model satisfy the three basic selection rules. The sum of fractions is between 0.95 and 1.05; each fraction is greater than -0.025; the RMS deviation between the reconstructed and experimental CD is less than 0.25 $\Delta\epsilon$. These acceptable solutions are subjected to another selection rule based on the helical content, as defined by Johnson [37]. The final solution is the average of all solutions that satisfy the four selection rules.

CONTIN/LL. This is a variant of the CONTIN method developed by Provencher and Glockner [38]. CONTIN uses the ridge regression procedure, which fits the CD spectrum of the test protein ($C\lambda^{obs}$) as a linear combination of the CD spectra of N reference proteins by minimizing the function

$$\sum_{\lambda=1}^{n} (C_{\lambda}^{calc} - C_{\lambda}^{obs})^2 + \alpha^2 \sum_{j=1}^{N} (v_j - N^{-1})^2$$

where C_λ is the spectrum at *n* wavelengths, α is the regularizer, and v_j is the coefficient of the CD spectrum for the *j* th reference protein in the linear combination used to construct the spectrum of the test protein, C_λ^{calc}. The selection rules $f_k \geq 0.0$ and $\Sigma f_k = 1.0$ are used as constraints. The method gives a range of solutions, depending on the value of α; smaller values of α give solutions similar to those from the normal least squares method and larger values tend to give solutions biased toward certain proteins, limiting the number of degrees of freedom.

In CONTIN/LL, the proteins in the reference set are arranged in the order of increasing RMS distance of the CD spectra from that of the protein analyzed, and the more distant proteins are deleted in a systematic manner to construct smaller reference sets. This results in a set of solutions, one for each LL combination, the number of which is determined by the number of reference proteins and the minimum number of proteins used for a solution. The selection rule based on helical content was used to screen the solutions. The final solution is the average of all solutions that satisfy the four selection rules.

4.2.6. Activity assay of the enzyme

The resultant modified alkaline protease was made into 4 ml enzyme solution using phosphate buffer and then used in all kinetic studies. Nitrile hydratase enzyme activity was measured by incubating with 10-45 mM of 3-cyanopyridine for exactly 6 h at 50 ˚C. The reaction was stopped by adding 0.1 ml of 1 M HCl solution and the precipitate was removed by centrifugation. The hydrolysis products of 3-cyanopyridine include nicotinamide and nicotinic acid (Fig. 4.3) were measured by using high-pressure liquid chromatography (HPLC) instrument.

4.2.6.1 Analytical methods.

HPLC was performed with a JASCO LC-2000 plus system equipped with a HiQ Sil C18Hs (reverse-phase column, 4.6 mm x 250 mm; KYA Technologies Corporation, Tokyo, Japan) at a flow rate of 1.0 ml/min at 30°C, with the following solvent system: acetonitrile-10 mM NaH_2PO_4-H_3PO_4 buffer (pH 2.8), 1:4 (vol/vol). In some cases, a Phenomenex Luna-NH_2 column (5µ, 250 x 4.6 mm; CA, USA) was used to detect the formation of nicotinic acid at a flow rate of 1.0 ml/min at 30°C, with the following solvent system: acetonitrile-10 mM NaH_2PO_4-H_3PO_4 buffer (pH 2.8), 3:1 (vol/vol). The absorbance was measured at 230 nm for both nicotinamide and nicotinic acid. The concentrations of substrate and product were determined in samples adequately diluted with the mobile phase.

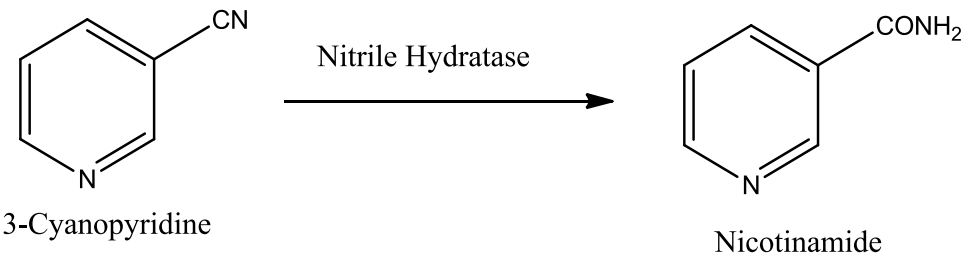

Fig. 4.3 Conversion of 3-Cyanopyridine to Nicotinamide in presence of NHase

4.2.7 Effect of temperature and pH on enzyme activity

The effect of temperature on the nitrile hydratase enzyme activity was observed by incubation with 15 mM of 3-cyanopyridine in 0.1M phosphate buffer solution having a pH=7.5 at temperatures ranging from 30 to 60 ˚C, and alternatively incubated at a fixed temperature of 50 ˚C at pH ranging from 6 to 9 for measure the effect of pH. The activity of nitrile hydratase at different pH and temperature were then measured as per previously described analytical method (Section 4.2.5.1).

4.3. Results and discussion

4.3.1 Component CD Spectra of Secondary Structures

The circular dichroism (CD) spectra of the native, Gdn-HCl denatured alkaline proteases exhibit characteristic peaks in the UV region (205-260 nm) as shown in Figure 4.4. The native alkaline protease showed a 20% residual molar ellipticity at 212 nm while with Gdn-HCl treatment it was reduced to 12%. This indicated nearly complete collapse of the globular structure of the protein.

The negative peak at 222 nm is attributable to the n–π* transition of the peptide, and the negative and positive peaks at 208 is attributable to the parallel excitation of the π–π* transition of α-helices in the peptide. [39-40] The negative peak at 196 nm is attributable to the n–π* transition of the peptide, and the positive peaks at 218 is attributable to the parallel excitations of the π–π* transition in β-strands of the peptide. The positive peak at 212 nm is attribute to π–π* transition and a negative peak at 195 nm is attribute to n–π* transition in random coil of the peptides. Variations in the CD spectra between these α-helix–rich proteins would arise from not

only differences in secondary-structure contents but also from ones in the arrangement of α-helices and β-strands in the tertiary structure (α/β and α+β classes).

Therefore, to evaluate the contribution of each secondary structure, the UVCD spectra of native, denatured and renatured (with cobalt metal ion) proteins were deconvoluted into the spectra of four components α-helices, β-strands, turns, and unordered structures using the SELCON3 program.[41] The spectra for each of these components averaged across all the proteins are shown in Table 4.1.

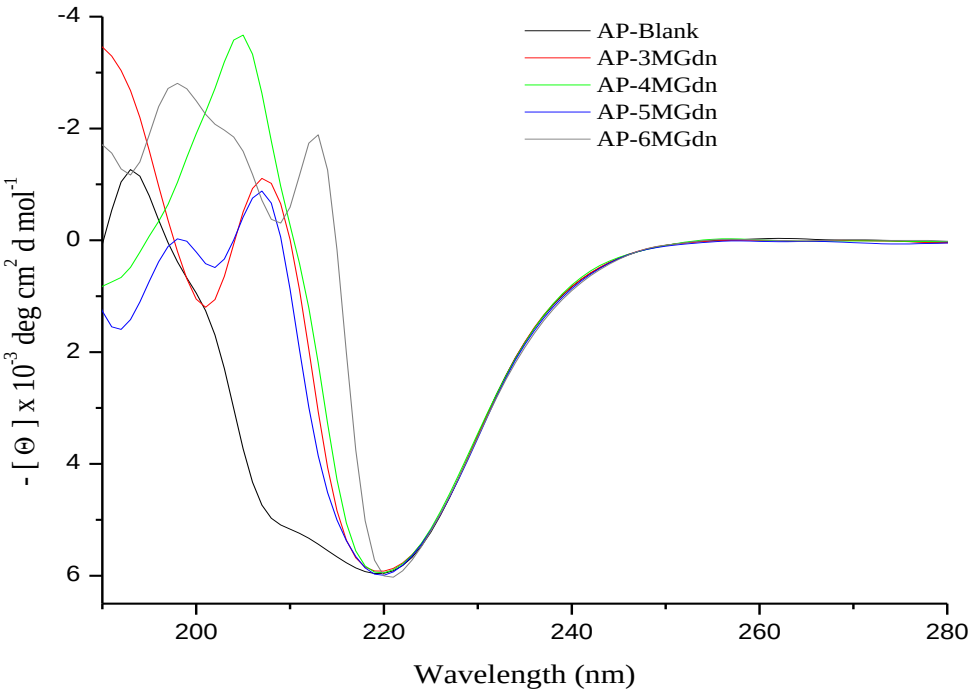

Fig. 4.4 CD spectrum of denatured alkaline protease in 3-6M Gdn-HCl

The native alkaline protease shows higher α-helix contents of 2.9% exhibiting two negative peaks at around 222 and 208, a positive peak at around 195 nm. Similar CD spectra were observed for 3-6M Guanidium Hydrochloride denatured alkaline

protease. However, gradual decrease in the α-helix contents in the range 2.9% to -3.37% with reference to native was observed. In general denaturation using increased Gdn-HCl concentration shows increase in hydrophobicity by cleavage of hydrogen bond between the amino acids in the well-arranged globular structure. The AP-4MGdn shows higher α-helix (1.48%) content compared to other denatured sample. In case of 3MGdn-Gdn denatured enzyme the ionic concentration may not be good enough to stabilize the secondary structure which ultimately results into the collapse of α-helix to turns (23.39%) and unordered (30.69%) contents. 5-6 MGdn-HCl denatured sample breaks most of the hydrogen bonding in the alkaline protease structure consequently showing higher turns (23–23.35%) and unordered (25.43 – 24.79%) contents.

The enzymes renatured in presence of cobalt metal ion shows α-helix content lower than the native alkaline protease as seen in Fig. 4.5. The folding of proteins is generally believed to be under thermodynamic control that leads to the production of active protein which has a stable conformation in the lowest energy state. Performance of SELCON3 Programs for analyzing renatured alkaline protease in Co metal ion CD Spectra for Reference Set 4 are shown in Table 4.2**.** AP-3MGdn-Co the unordered β-strands, turns and unordered content folded into distorted α-helix (2.99%), but in the case of AP-4MGdn-Co showed higher regular (1.14%) and distorted (6.65%) α-helix. The observed α-helix content of 5-6MGdn-Co samples was very small compared to other samples which presents as unordered content of 25.64% and 41.52% respectively. These increased unordered contents indicates that the denaturation of regular α-helix to distorted or into regular/distorted β-strands contents. Moreover, there is a possibility to produce regular α-helix on the

renaturation in presence of Co metal ion. However, when the turns and unordered contents are higher, it is quite difficult to achieve α-helices. The metal ions also accelerate the folding of denatured peptide chain by coordinating with its corresponding amino acids in their close proximity.

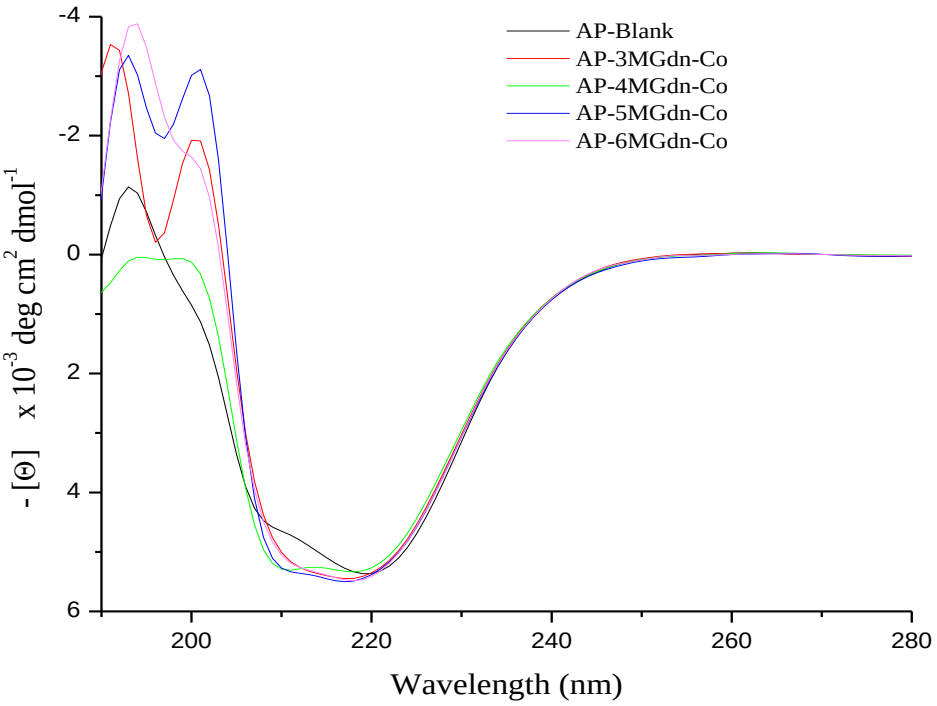

Fig. 4.5 CD spectrum of renatured alkaline protease in presence of Co metal ion

Table 4.1 Secondary content of AP-Blank, AP-3MGdn, AP-4MGdn, AP-5MGdn and AP-6MGdn from SELCON3 Program

Sample	$Helix_{\alpha R}$	$Helix_{\alpha D}$	$Strand_{\beta R}$	$Strand_{\beta D}$	Turns	Unordered	Total
AP-Blank	0.029	0.158	0.296	0.169	0.167	0.181	1.001
AP-3MGdn	-0.031	-0.048	0.344	0.157	0.215	0.282	0.919
AP-4MGdn	0.015	0.078	0.313	0.197	0.202	0.206	1.011
AP-5MGdn	-0.001	0.024	0.292	0.194	0.227	0.251	0.987
AP-6MGdn	-0.004	0.029	0.285	0.192	0.226	0.240	0.968

Table 4.2 Secondary content of AP-Blank, AP-3MGdn, AP-4MGdn, AP-5MGdn and AP-6MGdn from SELCON3 Program

Sample	$Helix_{\alpha R}$	$Helix_{\alpha D}$	$Strand_{\beta R}$	$Strand_{\beta D}$	Turns	Unordered	Total
AP-Blank	0.029	0.158	0.296	0.169	0.169	0.181	1.001
AP-3MGdn-Co	-0.002	0.030	0.295	0.197	0.197	0.255	1.002
AP-4MGdn-Co	0.011	0.064	0.285	0.196	0.196	0.208	0.962
AP-5MGdn-Co	-0.002	0.022	0.297	0.191	0.191	0.252	0.983
AP-6MGdn-Co	-0.031	-0.075	0.295	0.132	0.132	0.367	0.884

It is pertinent to compare the result obtained from SELCON3 method to those obtained with CONTIN/LL method. The ridge regression algorithm followed in the CONTIN/LL method gives different weights to different proteins in the reference set in fitting the experimental spectrum. This comparison can be attributed to the increased variety in the spectral and structural data used in the analysis resulting from the reference set 4. The largest improvements were observed for the secondary content of denatured and renatured alkaline proteases. AP-4MGdn sample shows the slight decrease of ordered strand (27.6%) to unordered (32.1%) but in renaturation the unordered content (30.73%) decreases compared to native (31.36%). AP-3MGdn the ordered (0.1%) and distorted α-helix (3.5%) contents were transformed to unordered (31.53%), the same trend also is observed for AP-4MGdn (unordered, 32.07%) and AP-5MGdn (unordered, 31.20%) samples as shown in Table 4.3.

The renatured samples in the presence of cobalt metal ion show all the contents of the secondary structure nearly close to the native alkaline protease except slight difference in the unordered contents. AP-4MGdn-Co shows ordered (0.2%) and distorted α-helix (3.7%) contents same as that of Table 4.4. The α-helical structures in proteins generally show smaller geometric variations, while the variations observed in β-strands and turns are much larger. The β-strands in proteins are often bent and/or

twisted and show larger variation of the (ϕ, ψ) angles than that in α-helices. Thus the CONTIN/LL method enables improving the secondary structure contents reference to native (alkaline protease) structure from experimental CD spectrum analysis.

The partly unfolded states were generated either by exposing the native protein to varying concentrations of Gdn-HCl from 3M to 6M. Thus, the unfolding pathway appears to be completely reversible, involving the same structural intermediates. Nevertheless, it appears reasonable that the core structure, resistant to denaturation by 3 to 6 M Gdn-HCl, acts as the nucleation site for the fast and correct refolding of alkaline protease molecules.[42] The folding process may occur in a successive assembly of "subdomains" in both directions of the core structure.[43-44] The characteristics of the CD of renatured alkaline proteases are different from those of the native with presence of turns and unordered content in the secondary structures, because those molecules contain many metal chelating sites through its coordinating amino acid residues. Thus, the peaks and troughs will be markers for the structural refolding as well as function recovery.

Table 4.3 Secondary content of AP-3MGdn-Co, AP-4MGdn-Co, AP-5MGdn-Co and AP-6MGdn-Co from CONTIN-LL Program

Sample	$Helix_{\alpha R}$	$Helix_{\alpha D}$	$Strand_{\beta R}$	$Strand_{\beta D}$	Turns	Unordered	Total
AP-Blank	0.002	0.037	0.285	0.150	0.213	0.314	1.001
AP-3MGdn	0.001	0.028	0.301	0.143	0.204	0.324	1.001
AP-4MGdn	0.002	0.037	0.276	0.147	0.217	0.321	1.000
AP-5MGdn	0.002	0.035	0.280	0.147	0.215	0.322	1.001
AP-6MGdn	0.002	0.034	0.303	0.152	0.207	0.302	1.000

Table 4.4 Secondary content of AP-3MGdn-Co, AP-4MGdn-Co, AP-5MGdn-Co and AP-6MGdn-Co from CONTIN-LL Programs

Sample	$Helix_{\alpha R}$	$Helix_{\alpha D}$	$Strand_{\beta R}$	$Strand_{\beta D}$	Turns	Unordered	Total
AP-Blank	0.002	0.037	0.285	0.150	0.213	0.314	1.001
AP-3MGdn-Co	0.001	0.035	0.289	0.148	0.211	0.315	0.999
AP-4MGdn-Co	0.002	0.037	0.292	0.151	0.210	0.307	0.999
AP-5MGdn-Co	0.001	0.032	0.288	0.146	0.213	0.321	1.001
AP-6MGdn-Co	0.002	0.033	0.294	0.149	0.210	0.312	1

4.3.2 Intrinsic Tyrosine Fluorescence

The UV-Visible spectrum of AP-Blank, AP-6MGdn and AP-6MGdn-Co is shown in Fig. 4.6. The native alkaline protease show absorbance at 275 nm and renatured in presence of Co metal ion shows absorbance at 275 nm and 280 nm. The fluorescence emission spectrum of the native and renatured (in presence of cobalt metal ion) enzyme samples following excitation at 285 nm is shown in Figure 4.7. The native protein exhibited a fluorescence emission peak at 306 nm, indicating that mostly the tyrosine residues were well buried within the protein structure. The renatured alkaline proteases did not produce significant peak towards red shift. This indicates that the tyrosine residues may not be interacting with cobalt metal ions during renaturation. Cobalt centered enzyme shows same peak as of native and the peak at 360 nm coexisted for charge transfer from coordinating residues of peptide to cobalt metal ion.

The observed tyrosine intensity of AP-4MGdn-Co enzyme is lower than the other renatured and native alkaline proteases at 306 nm apparently showing slightly higher intensity at 360 nm. This could be due to increase in number of coordination

between the amino acid residues with cobalt metal ions. The observations indicate that the reconstituted proteins may be delicately but distinctly different from the native AP.

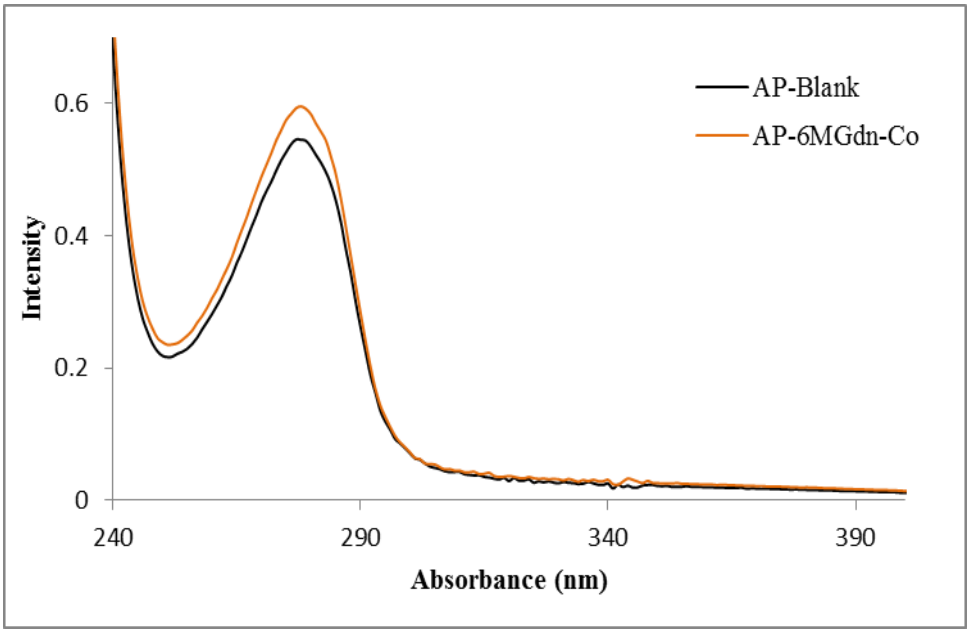

Fig. 4.6 UV-Visible spectra of AP-Blank, AP-6MGdn and AP-6MGdn-Co

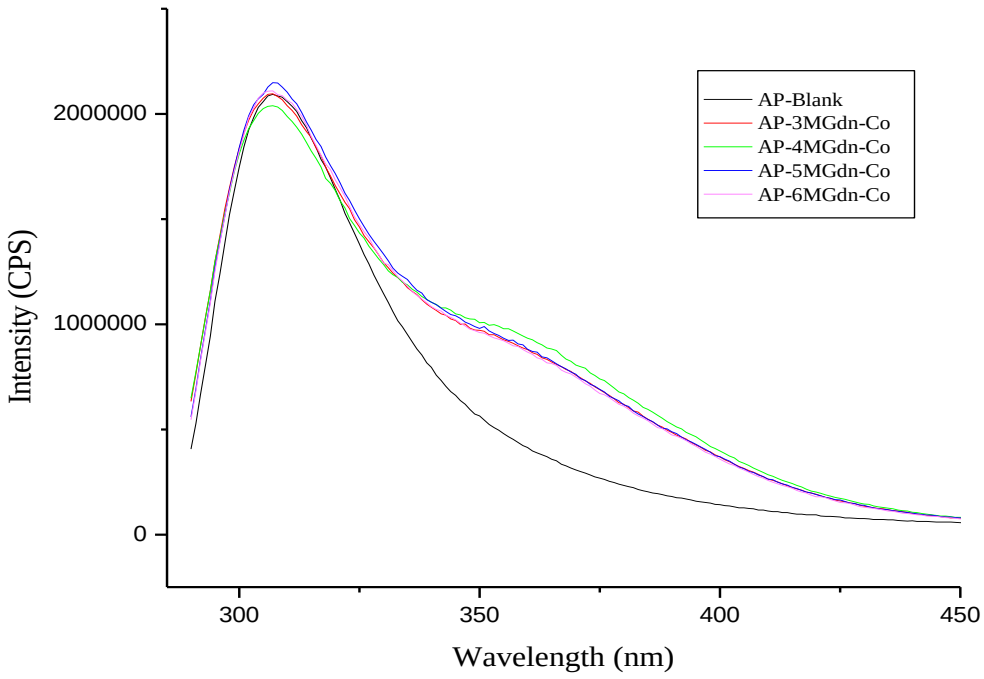

Fig. 4.7 Fluorescence emissions spectra of AP-3MGdn-Co, AP-4MGdn-Co, AP-5MGdn-Co and AP-6MGdn-Co

4.3.3 Inductive coupled plasma analysis

The ICP analysis data of calcium and cobalt metal ion are given in Table 4.5. The native alkaline protease shows higher content of calcium ion (3.5281 mg/L). The AP-3MGdn-Co, AP-4MGdn-Co, AP-5MGdn-Co and AP-6MGdn samples show very lower content. However, the AP-4MGdn-Co shows higher cobalt ion in their enzyme molecular structure, this could be the availability of cobalt metal ion to corresponding coordinating residues in close proximity. The ICP data also supports the expected protein folding in nano second phenomenon at molecular level of alkaline proteases.

Table 4.5 Inductive couple plasma (ICP) analysis of calcium and cobalt metal ion in native and AP-3MGdn-Co, AP-4MGdn-Co, AP-5MGdn-Co and AP-6MGdn-Co

Sample	Calcium (mg/L)	Cobalt (mg/L)
AP-Blank	3.5281	-
AP-3MGdn-Co	0.0305	0.0476
AP-4MGdn-Co	0.0165	0.0553
AP-5MGdn-Co	0.0103	0.0458
AP-6MGdn-Co	0.0101	0.0429

4.3.4 Nitrile Hydratase activity studies

The kinetic parameters of Michaelis–Menten equation were determined for AP-3MGdn-Co to AP-6MGdn-Co. Experiments were carried out by the production of nicotinamide using different substrate 3-cyanopyridine concentrations (5mM – 45mM) to obtain the values given in Table 4.6 and Fig. 4.8, the Lineweaver-Burk plot (Fig. 4.9) and the derived parameter values given in Table 4.7. For nitrile hydrolytic reaction catalyzed by AP-3MGdn-Co to AP-6MGdn-Co the value of saturation constant K_m = 1.87, 1.68, 2.43, 3.32 x 10^{-6} mol and the maximum reaction

velocity V_{max} = 7.97, 8.23, 7.59, 7.17 U/mg were observed for the AP-3MGdn-Co, AP-4MGdn-Co, AP-5MGdn-Co and AP-6MGdn-Co enzymes, respectively.

It shows lower apparent affinity of substrate (K_m) and higher V_{max} for the AP-4MGdn-Co enzyme, which led to altering the reaction towards the higher production of Nicotinamide. Most likely it was caused by the larger affinity to the regular coordination of amino acid residue with active centre cobalt metal ion that might have favored diffusion of substrate and product molecules towards the active site and vice versa. This observation is in good agreement with the data presented in Table 4.6.

Table.4.6 Experimental data of activity at different substrate (3-cyanopyridine) concentration

Conc. of 3-cyanopyridine (mM)	Conversion (%)	Rate of reaction x 10^{-2} (mol/min)	Enzyme activity x 10^{-2} (mol/min)	Specific activity x 10^{-4} (μ mol $mg^{-1}min^{-1}$)
AP-3MGdn-Co				
5	37.21	0.517	2.067	1.723
10	31.60	0.878	3.511	2.926
15	28.20	1.175	4.700	3.917
25	20.40	1.417	5.667	4.722
35	16.12	1.567	6.269	5.224
45	12.20	1.525	6.100	5.083
AP-4MGdn-Co				
5	41.85	0.581	2.325	1.938
10	34.95	0.971	3.883	3.236
15	29.51	1.230	4.918	4.099
25	22.42	1.557	6.228	5.190
35	17.15	1.667	6.669	5.558
45	13.36	1.670	6.680	5.567

AP-5MGdn-Co				
5	28.09	0.390	1.56	1.301
10	27.86	0.774	3.10	2.580
15	22.76	0.948	3.79	3.161
25	17.00	1.181	4.72	3.935
35	13.30	1.293	5.17	4.310
45	10.30	1.288	5.15	4.292
AP-6MGdn- Co				
5	20.07	0.279	1.115	0.929
10	22.48	0.624	2.498	2.082
15	18.70	0.779	3.117	2.597
25	13.30	0.924	3.694	3.079
35	10.10	0.982	3.928	3.273
45	8.30	1.038	4.150	3.458

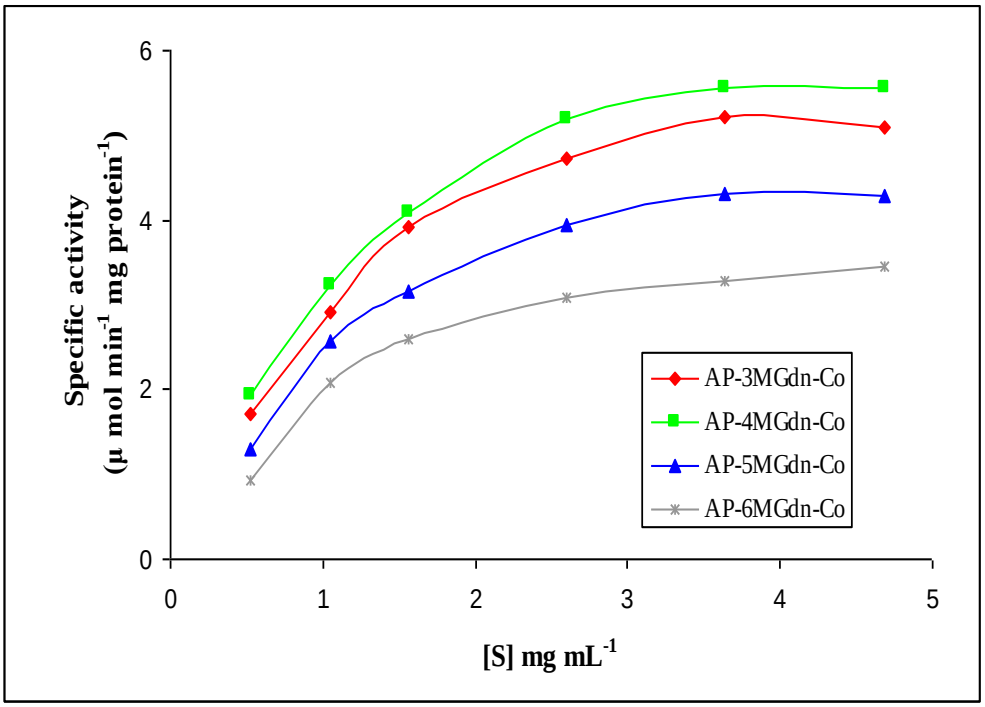

Fig. 4.8 Comparison of activity at different substrate (3-cyano pyridine) concentration

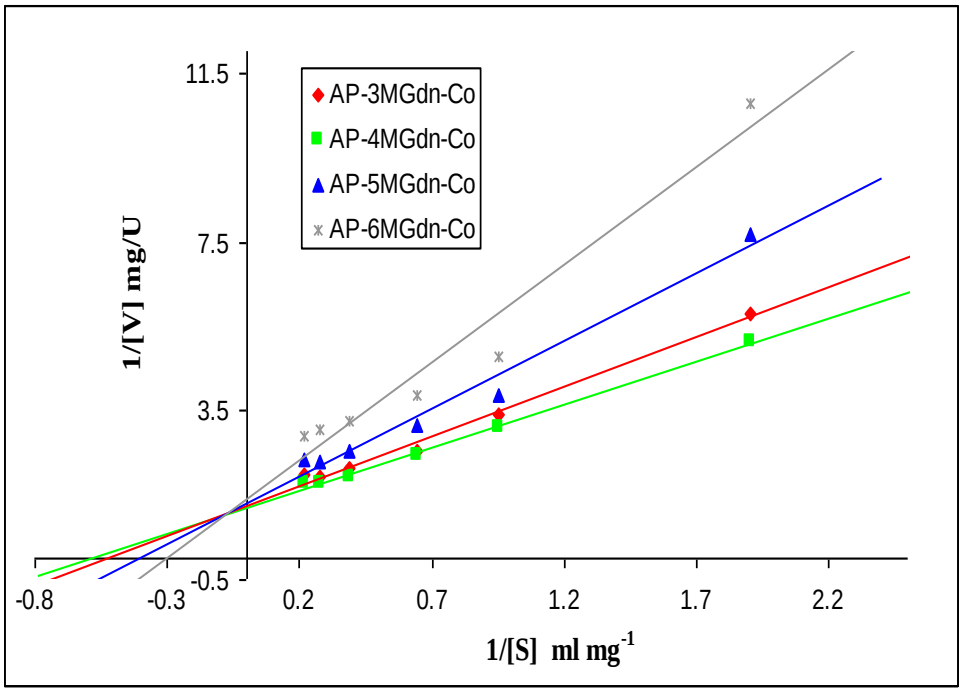

Fig. 4.9 L-B plot for kinetic parameters towards Nitrile Hydratase activity

Considering the structure and function of cobalt-containing NHases, the proposed model can be divided into three different stages.[45] Firstly, the binding of a nitrile occurs close to a hydroxide ion or a metal-bound water molecule. Secondly, either OH^- or the metal-bound water molecule (activated by OH^- as a general base) attacks the nitrile carbon atom, resulting in the formation of an imidate [R–C(–OH)=NH]. Finally, the imidate tautomerizes to an amide. As a consequence of the unique structure of the NHase active site, the hydration of nitriles is catalyzed with high efficiency.[46]

The turn over number k_{cat} = 0.299, 0.309, 0.285, 0.269 S^{-1} were observed for of AP-3MGdn-Co, AP-4MGdn-Co, AP-5MGdn-Co and AP-6MGdn-Co. Except AP-4MGdn-Co, somewhat lower values of both V_{max} and k_{cat} were obtained and the value of k_{cat}/ K_m was also slightly lower. It was expected that a restricted access of substrate

molecules to the active sites of catalyst, and concomitant diffusional limitations, would cause a dramatic change in kinetic parameters.

The only appreciable result appeared to be slightly higher values of maximum reaction velocity (0.823 U/mg) and specific constant (184000 M^{-1} S^{-1}) for AP-4MGdn-Co. It can be explained by differences in the proper co-ordination of amino acid residue with cobalt metal ion and the required arrangement of α-helix, β-strand, turn and unordered content in the globular structure to facilitate the diffusion of substrate and product molecules into the active sites.

Table 4.7 The derived kinetic parameters of the AP-3MGdn-Co, AP-4MGdn-Co, AP-5MGdn-Co and AP-6MGdn-Co from Lineweaver–Burk plot

Sample	K_m (x 10^{-6} M)	V_{max} (μmol mg^{-1}protein min^{-1})	k_{cat} (S^{-1})	k_{cat}/K_m (M^{-1} S^{-1})
AP-3MGdn-Co	1.87	0.797	0.299	160000
AP-4MGdn-Co	1.68	0.823	0.309	184000
AP-5MGdn-Co	2.43	0.759	0.285	117000
AP-6MGdn-Co	3.32	0.717	0.269	81000

4.3.5. Optimum Temperature and pH

The specific activity of the AP-3MGdn-Co, AP-4MGdn-Co, AP-5MGdn-Co and AP-6MGdn-Co enzyme, increased with increasing temperature up to 50 °C beyond which the activity showed a decrease as shown in Fig. 4.10. The AP-4MGdn-Co shows better specific activity relative to the other enzymes. The relative specific activity values for AP-3MGdn-Co, AP-4MGdn-Co, AP-5MGdn-Co and AP-6MGdn-Co enzyme at pH values ranging from 6 to 9 are given in Fig. 4.11.

Table 4.8 Experimental data of temperature effect on Nitrile Hydratase activity

Temp. (°C)	Conversion (%)	Rate of reaction x 10^{-3} (mol/min)	Specific activity x 10^{-4} (μ mol $mg^{-1}min^{-1}$)
AP-3MGdn-Co			
30	11.67	4.863	1.62
35	14.68	6.117	2.04
40	18.13	7.554	2.52
45	22.02	9.175	3.06
50	28.82	12.008	4.00
55	21.00	8.750	2.92
60	17.12	7.133	2.38
65	13.47	5.613	1.87
70	9.98	4.158	1.39
AP-4MGdn-Co			
30	13.38	5.575	1.86
35	16.63	6.929	2.31
40	19.46	8.108	2.70
45	23.76	9.900	3.30
50	29.51	12.296	4.10
55	22.83	9.513	3.17
60	18.31	7.629	2.54
65	14.56	6.067	2.02
70	11.05	4.604	1.53
AP-5MGdn-Co			
30	8.23	3.429	1.14
35	9.46	3.942	1.31
40	12.07	5.029	1.68
45	14.83	6.179	2.06
50	19.70	8.208	2.74
55	16.45	6.854	2.28
60	13.36	5.567	1.86
65	9.64	4.017	1.34
70	6.99	2.913	0.971
AP-6MGdn-Co			
30	7.50	3.125	1.04
35	8.43	3.513	1.17
40	11.21	4.671	1.56
45	13.74	5.725	1.91
50	18.70	7.792	2.60
55	13.89	5.788	1.93
60	10.95	4.563	1.52
65	7.24	3.017	1.01
70	4.78	1.992	0.664

Table 4.9 Experimental data of pH effect on Nitrile Hydratase activity

pH	Conversion (%)	Rate of reaction x 10^{-3} (mol/min)	Specific activity x 10^{-4} (μ mol $mg^{-1}min^{-1}$)
AP-3MGdn-Co			
6.0	12.07	5.029	1.68
6.5	13.05	5.438	1.81
7.0	19.36	8.067	2.69
7.5	28.20	11.750	3.92
8.0	18.13	7.554	2.52
8.5	15.00	6.250	2.08
9.0	9.02	3.758	1.25
AP-4MGdn-Co			
6.0	13.80	5.750	1.92
6.5	16.63	6.929	2.31
7.0	21.57	8.988	3.00
7.5	29.51	12.296	4.10
8.0	19.70	8.208	2.74
8.5	16.31	6.796	2.27
9.0	9.89	4.121	1.37
AP-5MGdn-Co			
6.0	8.94	3.725	1.24
6.5	10.28	4.283	1.43
7.0	13.45	5.604	1.87
7.5	19.70	8.208	2.74
8.0	12.48	5.200	1.73
8.5	9.87	4.113	1.37
9.0	7.93	3.304	1.10
AP-6MGdn-Co			
6.0	7.48	3.117	1.04
6.5	9.35	3.896	1.30
7.0	11.57	4.821	1.61
7.5	18.7	7.792	2.60
8.0	9.77	4.071	1.36
8.5	7.09	2.954	0.985
9.0	5.96	2.483	0.828

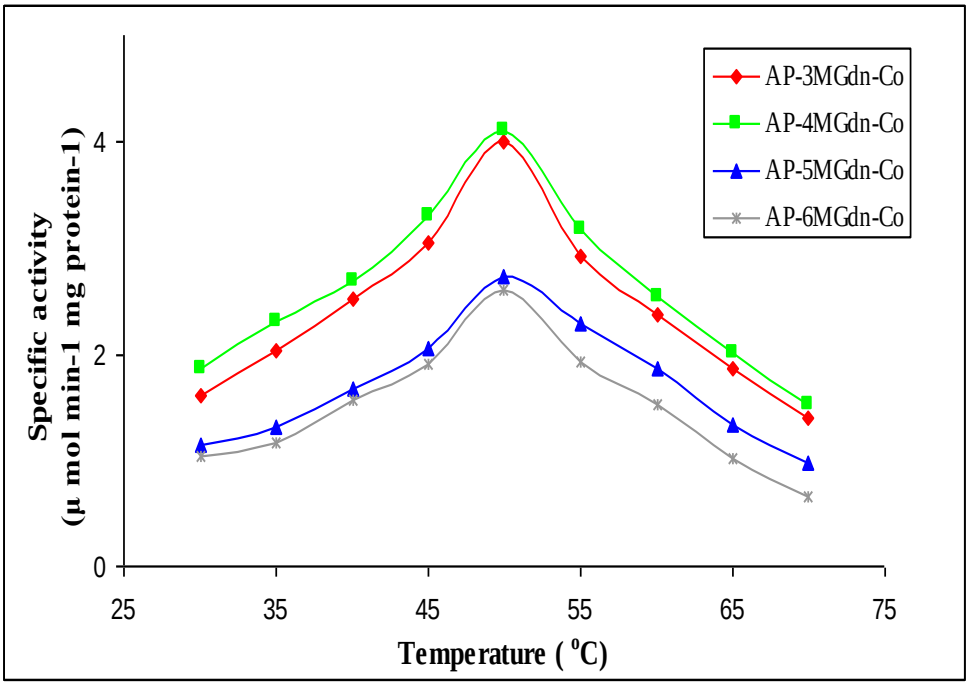

Fig. 4.10 Effect of temperature on Nitrile Hydratase activity

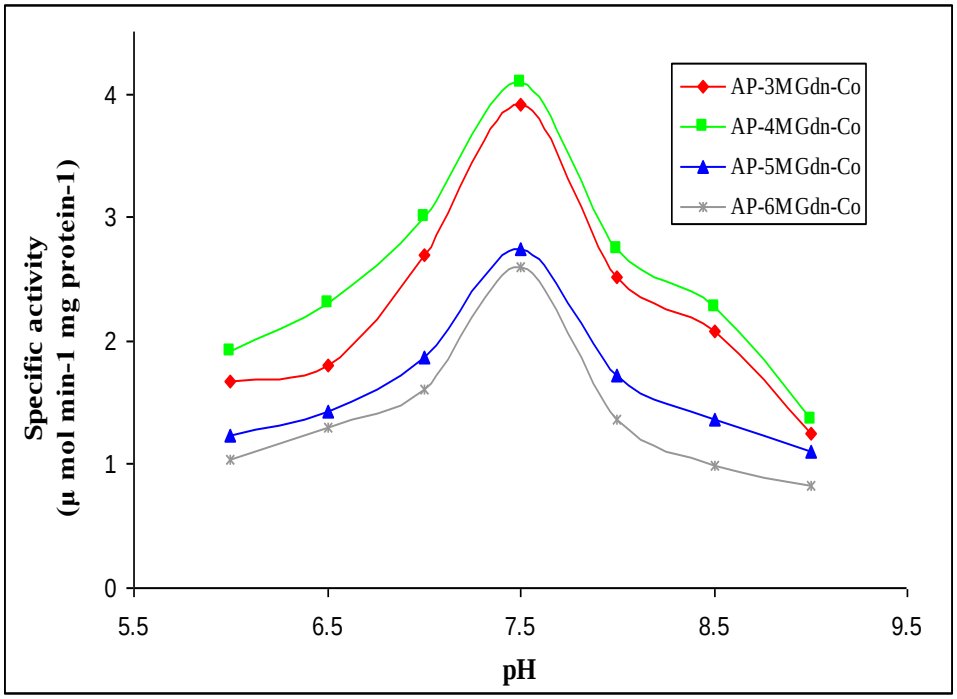

Fig. 4.11 Effect of pH on Nitrile Hydratase activity

All the enzymes shows, the specific activity increased with increasing pH value up to 7.5, after that the activity started to decrease. This could due to the destabilization of active center as well as the conversion nicotinamide to nicotinic acid at higher pH which render the interaction of 3-cyanopyride with active site cobalt metal ion.

4.4. References:

[1] Hui-Min Yu, Yue Shi, Hui Luob, Zhuo-Ling Tian, Yan-Qin Zhu, Zhong-Yao Shen, *J. Mol. Cat. B*: Enzym. 43 (2006) 80–85.

[2] S. Wu, R.D. Fallon, M.S. Payne, *Appl. Microbiol. Biotechnol*. 52 (1999) 186-190.

[3] O. Ikehata, M. Nishiyama, S. Horinouchi, T. Beppu, *Eur. J. Biochem*. 181 (1989) 563-570.

[4] M. Kobayashi, M. Nishiyama, T. Nagasawa, S. Horinouchi, T. Beppu, H. Yamada, *Biochim. Biophys. Acta* 1129 (1991) 23-33

[5] Y. Hashimoto, M. Nishiyama, T. Horinouchi, *Biosci. Biotechnol. Biochem*. 58 (1994) 1859-1865.

[6] W. Huang, J. Jia, J. Cummings, M. Nelson, G. Schneider, Y. Lindqvist, *Structure* 5 (1997) 691-699.

[7] S. Nagashima, M. Nakasako, N. Dohmae, M. Tsujimura, K. Takio, M. Odaka, M. Yohda, N. Kamiya, I. Endo, *Nat. Struct. Biol*. 5 (1998) 347-351.

[8] Y. Sugiura, J. Kuwahara, T. Nagasawa, H. Yamada, *J. Am. Chem. Soc*. 109 (1987) 5848-5850.

[9] B.A. Brennan, G. Alms, M.J. Nelson, L.T. Durney, R.C. Scarrow, *J. Am. Chem. Soc*. 118 (1996) 9194-9195.

[10] M. Nojiri, M. Yohda, M. Odaka, Y. Matsushita, M. Tsujimura, T. Yoshida, N. Dohmae, K. Takio, I. Endo, *J. Biochem*. (Tokyo) 125 (1999) 696-704.

[11] M.S. Payne, S. Wu, R.D. Fallon, G. Turdor, B. Stieglitz, I.M. Turner Jr., M.J. Nelson, *Biochemistry* 36 (1997) 5447-5454.

[12] T. Noguchi, J. Honda, T. Nagamune, H. Sasabe, Y. Inoue, I. Endo, *FEBS Lett*. 358 (1995) 9-12.

[13] M. Odaka, K. Fujii, M. Hoshino, T. Noguchi, M. Tsujimura, S. Nagasawa, M. Yohda, T. Nagamune, Y. Inoue, I. Endo, *J. Am. Chem. Soc*. 119 (1997) 3785-3791.

[14] D. Bonnet, I. Artaud, C. Moali, D. Petre, D. Mansuy, *FEBS Lett*. 409 (1997) 216-220.

[15] T. Nagamune, H. Kurata, M. Hirata, J. Honda, H. Koike, M. Ikeuchi, Y. Inoue, A. Hirata, I. Endo, *Biochem. Biophys. Res. Commun*. 168 (1990) 437-442.

[16] T. Nagasawa, K. Takeuchi, H. Yamada, *Eur.J. Biochem*. 196 (1991) 581-589.

[17] H. Komeda, M. Kobayashi, S. Shimizu, *J. Biol. Chem*. 271 (1996) 15796-15802.

[18] M. Nojiria, H. Nakayama, M. Odaka, M. Yohda, K. Takio, I. Endo, *FEBS Letters* 465 (2000) 173-177

[19] B. Song, J.H. Cho, D.P. Raleigh, *Biochemistry* 46 (2007) 14206-14214.

[20] C.N. Pace, *Methods Enzymol*. 131 (1986) 226-280.

[21] J.Y. Chang, *Biochemistry* 48 (2009) 9340-9346.

[22] L. Masino, S.R. Martin, P.M. Bayley, *Protein Sci*. 9 (2000) 1519-1529.

[23] C. Tanford, K. Kawahara, S. Lapanje, *J. Am. Chem. Soc*. 89 (1967) 729-736.

[24] C.N. Pace, *Crit. Rev. Biochem. Mol. Biol*. 3 (1975) 1-43.

[25] R, Gupta, S. Yadav, F. Ahmad, *Biochemistry* 35 (1996) 11925-11930.

[26] D. Bhattacharyya, T.K. Hazra, W.D. Behnke, P.L.G. Chong, A. Kurosky, J.C. Lee, S. Mitra, *Biochemistry* 37 (1998) 1722-1730.

[27] P. Zhuang, D.A. Butterfield, *Biophys. J.* 60 (1991) 623-628.

[28] S. Gianni, M. Brunori, C. Travaglini-Allocatelli, *Protein Sci*. 10 (2001) 1685-1688.

[29] B. Ahmad, T.A. Shamim, R.H. Khan, *J. Biochem*. 141 (2006) 251-259.

[30] K. Okrasa, R. J. Kazlauskas, *Chem. Eur. J*., 12 (2006) 1587–1596.

[31] M.B. Rao, A.M. Tanksale, M.S. Ghatge, V.V. Deshpande, *Microbiol. Mol. Biol. Rev*. 68 (1998) 597–635

[32] S.Y. Reddy ,K. Kahn, Ya-Jun Zheng, T.C. Bruice, *J. Am. Chem. Soc*., 124 (2002) 12979-12990.

[33] N. Sreerama, S.Y. Venyaminov, R.W. Woody, *Protein Sci*. 8 (1999) 370–380.

[34] K. Matsuo, R. Yonehara, K. Gekko, *J. Biochem*. 138 (2005) 79–88.

[35] P. Manavalan, W.C. Johnson, *Anal. Biochem*. 167 (1987) 76–85.

[36] I.H.M. van Stokkum, H.J.W. Spoelder, M. Bloemendal, R. van Grondelle, F.C.A. Groen, *Anal. Biochem*. 191 (1990) 110–118.

[37] W.C. Johnson, *Struct. Funct. Genet*. 35 (1999) 307–312.

[38] S.W. Provencher, J. Glockner, *Biochemistry* 20 (1981) 33–37.

[39] N. Sreerama, R.W. Woody, (2000) Circular dichroism of peptides and proteins in Circular Dichroism: Principles and Applications (N. Berova, K. Nakanishi, R.W Woody, eds.) 2nd ed., pp. 601–620, Wiley-VCH Press, New York

[40] R.W. Woody, A. Koslowski, *Biophys. Chem*. 101–102 (2002) 535–551

[41] N. Sreerama, R.W. Woody, *Anal. Biochem*. 287 (2000) 252–260

[42] A.R. Fersht, *Proc. Natl. Acad. Sci. U.S.A*. 92 (1995) 10869-10873.

[43] F.M. Hughson, P.E. Wright, R.L. Baldwin, *Science* 249 (1990) 1544-1548.

[44] M.H. Zehfus, G.D. Rose, *Biochemistry* 25 (1986) 5759-5765.

[45] M. Kobayashi, S. Shimizu *Nat Biotechnol*. 16 (1998) 733-736.

[46] M. Kobayashi, S. Shimizu, *Eur. J.Biochem.*, 261 (1999) 1-9.

Chapter 5

Summary, conclusion and future prospects

5.1 Summary and conclusion

Enzymes are the ubiquitous magicians of the biological world, catalyzing one substance into a material that is substantially different. Agriculture, manufacturing, pharmaceuticals, energy generation, all aspects of industry and human endeavor rely in some way on enzyme reactions. However, enzymes are fragile and operate within very specific temperatures and environments that reflect their cellular origins. This fragility has, until now, limited researchers ability to precisely control enzyme reactions or to reuse the enzymes. An enzyme is like a very efficient, environmentally friendly catalysts that doesn't require extreme conditions to operate, cells have thousands of enzymes carrying out the chemical reactions that sustain life, and many of these enzymes can be tapped for useful applications.

The possibilities for using immobilized enzymes to carry out desirable targeted chemical reactions are endless. New and highly diverse areas of research such as generating energy more efficiently in hydrogen fuel cells, purifying chemical and biological materials for prescription drug use, and detecting and neutralizing dangerous chemical and biological agents are just a few of the possible applications of targeted enzyme reaction.

Alkaline protease (22.5 kDa, EC 3.4.21.62) from Bacillus Licheniformis is an dairy industrial enzyme, which can hydrolyse the higher molecular weight casein into small casein molecules. Alkaline serine endopeptidase, was immobilized on surface modified SBA-15 and MCF materials by amide bond formation using carbodiimide as a coupling agent. The specific activities of free enzyme and enzyme immobilized on

SBA-15 and MCF were studied using casein (soluble milk protein) as a substrate. The highest activity of free enzyme was obtained at pH 9.5 while this value shifted to pH 10 for SBA-15 and MCF immobilized enzyme.

The highest activity of immobilized enzymes was obtained at higher temperature (60 ^{o}C) than that of the free enzyme (55 ^{o}C). Kinetic parameters, Michaelis-Menten constant (K_m) and maximum reaction velocity (V_{max}), were calculated as K_m = 13.375, 11.956, and 8.698 x 10^{-4} mg/ml and V_{max} = 0.156, 0.163 and 0.17 x 10^{-3} U/mg for the free enzyme and enzyme immobilized on SBA-15 and MCF, respectively. The reusability of immobilized enzyme showed 80% of the activity retained even after 15 cycles. Large pore sized MCF immobilized enzyme was found to be more promising than the SBA-15 immobilized enzyme due to the availability of larger pores of MCF, which could host the enzyme comfortably in its pores and offer facile diffusion of substrate and product molecules into the active sites of alkaline protease.

Cellulase from Penicillium funiculosum was covalently immobilized on functionalized MCF (Meso Cellular Foam) silica by imine bond formation followed by reduction using $NaBH_4$. The specific activities of free and immobilized enzyme were measured for hydrolysis of soluble carboxymethyl cellulose (CMC). The highest activity of MCF immobilized and native enzyme was obtained at optimum pH 5 and pH 4.5 respectively. Kinetic parameters, Michaelis–Menten constant (K_m) and maximum reaction velocity (V_{max}), were calculated as K_m = 0.025 ×10^{-2} mg/ml, V_{max} = 5.327 ×10^{-3} U/mg for the free enzyme and K_m = 0.024 ×10^{-2} mg/ml, V_{max} =9.794 ×10^{-3} U/mg for MCF immobilized enzyme respectively. The reusability of immobilized enzymes showed that 66% of its activity is retained even after 15 cycles.

Multi point covalent attachment of cellulase with solid carrier surface rigidified the enzyme and the availability of polar groups (-NH-, -OH). This could be electrostatically stabilizing the cellulase on surface as well as inside the pores of surface modified MCF during hydrolysis of soluble carboxymethyl cellulose. Surface modified MCF-AG's active functional groups are also involved in the hydrolysis of soluble carboxymethyl cellulose to some extent leading to higher activity of MCF immobilized cellulase. Uniform and ordered porous structure of modified MCF is found to be a promising material for immobilization of cellulase with 16.4 wt% enzyme loading.

The highly stable alkaline protease (22.5 kDa, EC 3.4.21.62) from Bacillus Licheniformis was denatured by increased concentration of 3M-6M Gdn-HCl and then renatured with cobalt metal ion in refolding buffer in order to design cobalt dependent Nitrile hydratase. The secondary structure fractions of the globular proteins from the CD spectrum of the denatured and renatured alkaline protease were analyzed using the reference set 4 in the member of the DICHROMWEB online server using the programs SELCON3 and CONTIN/LL. The observed secondary structure content values of renatured 4MGdn-Co shows ordered (0.2%) and distorted α-helix (3.7%) contents same as that of native alkaline proteases, but the unordered (30.73%) content was reduced (31.36%).

The creation of cobalt centered new active site was also supported by the fluorescence spectroscopy (appearance of a new peak at 360 nm) and ICP analysis (0.0476-0.0553 mg/L). The specific activities of all the modified enzymes were measured using the selective catalytic hydrolysis of 3-cyanopyridine to nicotinamide. Kinetic parameters, Michaelis–Menten constant (K_m), maximum reaction velocity

(V_{max}), turn over number (k_{cat}) and specific constant (k_{cat}/K_m) were calculated as K_m = 1.87, 1.68, 2.43, 3.32 x 10^{-6} mol; V_{max} = 7.97, 8.23, 7.59, 7.17 U/mg; k_{cat} = 0.299, 0.309, 0.285, 0.269 (S^{-1}); k_{cat}/K_m = 160000, 184000, 117000, 81000 for the AP-3MGdn-Co, AP-4MGdn-Co, AP-5MGdn-Co and AP-6MGdn-Co enzymes, respectively. The highest specific activity of AP-4MGdn-Co was obtained at optimum pH 7.5 and temperature 50 °C, due to the proper co-ordination of amino acid residue with cobalt metal ion and the appropriate arrangement of α-helix, β-strand, turn and unordered in the globular structure to facile the diffusion of substrate and product molecules into the active sites.

The Co-type Nitrile Hydratase was successfully designed from the alkaline protease by reversible denaturisation followed renaturisation in presence of cobalt metal ion. Co ion was spontaneously coordinate with the active amino acid residue which could be hydrolyzing the 3-cyanopyridine to nicotinamide without any NHase activator. Although it is unclear yet whether the low-spin trivalent state of the bound-metal and the coordinating residues stabilization were essential in the catalytic mechanism of nitrile hydration, the denovo enzyme engineering of Co-NHase will surely be an important for the industrial production of aromatic amides from its corresponding nitriles.

5.2 Future prospects

5.2.1 Immobilization of Biomolecules on porous materials

It has been shown that nanoporous materials can be used as carriers for enzyme immobilization.[1] As a result of the rapid growth of research in the preparation of nano structured materials with diverse physical and chemical properties, it should be possible to tailor supports to suit specific applications, once the underlying requirements of pore size, connectivity and surface chemistry are fully understood.[2-5] As described, there remains relatively little research so far on the applications of these enzyme–nanomaterials in real catalytic reactions, and demonstration of their utility remains a potential possibility.

In particular, if enzyme–nanomaterials composites can be prepared that retain their enantio selectivity, their applications in pharmaceutical and fine chemical industries can be exploited. There are also emerging biotechnologies that can benefit from composites of mesoporous solids with biological molecules as shown in Fig. 5.1. On a practical level, the large, tunable surface areas of the solids offer a vehicle for the delivery of drugs, which can include peptide-based pharmaceuticals.

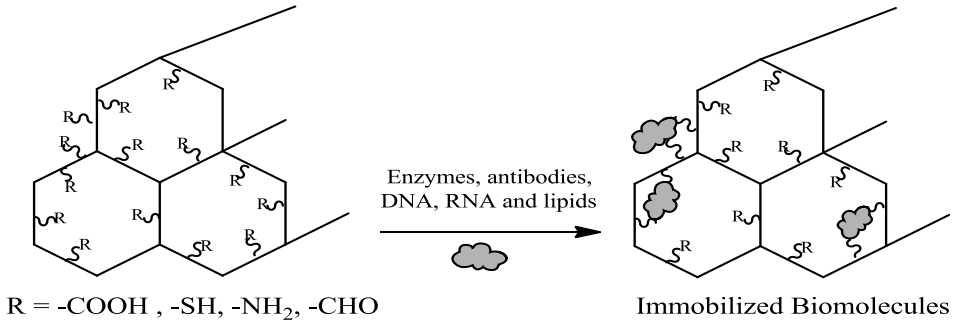

Fig. 5.1 Immobilization of various biomolecules on MPS's

Another area of enormous current interest is in the preparation of nanoparticles that can be taken into cells through the membrane. There is interest in loading such 'nanospheres' with magnetic and fluorescent inorganic species, (in order to visualize and manipulate them).[3] The high pore volume and large pore dimensions of mesoporous silica offer possibilities for hosting combinations of functional species. A triple-layer design for multifunctional nano materials incorporating functional species, such as fluorescent dyes or particles, quantum dots or nanomagnets and with a surface functionalized with organic groups.

It is possible to load such mesoporous nanoparticles with molecules that would not otherwise be able to pass through the membrane to act as a general transmembrane carrier, or to act as a transfection agent. Such mesoporous silica nanospheres have been described, among others and have been shown not to exhibit cytotoxicity. Drug delivery agents of this kind could be highly specific in their action.

Finally, many areas in biotechnology are still unexplored with the use of nanoporous silica materials. These include the immobilization of antibodies, DNA and RNAs, lipids and carbohydrates.[1,4,6] Close working relationship between materials scientists, chemists and biologists are key to the success of the promising future of nano porous silica–biomolecule hybrid materials.

5.2.2 Protein engineering of Metalloproteins

A most exciting development over the last few years is the application protein engineering techniques to enzyme technology. Protein engineering of enzymes is a faster, controlled, targeted and accurate method to optimize the properties of enzymes for a specific industrial application than the traditional method. It makes it doable to sidestep the high number of natural isolate screenings that would be necessary to find the enzyme with the desired properties.[7]

Metal ions play significant roles in most biological systems. Over the past two decades, there has been significant interest in the redesign of existing metal binding sites in proteins/peptides and the introduction of metals into folded proteins/peptides. The designed metal-binding sites also resulted in proteins with increased stability, altered activities and selectivity. It can be an effective approach for creating metal-binding sites with more complexity if the investigators are equipped with a thorough understanding of the structure and function of both the target and the template proteins. This approach can be enhanced further if it can utilize computer programs to help evaluate and modify the initial design through energy minimization.[8-11]

Recent research has focused on the effects of metal binding on the overall secondary and tertiary conformations of unstructured peptides/proteins. In this context, de novo design of metallo-peptides has become a valuable approach for studying the consequence of metal binding. It has been seen that metal ions not only direct folding of partially folded peptides but have at times also been the useful for properly folding random coil-like structures into stable secondary conformations.[12-15]

It is expected that the next few years will see the enhanced ability to coordinate small molecule substrates simultaneously with inorganic cofactors. In addition, greater attention is likely to be focused on how metals influence protein folding.

There are several approaches to the design and engineering of novel metallo proteins based on native protein scaffolds. Whether it is for redesign of an existing metal-binding site or to create a new one, both rational and combinatorial methods can be used. Another equally attractive empirical approach is the design of new metal-binding sites based on protein homology. This approach depends highly on the degree of sequence or structural homology with higher homology generally leading to a better chance of success. At the same time, factors that are common to both template protein and the target protein cannot be revealed from the design exercise. Furthermore, recent studies also showed that positive design in the secondary coordination sphere (such as hydrogen-bonding and hydrophobic interactions) is also quite important.[16-19] These problems also apply to the protein redesign approach. Despite these limitations, both approaches are extremely useful at elucidating the role of specific structural features in protein design and function and at revealing principles of protein design.

All the rational methods described above rely heavily on our knowledge of principles governing the structure and function of metal-binding sites. However, despite much progress made so far, our knowledge is still quite limited. For example, the high affinity and selectivity of many metal-binding sites remains to be elucidated. Fascinating new metal centers, such as the Fe, Co, Mn, Zn, Ni, Ca, Cu, etc. center in protein architecture, a multi nuclear metal center with M-M bonds, are being

discovered as shown in Fig. 5.2. To fill the gap of our knowledge and to keep pace with the rapid development of the field, combinatorial engineering of metal-binding sites is of great value. Combinatorial engineering using native protein scaffolds and focusing on a specific region of the protein can minimize this problem because structural space is much smaller than the sequence space.[20-22]

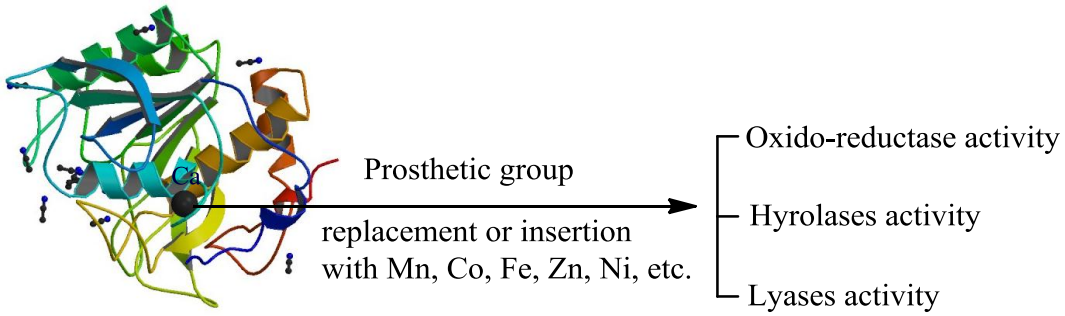

Fig. 5.2 Designing of various metal ion dependent enzymes

Recognizing the advantages and disadvantages of each approach, one can combine the advantages of two or more approaches. For example, rational approaches can be used to create a new metal-binding site and combinatorial searches can then be used to fine-tune the metal-binding affinity, selectivity, or in the case of catalytic sites the substrate-binding pocket. Most spectroscopic techniques routinely used in metallo protein design can confirm the success (or failure) of only certain main features of the design. It is difficult to reveal subtle changes from the design work. Since metallo protein design using native protein scaffolds makes it possible to choose a template protein of reasonable characteristics study using circular dichroism, fluorescence, NMR spectroscopies and crystallography.[13] With development of the many approaches described above, together with approaches, it will not be too long before we can design and make the same or may be even better enzyme molecule than nature does.

5.3 Reference:

[1] H.H.P. Yiu, P.A. Wright, J. Mater. Chem., 15 (2005) 3690–3700.

[2] C. Mateo, J.M. Palomo, G.F. Lorente, J.M. Guisan, R.F. Lafuente, Enzyme Microb. Technol., 40 (2007) 1451–1463.

[3] X. Gao, S. Nie, J. Phys. Chem. B, 107 (2003) 11575-11578.

[4] D.R. Radu, C.Y. Lai, K. Jeftinija, E.W. Rowe, S. Jeftinija, V.S.Y. Lin, J. Am. Chem. Soc., 126 (2004) 13216-13217.

[5] S. Hudson, E. Magner, J. Cooney, B.K. Hodnett, J. Phys. Chem. B 109 (2005) 19496-19506.

[6] M. Hartmann, D. Jung, J. Mater. Chem., 20 (2010) 844–857.

[7] S.J. Park, J.R. Cochran, Protein Engineering and Design, CRC Press, Taylor and Francis Group, Boca Raton, FL, 2010.

[8] H.W. Hellinga, Foldind Des., 3 (1998) R1-R8.

[9]) J.P. Glusker. Adv. Protein Chem., 42 (1991) 1-76.

[10] S. Karlin, Z.Y. Zhu, K.D. Karlin, Proc. Natl. Acad. Sci. U.S.A. 94 (1997) 14225-14230.

[11] K.D. Karlin, Z.Y. Zhu, S. Karlin, J. Biol. Inorg. Chem., 3 (1998) 172-187.

[12] D. Ghosh, V.L. Pecoraro, Curr. Opin. Chem. Biol., 9 (2005) 97–103.

[13] W.F. DeGrado, C.M. Summa, V. Pavone, F. Nastri, A. Lombardi, Annu. Rev. Biochem., 68 (1999) 779–819.

[14] J. Kaplan, W.F. DeGrado, Proc. Natl. Acad. Sci. USA, 101 (2004) 11566–11570.

[15] R.L. Koder, P.L. Dutton, Dalton Trans., (2006) 3045–3051.

[16] D.P. Hildebrand, J.C. Ferrer, H.L. Tang, M. Smith, A.G. Mauk, Biochemistry, 34 (1995) 11598-11605.

[17] J.A. Sigman, A.E. Pond, J.H. Dawson, Y. Lu, Biochemistry, 38 (1999) 11122-11129.

[18] T. Uno, A. Yukinari, Y. Tomisugi, Y. Ishikawa, R. Makino, J.A Brannigan, A.J. Wilkinson, J. Am. Chem. Soc., 123 (2001) 2458-2459.

[19] S.F. Marino, L. Regan, Chem. Biol., 6 (1999) 649-655.

[20] Y. Lu, S.M. Berry, T.D. Pfister, Chem. Rev., 101 (2001) 3047−3080.

[21] D. Ghosh, V.L. Pecoraro, Inorg. Chem., 43 (2004) 7902−7915.

[22] R.L. Koder, J.L.R. Anderson, L.A. Solomon, K.S. Reddy, C.C. Moser, P.L. Dutton, Nature, 458 (2009) 305-310.

Appendices

Appendix I

Determination of alkaline serine endo peptidase concentration

The alkaline serine endo peptidase enzyme solution concentration of 25, 50, 100 150, 200 and 250 µl was added into the 10 ml of phosphate buffer with EDAC (25 mg). To this 0.5 ml enzyme solution 2 ml of Bradford reagent was added and measure the absorption at 595 nm was measured a UV-vis-NIR scanning spectrophotometer (CARY 500 SCAN). The standard alkaline serine endo peptidase concentration curve was plotted and shown in Fig.1.

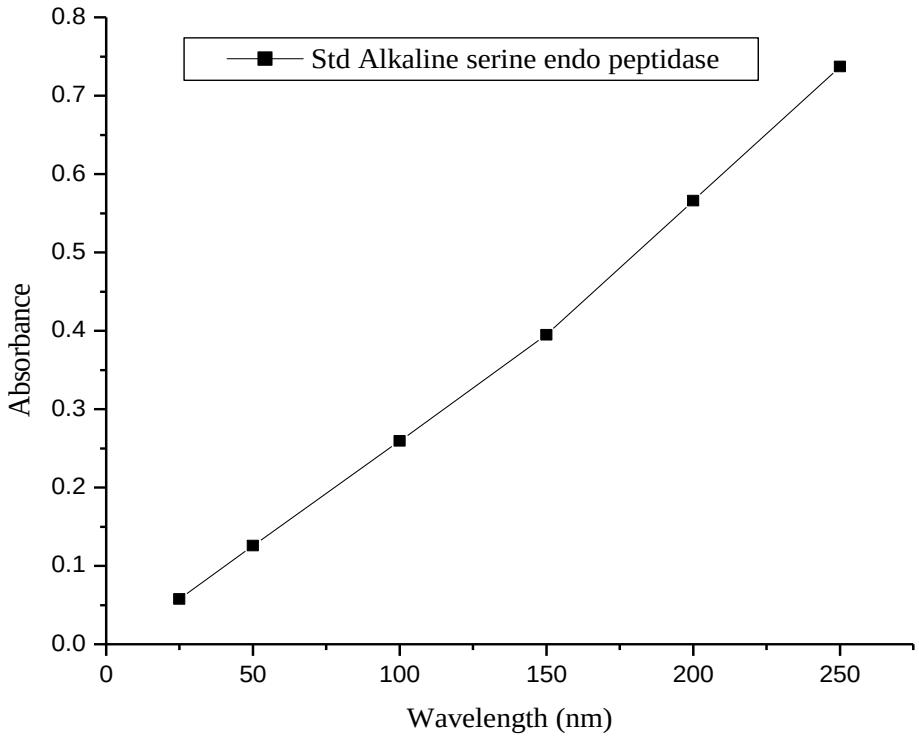

Fig.1 Standard alkaline serine endo peptidase concentration curve

The unknown enzyme concentration was determined from corresponding absorbance of the alkaline serine endo peptidase solution, which obtained from the enzyme immobilization by washing the excess enzyme using buffer solution.

Appendix II

Determination of tyrosine concentration

One of the casein hydrolyzed product of the tyrosine, various concentrations 0.025, 0.05, 0.10, 0.15, 0.20 and 0.25 mg/ml were prepared. 1 ml of this solution was added into 2 ml of 0.1 M bicarbonate buffer at pH 9.5, for exactly 20 min at 45 ^{o}C with a stirring speed of 150 rpm. To this solution 3 ml of 10 w/v of trichloroacetic acid was added and the precipitate was removed by centrifugation. The absorbance due to the tyrosine was measured at 280 nm using a UV-vis-NIR scanning spectrophotometer (CARY 500 SCAN). The standard tyrosine concentration curve was plotted and shown in Fig. 2.

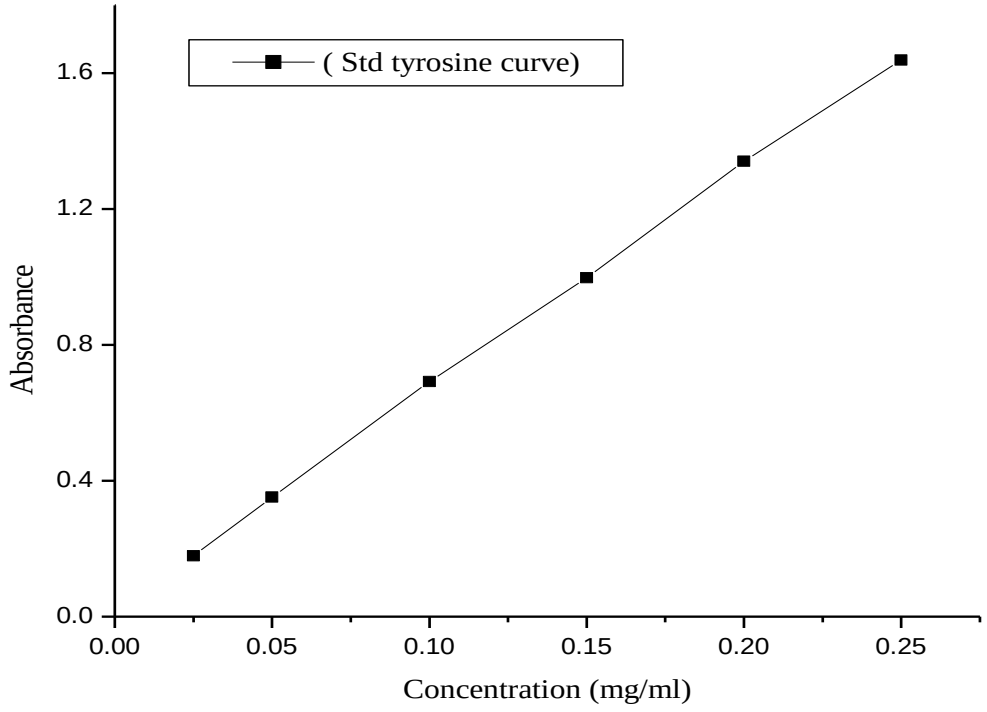

Fig. 2 Standard tyrosine concentration curve

Appendix III

Scanning electron microscopy (SEM) of SBA-15 and MCF

The meso porous material SBA-15 was synthesized as per described in section 2.2.2. Scanning electron microscopy (SEM) was performed on a Hitachi S-4000 scanning electron microscope. The samples were prepared by placing SBA-15 powder on double-sided carbon adhesive tape mounted on the sample holder. The SEM pictures of mesoporous SBA-15 particles after the calcination is shown in Fig. 3. Large fibrous structures 20–30 μm in length and 3–5 μm in diameter are observed. The fibrous structure is an agglomerate of long fibers that are constituted from small rod-like sub-particles 1–2 μm in length and 0.5 μm in diameter. The SBA-15 particles are something like spherically shaped with size approximately in the range of 20-30 μm.

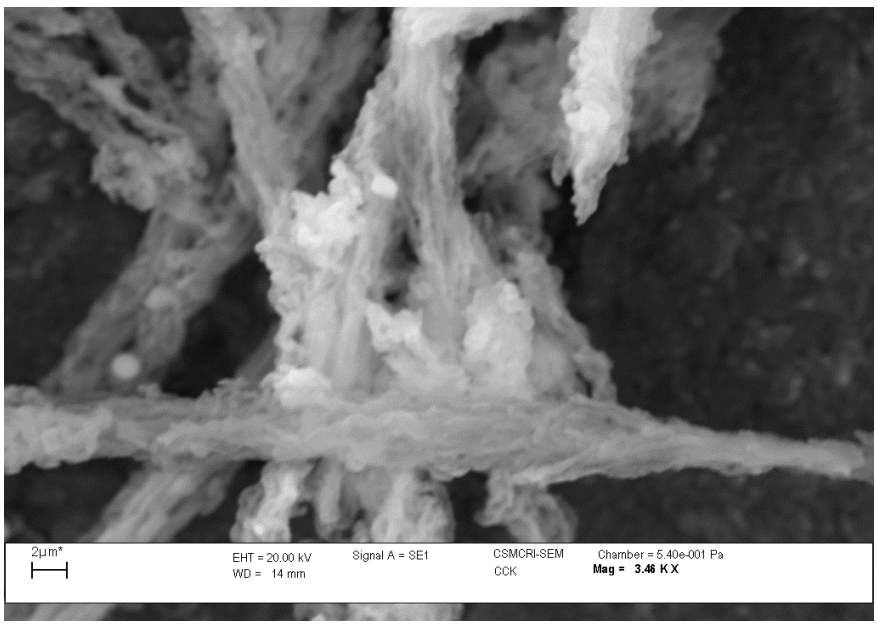

Fig. 3 SEM image of calcined SBA-15

The SEM picture clearly shows a large number of SBA-15 particles attaching closely with one another. The spines of one SBA-15 particle may be caught on the spine of another SBA-15. This way the bonding of large number of SBA-15 particles may take place. On the other hand, it could be due to vander Walls and electrostatic interaction between the adjacent SBA-15 particles.

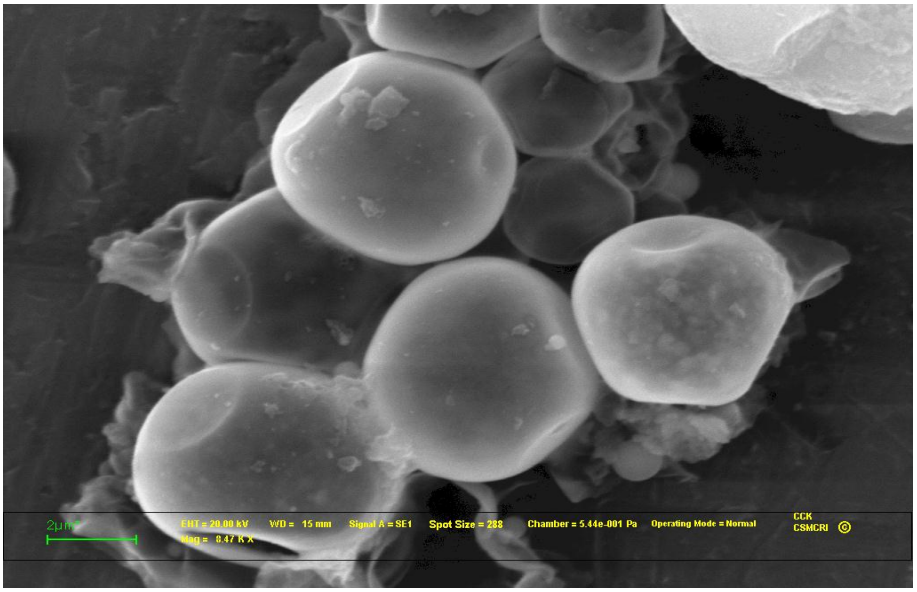

Fig. 4 SEM image of calcined MCF

Large spherical structures 4-8 µm in diameter are observed. It is clear that the pores are interconnected with gauge like structure. The formation of spherical micelles that yields mesocellular silica foams is driven by the requirement to cover the fixed amount of oil and polymer. The oil swells out the PPO chains until saturation, and then pure oil cores are formed at the center of the micelles. To cover the oil droplets with the minimum amount of polymer, the micelles become more spherical, yielding the spherical structure after calcination is shown in Fig. 5. The diameter of the spherical nodes that form at an oil-polymer ratio of 0.21 is ~ 220Å, the transition from cylinders of 110Å diameter to spheres of 220Å diameter is also possible.

Appendix IV

TEM image of the MCF

TEM was performed on 1230 Jeol Field Emission microscope at 120kV. The powder samples were mixed in ethanol and then ultrasonicated for 10min. A drop of the wet sample was placed on copper grid and then allowed to dry for 30 min before TEM analysis is shown in Fig.5.

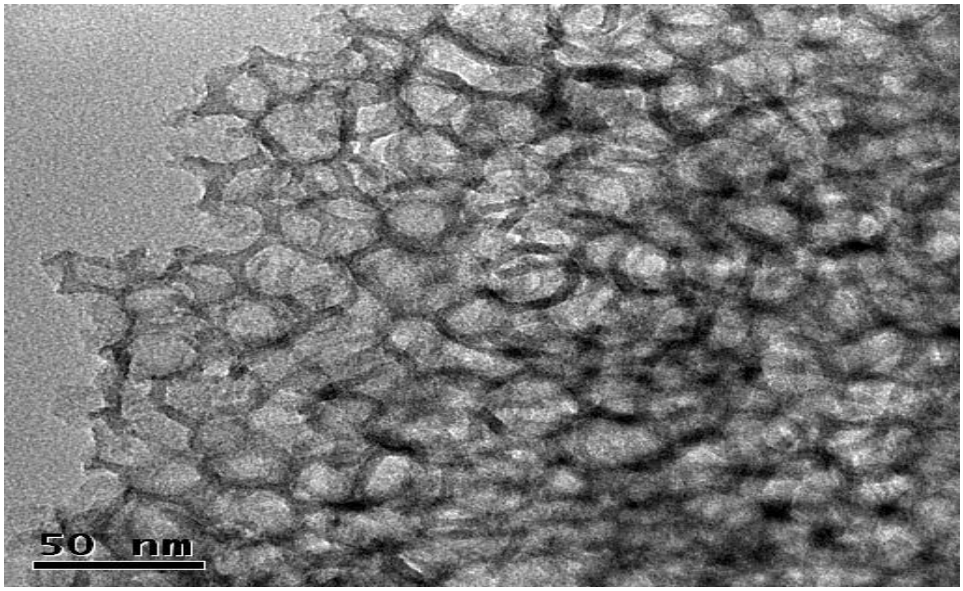

Fig. 5 TEM image of the calcined MCF

MCFs consist of uniform spherical cells 21-36 nm in diameter and possess surface areas up to 700 m^2/g. Uniform windows, 7-18 nm in diameter, interconnect the cells to form a continuous 3-D pore system, which makes the MCFs attractive candidates for supports for immobilization involving large molecules. The pore diameter of the pure-silica MCF sample estimated from the TEM image is around 220Å, which is in good agreement with that estimated from the BJH adsorption isotherm.

Appendix V

Determination of cellulase concentration

The various concentrations of cellulase enzyme 50, 75, 100, 125, 150 and 200 µl with phosphate buffer (pH=6) = 5 ml in total volume of 30 ml. To this 0.4 ml of enzyme solution 2 ml of Bradford reagent was added and measured the absorbance at 595 nm using UV-vis-NIR scanning spectrophotometer (CARY 500 SCAN). The standard cellulase concentration curve was plotted and shown in Fig. 6.

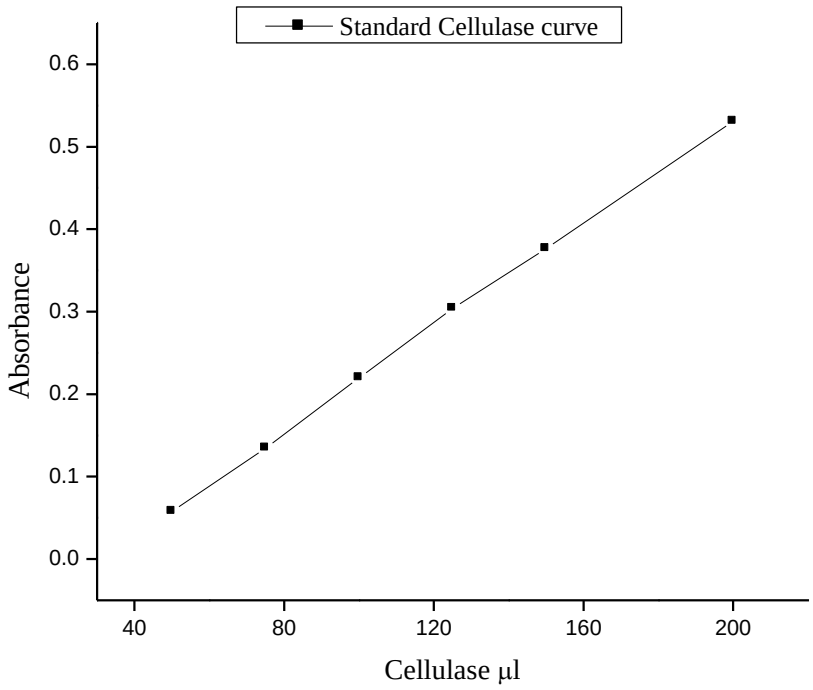

Fig. 6 Standard cellulase concentration curve

The unknown enzyme concentration was determined from corresponding absorbance of the cellulase solution, which obtained from the enzyme immobilization by washing the excess enzyme using buffer solution.

Appendix VI

Standard glucose curve:

The various concentration of glucose solution 0.2, 0.6, 1, 2, 3, 4 and 5 mg/ml were prepared. To this 1.5 ml solution, 3 ml of DNS reagent was added and kept at boiling water for 5 min and then kept to reach room temperature. 0.1 ml of this solution was diluted to 1 ml using distilled water and measured the absorbance at 540 nm using UV-vis-NIR scanning spectrophotometer (CARY 500 SCAN). The standard glucose concentration curve was plotted and shown in Fig. 7.

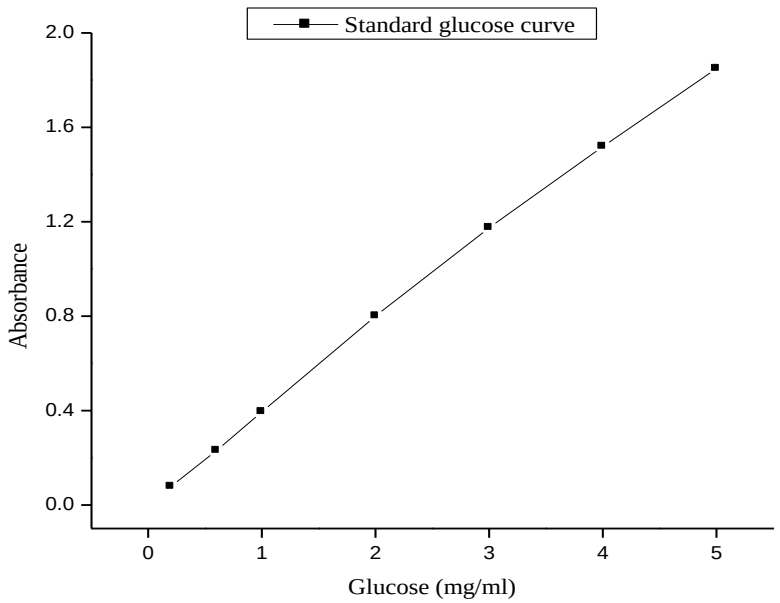

Fig. 7 Standard glucose concentration curve

LIST OF PUBLICATIONS:

1. "Immobilization of alkaline serine endopeptidase from *Bacillus licheniformis* on SBA-15 and MCF by surface covalent binding";
   Kayambu Kannan and Raksh Vir Jasra, *J. Mol. Catal. B: Enzymatic 56 (2009) 34–40*.
2. "Improved catalytic hydrolysis of carboxy methyl cellulose using cellulase immobilized on functionalized meso cellular foam"
   Kayambu Kannan and Raksh Vir Jasra, *J. Por. Mater. xxx (2010) xxx-xxx. DOI: 10.1007/s10934-010-9392-2 (Accepted)*
3. "De novo designing of nitrile hydratase from alkaline protease using reversible denaturation followed by renaturation in presence of cobalt metal ion"
   Kayambu Kannan and Raksh Vir Jasra (Communicated)
4. "A review of biochemical functions of enzymes in living systems"
   Kayambu Kannan and Raksh Vir Jasra (Under preparation)

PARTICIPATION IN SYMPOSIA / WORKSHOP :

- **Kayambu Kannan** and Raksh Vir Jasra, *Workshop on Immobilized enzyme for sensor application*, at Biochemistry Department, M.D University, Rohtak, India. August 24 to September 2, 2007.
- **Kayambu Kannan** and Raksh Vir Jasra**,** *Immobilization of Alkaline Serine Endopeptidase from Bacillus Licheniformis on SBA-15 and MCF by Surface Covalent Binding***,** 5th All Gujarat Research Scholars Meet, The M.S. University of Baroda, Vadodara, India. February 2008.
- **Kayambu Kannan** and Raksh Vir Jasra**,** *Surface Modified Mesoporous Materials for Enzyme Immobilization*, XXII-Gujarat Science Congress, Bhavnagar University, Bhavnagar, India. March 2008.
- **Kayambu Kannan** and Raksh Vir Jasra, National symposium on "Emerging Horizons in Catalysis". The M.S. University of Baroda, Vadodara, India. 25-26 September 2009.

Journal of Molecular Catalysis B: Enzymatic 56 (2009) 34–40

Contents lists available at ScienceDirect

Journal of Molecular Catalysis B: Enzymatic

journal homepage: www.elsevier.com/locate/molcatb

Immobilization of alkaline serine endopeptidase from *Bacillus licheniformis* on SBA-15 and MCF by surface covalent binding

Kayambu Kannan[a], Raksh Vir Jasra[a,b,*]

[a] *Discipline of Inorganic Materials & Catalysis, Central Salt & Marine Chemicals Research Institute, CSIR G.B. Marg, Bhavnagar 364002, Gujarat, India*
[b] *R&D Centre, Reliance Industries Limited, Vadodara Manufacturing Division, Vadodara 391346, Gujarat, India*

ARTICLE INFO

Article history:
Received 31 October 2007
Received in revised form 9 April 2008
Accepted 11 April 2008
Available online 26 April 2008

Keywords:
Alkaline serine endopeptidase
Casein hydrolysis
Enzyme immobilization
SBA-15
MCF
Enzyme reusability

ABSTRACT

An industrial enzyme, alkaline serine endopeptidase, was immobilized on surface modified SBA-15 and MCF materials by amide bond formation using carbodiimide as a coupling agent. The specific activities of free enzyme and enzyme immobilized on SBA-15 and MCF were studied using casein (soluble milk protein) as a substrate. The highest activity of free enzyme was obtained at pH 9.5 while this value shifted to pH 10 for SBA-15 and MCF immobilized enzyme. The highest activity of immobilized enzymes was obtained at higher temperature (60 °C) than that of the free enzyme (55 °C). Kinetic parameters, Michaelis–Menten constant (K_m) and maximum reaction velocity (V_{max}), were calculated as K_m = 13.375, 11.956, and 8.698×10^{-4} mg/ml and V_{max} = 0.156, 0.163 and 0.17×10^{-3} U/mg for the free enzyme and enzyme immobilized on SBA-15 and MCF, respectively. The reusability of immobilized enzyme showed 80% of the activity retained even after 15 cycles. Large pore sized MCF immobilized enzyme was found to be more promising than the SBA-15 immobilized enzyme due to the availability of larger pores of MCF, which offer facile diffusion of substrate and product molecules.

1. Introduction

Alkaline proteases are important enzymes having diverse applications in a wide variety of industries such as food, pharmaceutical, detergent, leather, silk, diagnostics, and for the recovery of silver from used X-ray films [1–4]. Alkaline serine endopeptidase from selected strain of *Bacillus licheniformis*, which hydrolyses casein, plays a vital role in dairy industries. Casein is a slowly digesting protein which is essential in building muscles in human body and is a major component of milk, whey and soy [5]. The industrial application of this enzyme requires specificity, stability at higher pH, temperature and reusability. Numerous techniques have been used for immobilization of free enzymes on solid support to obtain efficient biocatalysts [6]. Mesoporous silicas (MPSs) obtained by different templating methods demonstrate high potential as solid supports for enzyme immobilization [7–22]. These supports are environmentally acceptable, structurally more stable, and resistant to microbial attack. MPSs have a large specific surface area (~1000 m^2/g) and pore diameter, in the range of 2–50 nm, which can be tuned to host the enzymes of varied size. As such, the enzymes have considerable affinity towards the MPSs surfaces [7–14]. Besides, the MPSs surface can be modified with various anchor groups to covalently bind the enzyme molecules, which could reduce the enzyme leaching from the support during the recycling of the catalyst [14–22]. The uniform distribution of pores in MPSs favors the uniform loading of enzyme as well as facile diffusion of the substrate and product molecules inside the channels. The loading of an enzyme and its activity depend upon the surface area and pore size of the MPSs [17–22]. Among the MPSs, SBA-15 and MCF have been shown to be efficient supports for covalent immobilization of α-amylase, trypsin, chloroperoxidase, penicillin G acylase, organophosphorus hydrolase, glucose oxidase, glucoamylase, and invertase [8–11,14,19–22]. SBA-15 and MCF have pore sizes in the range of 9–25 nm and they possess 600–800 m^2/g surface area, which make them suitable to host the alkaline endopeptidase comfortably and also allow substrate and product molecules facile diffusion towards and from the active site of the enzyme [18,21]. The average size of the alkaline endopeptidase is 4.7 nm as shown in Fig. 1, produced using Chem3D Pro 10.0 from RCSB enzyme database [23].

Alkaline endopeptidase immobilized on polymeric support has been evaluated [24–26] for stability, activity and reusability with reference to free enzyme. In the present study, covalent immobilization of alkaline serine endopeptidase has been done through amide bond formation on modified SBA-15 and MCF. Surface

* Corresponding author. Tel.: +91 265 6693935; fax: +91 265 6693934.
E-mail address: rakshvir@ril.com (R.V. Jasra).

1381-1177/$ – see front matter © 2008 Elsevier B.V. All rights reserved.
doi:10.1016/j.molcatb.2008.04.007

J Porous Mater
DOI 10.1007/s10934-010-9392-2

Improved catalytic hydrolysis of carboxy methyl cellulose using cellulase immobilized on functionalized meso cellular foam

Kayambu Kannan · Raksh Vir Jasra

Abstract Cellulase from *Penicillium funiculosum* was immobilized on functionalized MCF (Meso Cellular Foam) silica by imine bond formation followed by reduction using $NaBH_4$. The specific activities of free and immobilized enzyme were measured for hydrolysis of soluble carboxymethyl cellulose (CMC). The highest activity of MCF immobilized and native enzyme was obtained at optimum pH 5 and 4.5 respectively. Kinetic parameters, Michaelis–Menten constant (*K*m) and maximum reaction velocity (*V*max), were calculated as *K*m = 0.025×10^{-2} mg/mL, *V*max = 5.327×10^{-3} U/mg for the free enzyme and *K*m = 0.024×10^{-2} mg/mL, *V*max = 9.794×10^{-3} U/mg for MCF immobilized enzyme respectively. The reusability of immobilized enzymes showed that 66% of its activity is retained even after 15 cycles. The availability of polar groups (–NH–, –OH) and large pore size of surface modified MCF could be electrostatically stabilizing the cellulase. Functionalized MCF was found to be a promising material for stabilizing cellulase with 16.4 wt% loading of enzyme.

K. Kannan · R. V. Jasra (✉)
Discipline of Inorganic Materials & Catalysis, Central Salt & Marine Chemicals Research Institute, Council of Scientific and Industrial Research (CSIR), G.B. Marg, Bhavnagar, Gujarat 364002, India
e-mail: rvjasra@gmail.com; rakshvir.jasra@ril.com

K. Kannan
e-mail: kanna.kp@gmail.com

Present Address:
K. Kannan · R. V. Jasra
R&D Centre Reliance Technology Group, Reliance Industries Limited, Vadodara Manufacturing Division, Vadodara 391346, Gujarat, India

Keywords Cellulase · Covalent bonding · Functionalized MCF · Soluble CMC hydrolysis · Enzyme stabilities · Reusability

1 Introduction

The abundance and relatively low cost of lignocellulosic materials make them attractive as a feedstock for the production of ethanol from renewable resources [1–5]. Ethanol is a potential future fuel having reduced net greenhouse gas emission. The enzymatic process has the potential to convert the lignocellulosic materials to ethanol with a high yield and low production cost [6, 7]. However, the recalcitrance of the lignocellulosic matrix to enzymatic attack necessitates pretreatment of the material in order to enhance the accessibility of the substrate to the enzyme. High-pressure steam treatment with small amount of acid catalyst such as sulphuric acid or sulphur dioxide, reduces the cellulose crystallinity [8–11]. Though, there have been efforts to reduce cellulase enzyme cost (http://eere.energy.gov/), yet the production cost of enzymes is still too high. Immobilization of enzyme is one of the methods to reduce the cost by reusing same enzyme while retaining its specificity and stability. Therefore, research efforts have been directed to immobilize enzyme using inorganic, organic and hybrid supports [15]. Moreover, immobilized enzymes can also be used in fixed bed type reactor, which can be used in a continuous mode. Mesoporous silicas (MPSs) have emerged as potential solid supports for enzyme immobilization [12]. These supports are environmentally acceptable, structurally stable, and resistant to microbial attack. Besides, the MPSs surface can be modified with various anchor groups to covalently bind the enzyme molecules, which could reduce the enzyme leaching from

Published online: 30 May 2010